Stony Brook University

The Role of TolC in *Francisella tularensis* Virulence

A Dissertation Presented

by

Christopher Richard Doyle

to

The Graduate School

in Partial Fulfillment of the

Requirements

for the Degree of

Doctor of Philosophy

in

Molecular Genetics and Microbiology

Stony Brook University

May 2014

Stony Brook University

The Graduate School

Christopher Richard Doyle

We, the dissertation committee for the above candidate for the
Doctor of Philosophy degree, hereby recommend
acceptance of this dissertation.

David G. Thanassi, Ph.D. (Dissertation Advisor), Professor
Department of Molecular Genetics and Microbiology

Jorge L. Benach, Ph.D. (Chairperson of Defense), Distinguished Professor and Chair
Department of Molecular Genetics and Microbiology

Adrianus W.M. van der Velden, Ph.D., Assistant Professor
Department of Molecular Genetics and Microbiology

Wei-Xing Zong, Ph.D., Professor
Department of Molecular Genetics and Microbiology

Anthony T. Maurelli, Ph.D., Professor
Department of Microbiology and Immunology
Uniformed Services University of the Health Sciences

This dissertation is accepted by the Graduate School.

Charles Taber
Dean of the Graduate School

Abstract of the Dissertation

The role of TolC in the virulence of *Francisella tularensis*

By

Christopher Richard Doyle

Doctor of Philosophy

in

Molecular Genetics and Microbiology

Stony Brook University

2014

Francisella tularensis is a Gram-negative, facultative intracellular pathogen and the causative agent of tularemia. *F. tularensis* is a Tier 1 agent of bioterrorism that is highly lethal via the pulmonary route of infection. *F. tularensis* invades host cells, escapes the phagosome, and replicates in the cytosol prior to being released upon host cell death. The molecular mechanisms behind the virulence of *F. tularensis* are largely unknown. Among the described virulence factors of *F. tularensis* is a functional type I secretion system (T1SS). The T1SS is important for the secretion of virulence factors from the bacterial cytoplasm to the extracellular environment. The *F. tularensis* T1SS consists of a periplasm-spanning outer membrane protein, TolC, which interacts with inner membrane adapter and transport proteins to form a contiguous channel. TolC has been shown to be important for the virulence of multiple *F. tularensis* subspecies. Infection of host cells with a *F. tularensis* live vaccine strain (LVS) Δ*tolC* mutant leads to increased caspase-3 activation and host cell death compared to cells infected with the wildtype LVS. The LVS Δ*tolC* mutant also elicits increased secretion of proinflammatory cytokines from infected cells when compared to cells infected with the wildtype LVS.

The work described here investigates the temporal induction of host cell apoptosis during LVS infection and the role that TolC plays in modulating this process. I show that the LVS delays

activation of the intrinsic apoptotic pathway to allow for bacterial replication during infection and that TolC is necessary for this inhibition. Chromosomal deletion of *tolC* in the highly virulent, human pathogenic Schu S4 strain showed that TolC is necessary for virulence and inhibiting cell death during infection, demonstrating that TolC function is conserved across *F. tularensis* subspecies. Finally, I investigated the efficacy of the LVS Δ*tolC* mutant strain as a live vaccine against tularemia. My results suggest that the Δ*tolC* mutant strain may be a safer, more effective tularemia vaccine compared to the parental LVS. Taken together, my work characterizes the role of TolC as a major *F. tularensis* virulence factor aimed at suppressing innate immune responses during infection.

Table of Contents

List of Tables

List of Figures

List of Abbreviations

ABC: ATP-binding cassette

AIM2: Absent in melanoma 2

BHI: Brain heart infusion broth

BMDM: Bone marrow-derived macrophage

BMIM: Bone marrow infection medium

BMM: Bone marrow medium

BSL3: Biosafety level 3

CDM: Chamberlain's defined medium

CFU: Colony-forming unit

CR3: Complement receptor 3

FBS: Fetal bovine serum

FCP: Francisella-containing phagosome

FcγR: Fc gamma receptor

FPI: *Francisella* pathogenicity island

IL-18: Interleukin 18

IL-1β: Interleukin 1 beta

IM: Inner membrane

LD_{50}: Median lethal dose

LDH: Lactate dehydrogenase

LPS: Lipopolysaccharide

LVS: Live vaccine strain

MAC: Membrane attack complex

MDM: Monocyte-derived macrophage

MFP: Membrane fusion protein

MHB: Mueller-Hinton broth

MOI: Multiplicity of infection

MR: Mannose receptor

OD_{600}: 600 nm optical density

OM: Outer membrane

PARP: Poly-ADP-ribose polymerase

RNS: Reactive nitrogen species

ROS: Reactive oxygen species

RTX: Repeat-in-toxin

SPA: Surfactant protein A

SR: Scavenger receptor

STS: Staurosporine

T1SS: Type I secretion system

TLR4: Toll-like receptor 4

TNFα: Tumor necrosis factor alpha

Acknowledgments

The work contained in the following pages would not have been possible without the help, guidance, and friendship of so many people, inside the lab and out. I will forever appreciate my friends, family, and colleagues in the Microbiology Department and CID for all of their help during my time at Stony Brook.

Over the past several weeks, I've realized that when I started my career at Stony Brook five and a half years ago, I knew nothing. I'd taken lab courses in college and worked under a postdoc in a lab at UMass, but I didn't know how to work in a lab, design an experiment, or even begin to think like a scientist. Looking back, I realize that I owe a lot of who I am today as a scientist to David Thanassi and the members of his lab. Under David, I not only learned how to work in a lab, but also learned to write and think like a scientist. From day one, David has given me tremendous freedom to take this project to where it is now. At first, as is the case with most new graduate students, my mind was all over the place, I was easily sidetracked in the lab, and I know it was more than a bit of a headache at times for David to keep me focused. As time passed, I noticed David slowly becoming more and more okay with experiments I was proposing and doing. I'm not sure if this was intentional or not, but I gradually started to feel like I knew what I was doing here and that a lot of what was going on in my head, scientifically speaking, was correct. To this end, I owe my still-young scientific career to David and am extremely thankful that he, for whatever reason, chose me in 2009.

I've made some wonderful friends over the past several years, and because of them, my time at Stony Brook was never uneventful. I've lived in six different places over the last five years, with at least a dozen different people. If nothing else, these various living arrangements have taught me that having real friends goes beyond consistent physical proximity. I've had the privilege to make numerous real friends here, in science and out. I'm not going to list most of them for fear of leaving someone out, but these people know who they are. The one true friend I want to thank here – if for no reason other than that I'd never hear the end of it if I didn't – is Becc. I'm no wordsmith when it comes to things like this, but just know that I appreciate everything big and small that you've done and continue to do for me.

Finally, none of this – college, graduate school, or a Ph.D. – would have been possible without the support of my family, specifically my parents. I'm the oldest of five kids, all of whom have gotten into their fair share of trouble over the years. I can't imagine having even one child of my own, so to try and figure out how my parents had five of us in a 7 year span and raised us all boggles my mind. Without them, there's little chance I would have finished my undergraduate degree, even less of a chance that I would have gone to grad school, and zero chance I would have finished grad school. Obviously all children are grateful and love their parents, but my gratitude and appreciation for everything they've done for me, specifically over the last 5-6 years, goes beyond that, and goes beyond simple words that I can write on these pages.

CHAPTER 1: Introduction

I. *Francisella tularensis*

Discovery and Early Characterization. *Francisella tularensis* is a Gram-negative bacterium and the causative agent of tularemia. *F. tularensis* was initially isolated from rats and squirrels displaying plague-like symptoms in Tulare Co., California, in 1911 (1). Further characterization of *F. tularensis* was performed by Dr. Edward Francis, a United States Public Health Services physician. Dr. Francis' early work characterized *F. tularensis* as a facultative intracellular, nonmotile coccobacillus, and laid the groundwork for subsequent investigation (1). In 1919, Dr. Francis determined that *F. tularensis* could be transmitted to humans via infected arthopods, and named the disease caused by *F. tularensis* – also known as rabbit fever, Ohara's disease, and deer fly fever – tularemia (1). Dr. Francis subsequently established that the plague-like disease previously observed in rodents and tularemia observed in humans were both caused by *F. tularensis*, thus linking rodents, arthropods, and humans in the *F. tularensis* infection cycle (1). In honor of Dr. Francis' seminal work, the bacterium formerly known as *Bacterium tularense* was named *F. tularensis* in 1959.

Nomenclature. Genetic characterization of the *Francisella* genus has accelerated with advances in nucleic acid sequencing technologies, and new species and subspecies are being identified on an increasing basis (2-5). To date, the *Francisella* genus consists of six species: *F. tularensis*, *F. novicida*, *F. philomiragia*, *F. noatunensis*, *F. piscicida*, and *F. hispaniensis*. Of these species, *F. tularensis* is the most virulent to humans. Accordingly, *F. tularensis* is the most extensively studied *Francisella* species. The *F. tularensis* species consists of four subspecies: *tularensis*, *holarctica*, *mediasiatica*, and *japonica*. Of all *Francisella* species and subspecies characterized to date, only two cause significant disease in immunocompetent humans. *F. tularensis* subsp. *tularensis*, also known as Type A *Francisella*, is highly infectious and causes severe cases of tularemia in humans that are often fatal. *F. tularensis* subsp. *holarctica*, also known as Type B *Francisella*, is comparably less virulent and causes a mild disease in humans that is rarely fatal (6, 7). The live vaccine strain (LVS) is derived from a subsp. *holarctica* isolate and is discussed in detail below. Finally, *F. novicida* can cause disease in immunocompromised individuals, but is avirulent to immunocompetent humans. The

majority of the remainder of this dissertation will focus on the *F. tularensis* subsp. *tularensis* Schu S4 strain and the *F. tularensis* subsp. *holarctica*-derived LVS.

Distribution. *F. tularensis* is naturally found throughout the world, and small, sporadic tularemia outbreaks often occur (8-10). Type A strains are generally found in North America, while Type B strains are more prevalent in Europe and Asia (11). *F. tularensis* was not thought to exist in the southern hemisphere, but a recent report implicated Type B *F. tularensis* in a case of human tularemia in Australia (12). Infection with Type A *F. tularensis* is responsible for the majority of tularemia cases in the United States (Figure 1.1). Until recently, all Type A strains were considered to be equally virulent to humans. However, advances in DNA sequencing and molecular diagnostics have led to further classification of Type A strains into the A1 and A2 subclades, with Type A1 strains exhibiting higher virulence to humans compared to A2 strains (13, 14). *F. tularensis* has been isolated from various small mammals, including rabbits, hares, squirrels, rats, mice and other rodents (15-17). Additionally, *F. tularensis* has been found in freshwater amoebae, fish, crustaceans, and a variety of insects, including ticks, deer flies, and mosquitoes (15-17). The severity of tularemia in humans, discussed below, is dependent on a variety of factors, including the route of transmission, infectious dose, and the specific subspecies of *F. tularensis* responsible for infection.

Tularemia. *F. tularensis* is the etiological agent of tularemia in humans. Tularemia is a febrile, plague-like illness that is characterized by several distinct clinical manifestations that primarily result from ulceroglandular, oculoglandular, oropharyngeal, and pneumonic forms of disease (18). Ulceroglandular tularemia is the most common disease form and usually occurs following inoculation of *F. tularensis* into the skin via the bite of an infected arthropod or through the handling of infected animal carcasses. Ulceroglandular tularemia is characterized by an initial lesion at the site of infection, followed by flu-like symptoms, lymphadenopathy and systemic dissemination of *F. tularensis* in severe cases (18, 19). Oculoglandular tularemia is another relatively common disease manifestation that most commonly occurs following inoculation of *F. tularensis* into the eye following contact with contaminated water or raw meat, and is characterized by conjunctivitis and systemic dissemination of *F. tularensis* (18, 20). Oropharyngeal tularemia occurs following ingestion of contaminated water or meat, and is characterized by pharyngitis, lymphadenopathy, and diarrhea (18, 21). Compared to the

pneumonic form of disease, ulceroglandular, oculoglandular, and oropharyngeal forms of tularemia are relatively benign and rarely result in death.

Pneumonic tularemia is the most severe form of the disease. Like all forms of tularemia, disease severity is dependent on the inoculating dose and *Francisella* species responsible for the infection. Pneumonic infection with Type A *Francisella* strains is highly problematic, with untreated mortality rate estimates ranging from 20-60% following infection (22). The disease severity of pneumonic tularemia is compounded by the fact that as few as ten organisms can cause lethal disease, and that *F. tularensis* is easily aerosolized, facilitating inhalation of bacteria (23). For these reasons, *F. tularensis* was a significant component of former biological warfare programs in many countries, including the United States, Japan, and the former Soviet Union (22). Fears surrounding its use as a bioweapon continue to shape various aspects of science policy. Today, *F. tularensis* is designated as a Tier 1 Select Agent and Category A bioterrorism agent by the United States Centers for Disease Control and Prevention, one of just three bacteria to fall into both of these highly regulated categories (24).

II. Tularemia vaccine development.

Early attempts. Given the high infectivity of *F. tularensis* and the high rates of morbidity and mortality associated with tularemia, there has long been a recognized need for an effective tularemia vaccine. In the United States, early studies in search of a tularemia vaccine consisted of vaccinating volunteers with crude preparations of killed *F. tularensis*. These vaccine preparations were largely ineffective and led to a variety of adverse side effects (25, 26). Subsequent human studies using an acid-extracted and phenol-purified inactivated vaccine were inconclusive (27). Studies of similar vaccines in nonhuman primates revealed that killed vaccines did not prevent symptoms and conferred limited protection against highly virulent strains (28). Together, these early vaccine studies suggested that vaccination with killed or inactivated bacteria would not suffice, and suggested that effective vaccination against tularemia would likely require live, replicating bacteria.

The LVS. In 1956, the United States obtained an attenuated vaccine strain, the LVS, from the former Soviet Union. The LVS was derived from repeated in vitro and in vivo passage of a virulent *F. tularensis* subsp. *holarctica* strain (29). Since its isolation, the LVS has been extensively studied as a tularemia vaccine. Initial evaluation of the LVS as a vaccine was carried out by the United States Army in the late 1950's and 1960's. These studies consisted of vaccinating individuals via scarification prior to aerosol administration of the *F. tularensis* subsp. *tularensis* Schu S4 strain, which is a prototypical Type A *Francisella* strain used in many *F. tularensis* studies today. Scarification with the LVS protected against lethal subcutaneous challenge but was ineffective against high-dose aerosol challenge with the Schu S4 strain (25, 30). In subsequent studies, aerosol vaccination with the LVS improved vaccine efficacy, but increased the likelihood of developing tularemia independent of secondary challenge (31). Additionally, the genetic basis for the LVS's attenuation remains poorly understood. For these reasons, the LVS remains unlicensed as a vaccine in the United States. Despite this, the LVS has been used to vaccinate at-risk individuals in the United States Army's biomedical research labs, and is often used as a benchmark against which to compare new tularemia vaccines.

Subunit vaccines. Our incomplete understanding of the LVS and the need for a safe, effective tularemia vaccine has driven recent attempts at creating novel subunit vaccines composed of various *F. tularensis* components. Subunit vaccines are an intriguing option in the search for a safe, effective vaccine, as they are composed of noninfectious material and are of a defined composition. However, attempts at using crude *F. tularensis* outer membrane preparations, purified lipopolysaccharide (32), or a variety of immunogenic proteins have proven partially effective at best (33, 34). This observation, combined with the inability of previous killed vaccines to elicit protective immunity, suggests that an effective tularemia vaccine will likely be composed of multiple antigens and be able to elicit sustained cellular and humoral immune responses. In this regard, live, rationally attenuated *Francisella* vaccine strains may hold the most significant promise.

Live attenuated vaccines. Live attenuated vaccines have been used for successful vaccination against the bacterial pathogens responsible for typhoid fever, cholera, and tuberculosis (35, 36). Even for tularemia, the LVS remains one of the most effective vaccines to date. Recently, the search for a successful live vaccine against *Francisella* has accelerated.

The use of attenuated *F. novicida* mutants as live vaccines has been largely ineffective against Type A challenge, despite conferring protection against homologous challenge (37, 38). Early attempts at using LVS-derived mutants as vaccines conferred partial, route-dependent protection against Type A challenge, though levels of protection were similar to those conferred by the wildtype LVS. These LVS derivatives included mutants defective for capsule production (Δ*capB*), LPS biosynthesis (Δ*wbtA*), and antioxidant activity (Δ*sodB*), among others (39-43). On the other end of the *Francisella* virulence spectrum, several studies have recently examined the ability of attenuated Type A *F. tularensis* deletion mutants to confer protective immunity against aerosol challenge with virulent *F. tularensis*. These Type A mutant strains include strains lacking genes that contribute to capsule production (Δ*capB*), amino acid biosynthesis (Δ*aroD*), guanine biosynthesis (Δ*guaA*/Δ*guaB*), and stress tolerance (Δ*clpB*) (44-46). Studies using these strains, though limited in number, suggest that it is possible to use highly attenuated Type A mutants as live vaccines, but demonstrate that protection is modest, particularly following inhalational challenge. The fine balance between virulence and attenuation represents a major obstacle in the development of live vaccine strains, as many attenuated vaccine candidates are actually overattenuated, in that they are unable to persist within the host long enough to elicit significant immune responses. As a result, overattenuated mutant strains offer little in terms of adaptive immunity and are minimally effective (47-50). Together, these studies suggest that a safe, effective tularemia vaccine could be created using an *F. tularensis* derivative that is attenuated for virulence, but able to persist, spread, and elicit effective adaptive immune responses within the host.

III. *Francisella* pathogenesis and virulence mechanisms.

F. tularensis is a stealth, facultative intracellular pathogen, and many aspects of its life within the host are characterized by immune evasion. This is evident in human cases of tularemia, as well as in non-human primate and mouse models of tularemia, where little proinflammatory responses are observed during early stages of infection, despite high bacterial burden. The ability of *F. tularensis* to interfere with various aspects of host innate immune responses is critical to its ability to infect, replicate, disseminate, and cause disease. *F. tularensis* possesses virulence factors and other characteristics that allow bacteria to evade host responses before, during, and after infection of host cells. The current understanding of *F. tularensis* pathogenesis

and immunomodulatory capacity as it relates to the various stages of host cell infection is outlined below and summarized in Figure 1.2.

Extracellular immune evasion. The extracellular environment encountered by *F. tularensis* prior to infection of host cells is riddled with antibacterial components of the innate immune system, including antibodies, complement, and circulating immune sentinel cells. Normally, these innate immune components rapidly and efficiently respond to infection by direct bacterial killing and induction of inflammatory responses aimed at clearing the infection. Given the observation that induction of inflammatory responses following *F. tularensis* infection does not occur until 2-4 days post-infection (51-56), it is not surprising that *F. tularensis* possesses mechanisms which enable bacteria to evade extracellular immunity during infection. Two of the more well-characterized bacterial mechanisms of extracellular immune evasion include a tetra-acylated LPS and the ability of *F. tularensis* to evade complement-mediated lysis.

LPS is a major structural component of the Gram-negative outer membrane. LPS consists of a surface-exposed O-antigen polysaccharide, which is linked to membrane-embedded lipid A molecules via inner and outer core oligosaccharides. The LPS in most Gram-negative bacteria, such as *Escherichia coli*, contains a hexa-acylated lipid A which is recognized and bound by toll-like receptor 4 (TLR4) at the surface of host cells (57). TLR4 recognition of LPS leads to proinflammatory signaling and is a major contributing factor to the excessive inflammation seen during cases of sepsis (58, 59). *F. tularensis* effectively avoids LPS-TLR4 signaling and inflammation due to the presence of a non-reactogenic hypo-acylated lipid A, a bacterial modification which appears to be conserved in several Gram-negative pathogens (60-62).

In addition to avoiding extracellular LPS-TLR4 signaling, *F. tularensis* also effectively disrupts the bactericidal effects of the complement cascade. Complement is a critical component of the innate immune system. During bacterial infection, complement components serve to directly or indirectly kill invading bacteria (63). Direct complement-mediated bacterial killing results from the assembly of the pore-forming membrane attack complex (MAC) at the bacterial surface and subsequent bacteriolysis (63). MAC assembly relies on the sequential binding of complement components, including C3b, at bacterial surfaces. In one early *F. tularensis* study, the presence

of an exopolysaccharide capsule was linked to avoidance of MAC-mediated lysis (64-66). In addition to capsule-dependent complement evasion, *F. tularensis* avoids complement-mediated lysis by recruiting a host protease, factor H, to the bacterial surface (64). At the *F. tularensis* surface, factor H cleaves C3b into iC3b, which not only stops MAC assembly and prevents bacteriolysis, but also serves a role in facilitating the silent entry of *F. tularensis* into host cells via complement receptor 3 (CR3; discussed below) (67).

Invasion of host cells. *F. tularensis* is a facultative intracellular pathogen that prefers to replicate within the cytosol of host cells. Accordingly, the first step in the establishment of *F. tularensis* infection is entry into host cells. Due to the macrophage's well-established role in innate immunity, many studies have focused on the ability of *F. tularensis* to enter, survive inside, and replicate within macrophages. However, *F. tularensis* can invade and replicate within a wide variety of other cell types, including dendritic cells, monocytes, neutrophils, lung epithelial cells, hepatocytes, fibroblasts, endothelial cells, and erythrocytes, observations that underscore the high degree of *F. tularensis* flexibility during infection (68-74). Host receptors used by *F. tularensis* for entry include nucleolin and lung surfactant protein A (SPA), as well as CR3, mannose receptor (MR), scavenger receptor (SR), and Fcγ receptors (FcγR) (75-78). Receptor utilization depends primarily on the opsonization state of *F. tularensis*. Serum-opsonized bacteria primarily enter cells via CR3, and to a lesser extent, nucleolin, SPA, MR, and SRA, while antibody-opsonized bacteria enter primarily via FcγR (79). To date, the only host cell receptor linked to invasion of non-opsonized bacteria is MR (79). Utilization of host cell receptors for entry enhances *F. tularensis* uptake, and as is the case for CR3-mediated entry, reduces the secretion of proinflammatory cytokines, such as tumor necrosis factor alphpa (TNFα), interleukin-6, and interleukin-1-beta (IL-1β), which are normally secreted following bacterial entry into host cells (67, 79).

Phagosomal modification and escape. Following invasion into host cells, *F. tularensis* resides in a membrane-bound vacuole, the *Francisella*-containing phagosome (FCP). Once inside the FCP, *F. tularensis* actively disrupts various aspects of innate immunity that normally function to degrade newly phagocytosed pathogens. These *F. tularensis*-induced modifications include inhibition of the production and activity of reactive oxygen species and reactive nitrogen

species (ROS and RNS, respectively), and inhibition of phagosome-lysosome fusion, both of which are critical for the effective bactericidal function of phagosomes (80).

NADPH oxidase is a multiprotein complex that facilitates the conversion of molecular oxygen to the ROS, superoxide, and contributes to the formation of RNS at the phagosomal membrane (81, 82). NADPH oxidase-generated ROS/RNS are bactericidal, as they disrupt various aspects of normal bacterial function, including protein synthesis and DNA stability (82, 83). In studies using human neutrophils, *F. tularensis* was found to actively inhibit assembly of the ROS/RNS-generating NADPH oxidase complex at the FCP membrane through the action of the acid phosphatases AcpA/B/C and Hap (84). As an additional counteractive mechanism, *F. tularensis* encodes three antioxidant enzymes: a catalase (KatG), and two superoxide dismutase enzymes (SodB/C), which are all important for oxidative stress resistance (85-87). Recent work also highlighted the important role that amino acid transporters play in the ability of *F. tularensis* to evade ROS and escape from the FCP, as bacteria deficient for the glutamate transporter, GadC, were sensitive to ROS, did not escape from the FCP, and were avirulent (88).

A substantial portion of the phagosome's ROS/RNS-independent bactericidal function is dependent on fusion of phagosomes with lysosomes. Lysosomes are highly acidic organelles that contain luminal degradative enzymes and antimicrobial peptides such as cathepsins and cathelicidins, respectively (89). During *F. tularensis* infection of host cells, phagosome-lysosome fusion is not observed; FCP's do not acquire lysosomal markers or contain lysosomal hydrolases such as cathepsins (71, 90, 91). Instead, *F. tularensis* physically disrupts the FCP membrane and escapes into the host cell cytosol. The ability of *F. tularensis* to escape from the FCP into the cytosol is critical for its virulence, as bacterial replication occurs primarily within the cytosol. Recent work has highlighted several proteins encoded by *Francisella* pathogenicity island (FPI) genes as being important for *F. tularensis* escape into the cytosol, including IglA/B/C/D, MglA, FevR, and MigR (79, 92, 93). Several other proteins, distinct from those encoded by FPI genes, contribute to the ability of *F. tularensis* to escape from the phagosome. These proteins include acid phosphatases (AcpA/B/C and Hap), biosynthetic enzymes (CarA/B, PyrB) and proteins of unknown function (FTT1103 and FTT1676) (Figure 1.2) (79, 94, 95). However, precise characterization of the specific bacterial factors and mechanisms responsible

for inhibiting phagosome-lysosome fusion remains incomplete and is an area of active research in the field.

***F. tularensis* cytosolic replication.** Following escape from the FCP, *F. tularensis* enters the cytosol, a relatively permissive environment compared to the FCP. Even though *F. tularensis* spends the majority of its intracellular life within the cytosol, many mechanisms by which bacteria persist and replicate within host cells are poorly understood. This is partly due to the fact that internalization and phagosomal escape are prerequisites for cytosolic replication. As a result, many genetic approaches aimed at identifying genes required for intracellular replication also identify genes required for invasion and phagosomal escape. However, there have been several proteins identified that are specifically required for *F. tularensis* growth within the cytosol. These include biosynthetic proteins required for DNA synthesis (PurM/C/D), a transpeptidase required for cytosolic glutathione utilization (Ggt), and several proteins of unknown function (DipA, RipA, and FTT0989) (Figure 1.2) (48, 96-98).

Host cell death responses to *F. tularensis.* Following extensive cytosolic replication, *F. tularensis* triggers programmed death of infected cells. Host cell death responses to *F. tularensis* infection are characterized by caspase-3-mediated apoptosis and caspase-1-mediated pyroptosis (99). Pyroptosis is a form of programmed cell death that is initiated in response to the detection of cytosolic damage-associated molecular patterns, such as the presence of foreign DNA, RNA, and toxins (100). Pyroptotic responses to *F. tularensis* are initiated following release of DNA from dead or dying bacteria within the host cell cytoplasm and host sensing of this DNA via the cytosolic DNA sensor, absent in melanoma 2 (AIM2) (101, 102). Recognition of *F. tularensis* DNA by AIM2 triggers activation of caspase-1, cleavage and release of the proinflammatory cytokines IL-1β and interleukin-18 (IL-18), and pyroptotic cell death (101). Apoptotic cell death, on the other hand, is not inherently proinflammatory, in that apoptosis is not associated with the cleavage and release of cytokines. Apoptosis can be divided into two main pathways: the extrinsic and intrinsic pathways (Figure 1.3) (103). Apoptosis via the extrinsic pathway is initiated following external engagement of death receptors by ligands such as TNFα or Fas ligand, and is characterized by activation of caspase-8 (Figure 1.3) (103). The intrinsic apoptotic pathway is triggered following intracellular stresses that lead to mitochondrial damage, such as nutrient deprivation, DNA damage, or infection, and is

characterized by caspase-9 activation (Figure 1.3) (103). Importantly, the extrinsic and intrinsic apoptotic pathways both converge on caspase-3 activation, leading to nuclear condensation, DNA fragmentation, cleavage of various cellular proteins, including poly-ADP-ribose polymerase (PARP), and cell death.

To date, apoptotic responses to *F. tularensis* have been understudied compared to pyroptotic responses. The limited number of studies examining apoptosis during *F. tularensis* infection of host cells demonstrate that *Francisella* can actively delay induction of apoptosis in infected macrophages and neutrophils (104-106). Notably, infection of mice with fully virulent Type A *F. tularensis* results in extensive activation of caspase-3, but minimal activation of caspase-1 (107). Additionally, infection of caspase-1/11-deficient mice with Type A *F. tularensis* leads to pathological changes similar to those observed during infection of WT mice (99, 107), and a role for caspases -1 and -11 in immunity against *Francisella* has only been confirmed using attenuated or lower virulence strains such as the LVS or *F. novicida* (101, 102, 108, 109). In contrast, infection of caspase-3-deficient mice with Type A *F. tularensis* results in lower levels of macrophage cell death and increased spread of bacteria within infected livers compared to infection of WT mice (99, 107). Together, these results suggest a central role for apoptosis in the pathogenesis of tularemia and highlight the importance of studying apoptotic responses during infection (Figure 1.4) (99, 107).

While the ability of *F. tularensis* to prevent induction of pyroptosis during cytosolic replication appears to be due primarily to maintenance of bacterial structural integrity (93, 110), the mechanisms by which *F. tularensis* inhibits apoptotic responses during early stages of cytosolic replication are not characterized. *F. tularensis* replication within the cytoplasm eventually triggers host cell lysis and the release of intracellular bacteria for additional rounds of infection (Figure 1.2). The ability of *F. tularensis* to invade, survive, and replicate within host cells prior to host cell death is critical for its virulence. Despite significant advances in our understanding of the bacterial factors responsible for facilitating certain aspects of these critical processes, many questions remain unanswered. Specifically, the mechanisms by which *F. tularensis* secretes proteins to evade intracellular immune responses, including induction of host cell death, is poorly understood. To address this fundamental gap in knowledge, our lab began investigating protein secretion mechanisms of *F. tularensis*.

***Francisella* secretion systems.** Gram-negative bacteria encode a variety of specialized protein secretion systems that facilitate the transport of proteins across the Gram-negative double membrane. These secretion systems transport proteins in two general ways. Some secretion systems, including the type II, V, and chaperone-usher systems, transport proteins in a stepwise fashion across the inner membrane (IM), into the periplasm, and across the outer membrane (OM) (Figure 1.5). Other secretion systems, including the type I, III, IV, and VI systems, directly transport proteins from the bacterial cytosol into the extracellular environment in a single step (Figure 1.5). Additionally, all Gram-negative bacteria examined to date release OM-derived, protein-containing vesicles from their surface (111). Importantly, secretion systems and the effector proteins secreted through these systems are critical for the ability of many pathogens to cause disease.

The first *F. tularensis* genome was sequenced in 2005 (112). Given our lab's interest in Gram-negative protein secretion and the gap in knowledge surrounding *F. tularensis* protein secretion mechanisms, we examined the *F. tularensis* genome for the presence of protein secretion systems. This analysis revealed that *F. tularensis* lacks many secretion systems commonly used by intracellular pathogens, including the type III and type IV systems, to deliver virulence factors into host cells. At the time, our analysis indicated that *F. tularensis* encoded a type II-like secretion system responsible for assembling type IV pili at the bacterial surface (113), and a type I secretion system (T1SS; discussed below) (114). More recently, our lab demonstrated a role for OM vesicles in *Francisella* protein secretion and delivery to host cells (115), and other groups identified a type VI secretion system encoded by FPI genes (92). The finding that *F. tularensis* – a facultative intracellular pathogen – does not encode either the type III or IV secretion systems is surprising. Type III secretion systems are used by many intracellular pathogens, such as *Yersinia*, *Salmonella*, and *Shigella*, to deliver effector proteins directly into host cells during infection. Similarly, type IV secretion systems are employed by *Legionella*, *Bordetella*, and *Helicobacter*, among others, to facilitate intracellular bacterial growth and survival. Given the lack of type III and IV systems, our lab began examining the contributions of TolC, the OM component of the T1SS, to *F. tularensis* virulence.

IV. The type I secretion system.

Overview. Type I secretion systems consist of three proteins: a periplasm-spanning OM pore protein, an IM ATP-binding cassette (ABC) pore protein, and a IM/periplasmic membrane fusion protein (MFP) (Figure 1.6). The prototypical and most well-studied T1SS facilitates the secretion of α-hemolysin (HlyA) from *E. coli*, and is composed of the OM pore protein, TolC, the IM-ABC protein, HlyB, and the MFP, HlyD (116, 117). In addition to its role in protein secretion via the type I pathway, TolC participates in multidrug efflux (Figure 1.6). Multidrug efflux machineries are similar to the T1SS in that they consist of three proteins: an IM transporter, MFP, and OM pore protein (118). In contrast to the T1SS, most multidrug efflux systems export various drugs and harmful small molecules in an ATP-independent manner, and instead rely on H^+ motive force to facilitate efflux (118, 119). Importantly, the role of TolC in multidrug efflux is independent of its role in type I protein secretion and is dependent on specific interactions with multidrug efflux-specific MFP's and IM transporters, such as AcrA and AcrB (120, 121) (Figure 1.6).

Structure. Crystal structures for different protein components of the *E.coli* T1SS and multidrug efflux systems, including TolC, have been solved (122). TolC is a homotrimeric protein consisting of 55 kDa monomers. Together, three TolC monomers form a membrane-spanning "channel-tunnel", with two distinct domains: an OM β-barrel pore domain, and a periplasmic α-helical tunnel domain (Figure 1.6) (122). The periplasmic domain of TolC interacts with both the MFP and IM-ABC protein during secretion of proteins. HlyB is the prototypical IM-ABC protein involved in the secretion of HlyA via the type I pathway (Figure 1.6). HlyB is thought to function as a dimer, with two transmembrane domains forming a pore through the IM, and two cytosolic nucleotide binding domains that are involved in ATP hydrolysis and direct recognition of proteins targeted for secretion (123). Finally, HlyD is a homohexameric protein that is anchored in the IM, though the majority of the protein is periplasmic. HlyD locks the TolC-HlyB complex in place during the secretion process, thus completing the assembly of the channel from the cytoplasm to the external environment (124).

Secretion mechanism. During protein secretion via the type I pathway, a contiguous channel is formed from the bacterial cytosol to the external environment to allow for protein export. As it

is the most well characterized T1SS, mechanistic aspects of HlyA secretion from *E. coli* will be discussed below. In its inactive state, the membrane-embedded pore domain of TolC is open to the external environment, while the periplasmic α-helical tunnel is closed at the IM side (122). Additionally, HlyD and HlyB form a stable complex at the IM in the absence of TolC (125, 126). Though the exact mechanisms of protein secretion via the type I pathway are not completely understood, recent work has clarified several key steps in the translocation process. Secretion is initiated when the C-terminal secretion signal (discussed below) of a substrate protein, such as HlyA, is recognized and bound by cytoplasmic regions of an IM-ABC protein, such as HlyB (125) (127). This binding event causes a conformational change in the HlyB-HlyD complex and allows for TolC interaction with the complex (124). Additional studies examining the interaction of TolC with MFP's, such as AcrA or HlyD, demonstrated that specific TolC-MFP interactions are dependent on conserved RXXXLXXXXXX[T/S] (RLT/RLS) amino acid motifs on the MFP during secretion or efflux (128). Interaction of the MFP/IM-ABC complex with TolC leads to the formation of an envelope-spanning secretion channel. Following channel formation, ATP hydrolysis by IM-ABC proteins, such as HlyB, drives secretion of unfolded effector proteins through TolC into the extracellular environment.

T1SS effectors. The T1SS is responsible for the export of a wide variety of proteins from many phylogenetically distant Gram-negative organisms (Table 1.1). Identification of effector proteins has led to a general consensus with regard to their physical and biochemical makeup. Most T1SS effectors are members of the repeat-in-toxin (RTX) family of proteins, which contain a variable number of repeating GGXGXDXUX amino acid motifs (129). Additionally, most T1SS effectors have few cysteine residues and have low pI values of around 4 (130). Though not completely understood, recent work examining C-terminal amino acid sequences of T1SS effectors suggests that the last 50-60 amino acids of effectors represent a secretion signal that targets the protein to the IM ABC transporter to initiate the secretion process (131-134). The presence of a C-terminal secretion signal is supported by the fact that chimeric proteins containing the last 60 amino acids of HlyA are secreted via the T1SS (133). Despite the general consensus for the presence of a C-terminal signal sequence, analysis of primary amino acid sequences reveals little insight into the signal, as minimal primary sequence homology is observed between the C-termini of known effectors (130). Together, these observations lead to a model where the C-terminal secretion signal forms a distinct secondary structure, which can be recognized and bound specifically by the IM ABC to initiate the secretion process (130, 135).

To date, no *F. tularensis* T1SS effectors have been identified. Identification of these effectors is an active area of research in the lab and will be discussed in Chapter 5.

V. Contributions of TolC to *Francisella* virulence.

TolC is critical for the secretion of proteins via the type I pathway. Bioinformatic analysis of the *F. tularensis* genome identified two proteins, TolC and FtlC, as homologous to the *E. coli* TolC protein (114). To begin to investigate the role of type I protein secretion in *Francisella*, virulence, our lab constructed LVS Δ*tolC* and Δ*ftlC* deletion mutants (114). These mutants exhibited no growth defects in a variety of media commonly used for *F. tularensis* cultivation. Importantly, whereas both the LVS Δ*tolC* and Δ*ftlC* mutants contributed to multidrug efflux, only the Δ*tolC* mutant showed virulence defects. This previously published work is summarized below.

TolC is a critical LVS virulence factor in mice. Our lab previously demonstrated that TolC is critical for the virulence of the LVS in intranasal and intradermal mouse models of infection, as mice infected with a LVS Δ*tolC* mutant exhibited increased survival compared to those infected with the wild-type (WT) LVS (Figure 1.7A) (114, 136). This work also demonstrated that the WT LVS and Δ*tolC* mutant induce similar pathology in infected organs, and are both able to spread systemically from the site of infection (136). However, the Δ*tolC* mutant colonized organs at lower levels compared to the WT LVS and replicated to lower levels within these organs compared to the WT (Figure 1.7B) (136). Subsequent examination of murine bone marrow-derived macrophages (BMDM) infected with the WT LVS or Δ*tolC* mutant revealed a similar replication defect for the Δ*tolC* mutant (Figure 1.8) (114). Together, these early studies demonstrated that TolC is a virulence factor of the LVS that may be important for facilitating efficient intracellular replication during infection.

The LVS Δ*tolC* mutant is hypercytotoxic to host cells and elicits increased secretion of proinflammatory cytokines from human cells compared to the WT. To further investigate the molecular basis for the LVS Δ*tolC* mutant's virulence attenuation in mice and decreased

replication within host cells, as well as to identify potential differences in the immune responses of cells infected with the WT LVS or the Δ*tolC* mutant, our lab conducted a series of cell culture-based experiments. Using the release of a cytosolic enzyme, lactate dehydrogenase (LDH), as a readout for cell death, our lab determined that the Δ*tolC* mutant was hypercytotoxic to BMDM and human monocyte-derived macrophages (MDM) when compared to cells infected with the WT LVS (Figure 1.9) (136). Subsequent studies indicated that the Δ*tolC* mutant's hypercytotoxicity was associated with increased activation of caspase-3 and occurred independently of caspase-1 (Figure 1.10) (136). Since completion of the experiment shown in Figure 1.10A, it was demonstrated that the caspase-$1^{-/-}$ mice used therein are also deficient in caspase-11 expression (137), demonstrating that the Δ*tolC* mutant's hypercytotoxicity also occurs independently of caspase-11. Additionally, further investigation using human MDM demonstrated that infection with the LVS Δ*tolC* mutant elicited increased secretion of the proinflammatory cytokines monocyte chemotactic protein-1, interleukin-8, and interleukin-1-beta (IL-1β), compared to secretion from MDM infected with the WT (Figure 1.11) (136). Together, these results indicated that TolC is a critical LVS virulence factor that functions to dampen host cell death and proinflammatory responses during infection.

Based on the established role of TolC in protein secretion from Gram-negative bacteria, the absence of many secretion systems in *F. tularensis*, and the established role for TolC in the virulence of the LVS, we hypothesized that TolC facilitates secretion of effector proteins aimed at inhibiting host innate immune responses during infection. Additionally, we hypothesized that the differential immune responses triggered during infection with the Δ*tolC* mutant would lead to enhanced adaptive immune responses compared to those seen following infection with the WT LVS. This dissertation details my work on the role of TolC during *F. tularensis* infection. **The following studies consisted of three specific aims: i. Determining the mechanism of TolC-mediated inhibition of host cell death during infection; ii. Evaluating the LVS Δ*tolC* mutant as a live attenuated tularemia vaccine; and iii. Characterizing the contribution of TolC to virulence of the human pathogenic Schu S4 strain.**

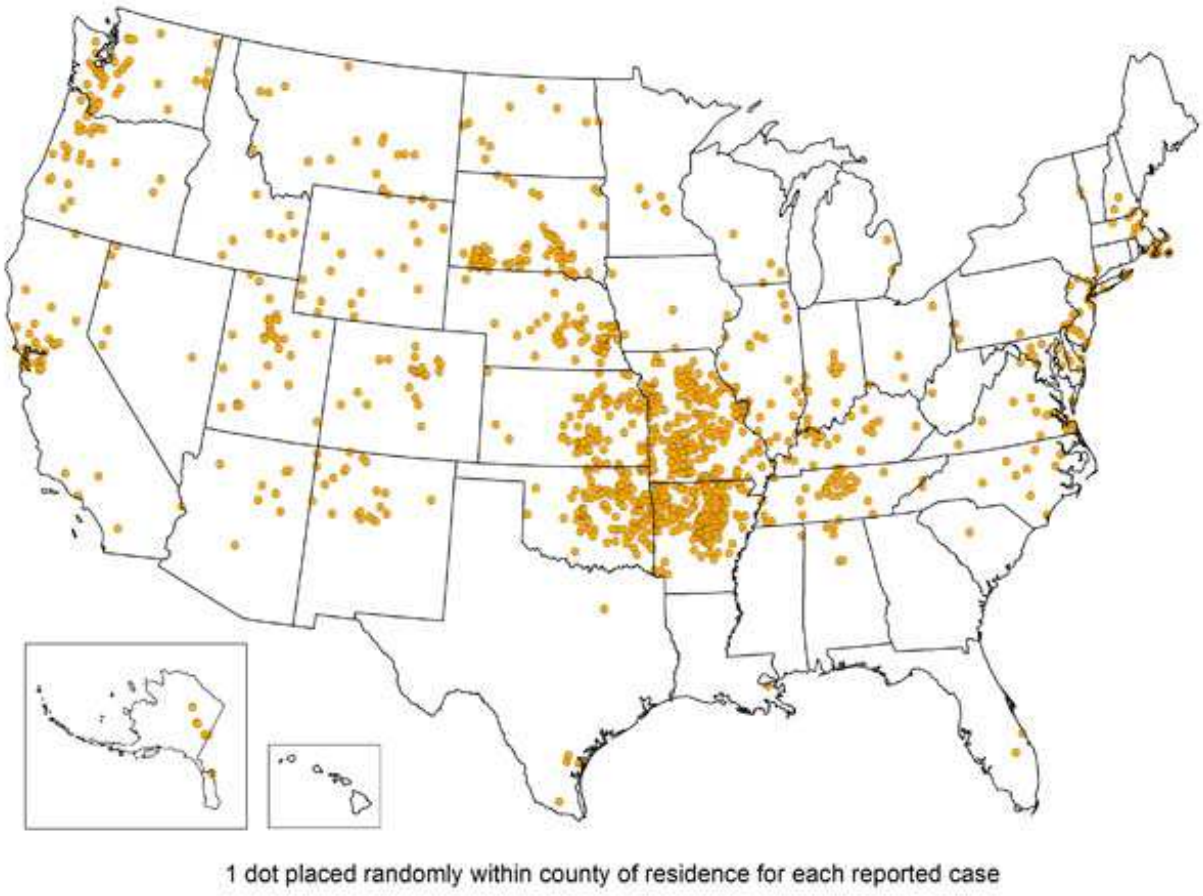

Figure 1.1: Incidence of tularemia in the United States: 2003-2012. Map showing the distribution of confirmed cases of tularemia in the United States from 2003-2012. Tularemia has been reported in all states except Hawaii, with foci in the northwest, midwest, and Martha's Vineyard areas. One dot represents one tularemia case. Figure is reprinted with permission from the US Centers for Disease Control and Prevention.

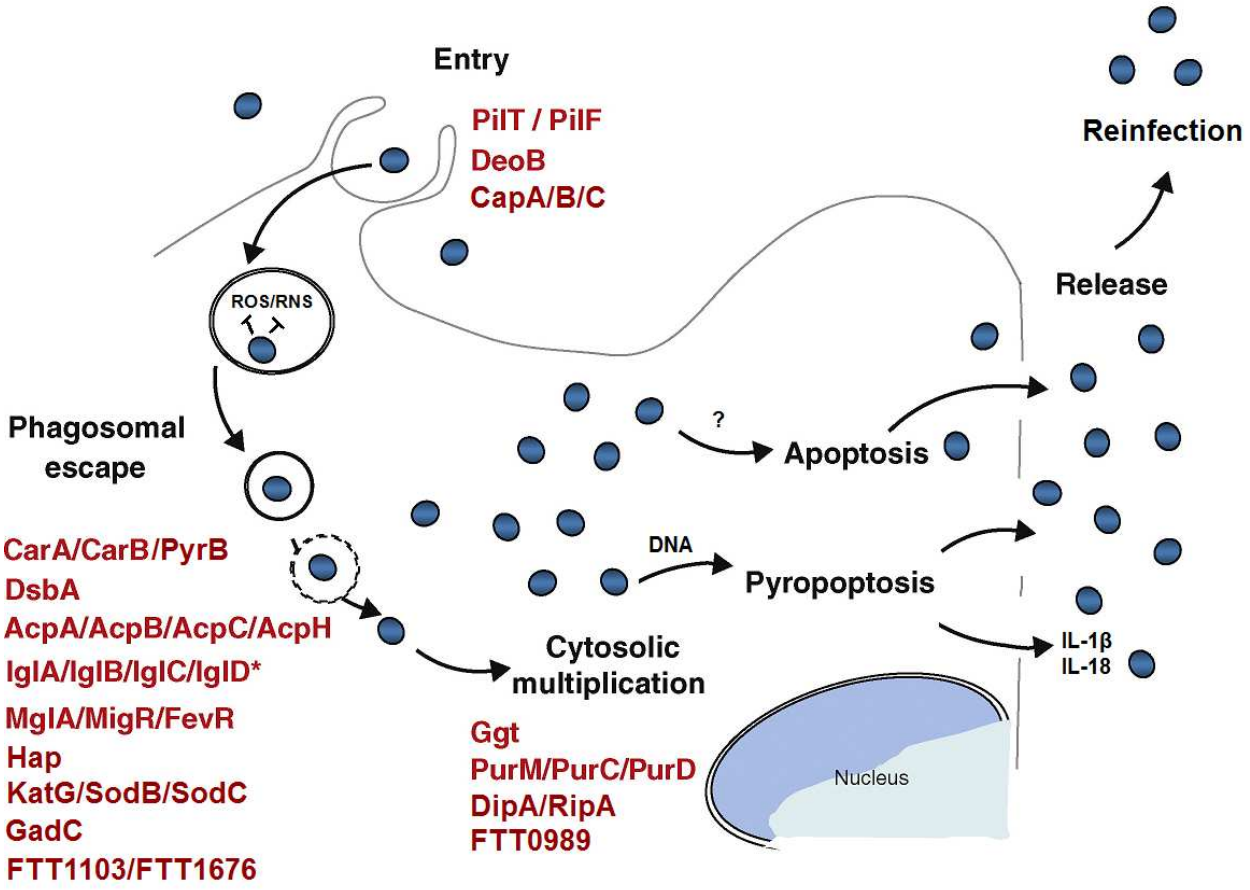

Figure 1.2: Virulence factors and their contribution to the *F. tularensis* intracellular lifecycle. Proteins identified to be important for various aspects of the F. *tularensis* intracellular lifecycle are outlined. Figure adapted and reprinted with permission from (95).

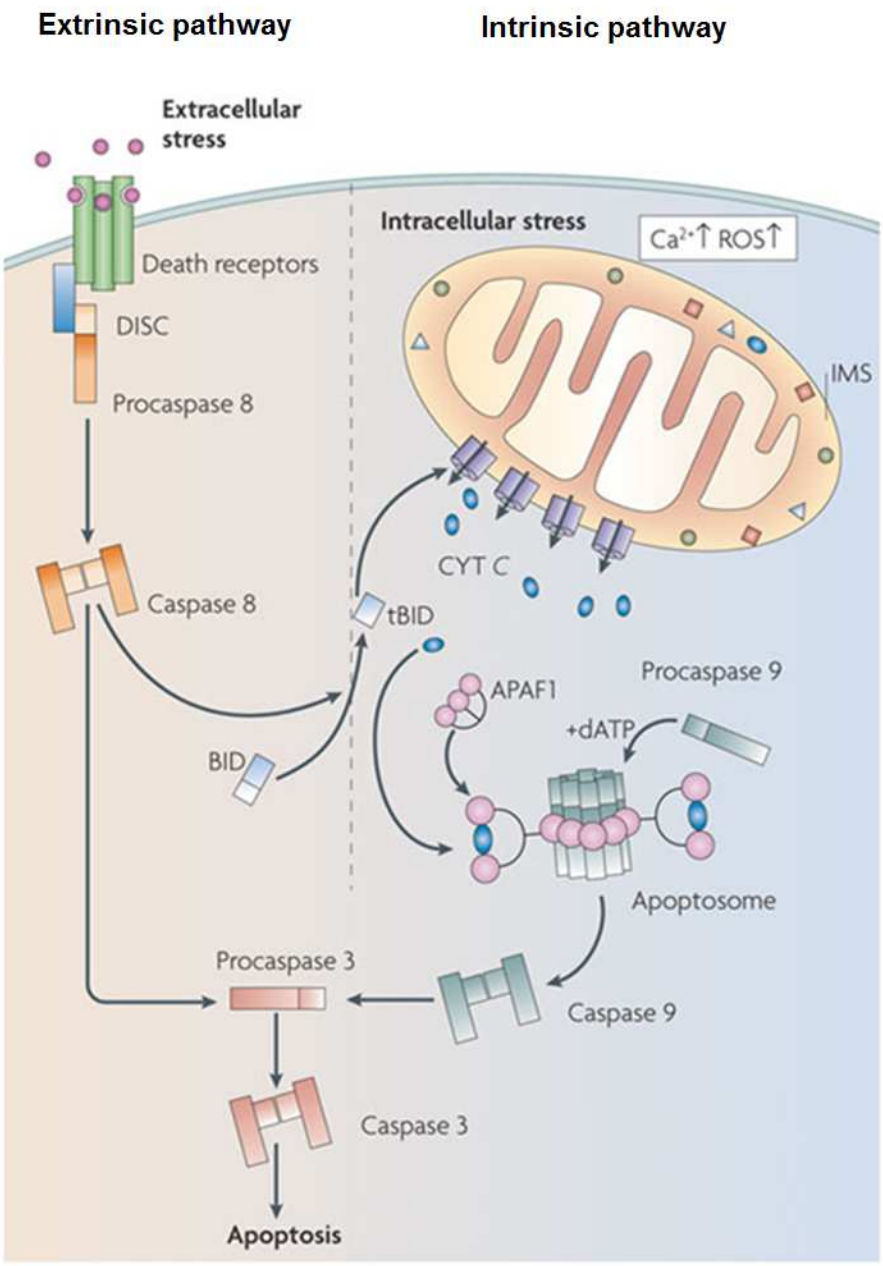

Figure 1.3: Overview of apoptosis. Apoptosis is a form of programmed cell death initiated in response to a variety of external or internal stimuli. The extrinsic apoptotic pathway is activated following stimulation of death receptors and is characterized by caspase-8 activation. The intrinsic apoptotic pathway is activated in response to intracellular stress and is characterized by activation of caspase-9. Both pathways converge on activation of caspase-3 and apoptosis. Adapted and reprinted with permission from (138).

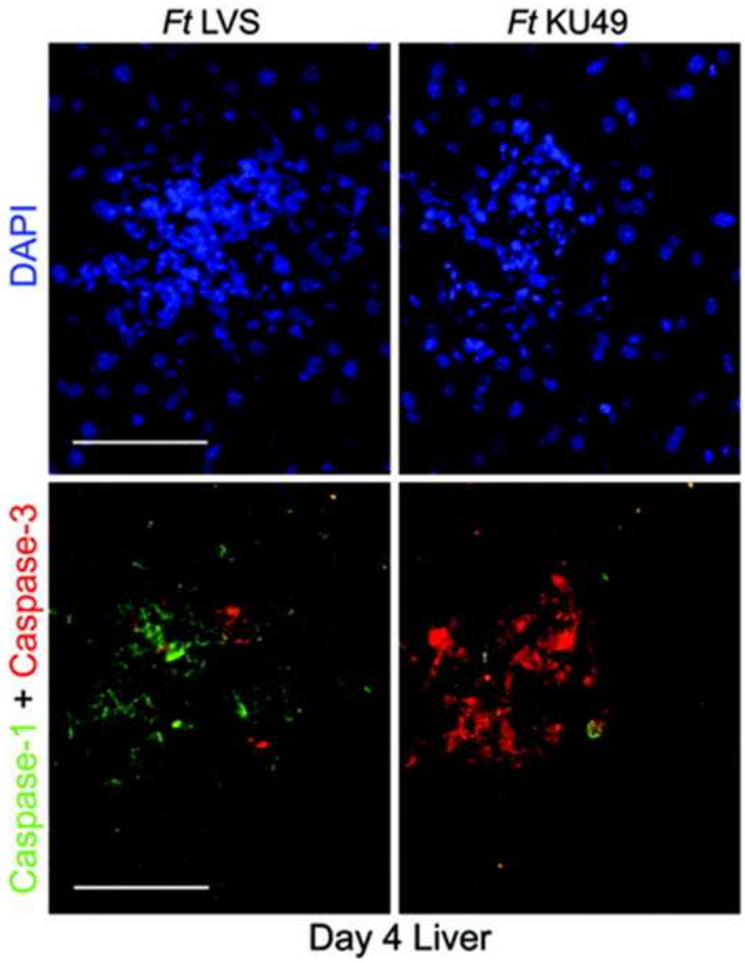

Figure 1.4: Programmed cell death during *F. tularensis* infection. Mice were infected intranasally with 5.5 x 10^3 CFU of the attenuated LVS or 38 CFU of the Type A, human pathogenic KU49 strain. Livers were collected 4 days post-infection and analyzed by immunofluorescence for the presence of cleaved caspase-1 and -3. Upper images show DAPI staining of nuclei (blue), whereas the lower images show the distribution of cleaved caspase-1 (green) and cleaved caspase-3 (red). Image is reprinted with permission from (107).

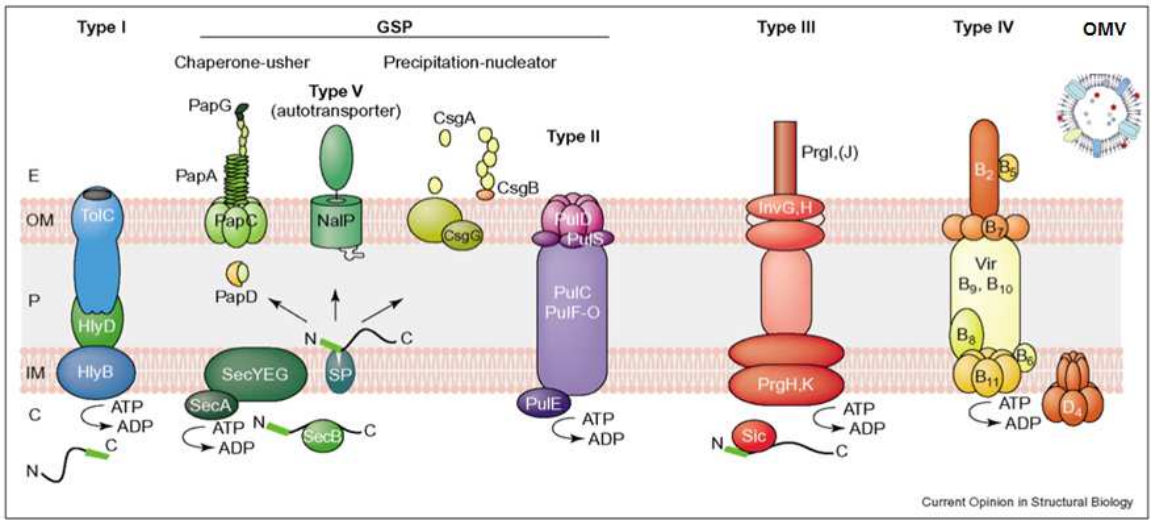

Figure 1.5: Protein secretion from Gram-negative bacteria. The cell wall of Gram-negative bacteria contains an inner and outer lipid bilayer membrane (IM and OM), which complicates the secretion of proteins from the bacterial cytoplasm to the external environment. To overcome this problem, bacteria encode a variety of specialized protein secretion systems, shown above. These systems specifically transport proteins from bacteria into the extracellular environment either directly (Type I, III, IV, and VI), or following initial transport of proteins into the periplasm (Type II, V, and chaperone-usher). In addition to the more well-characterized secretion systems, outer membrane vesicles (OMV) may specifically transport proteins from bacteria. The recently characterized Type VI secretion system is not shown. Adapted and reprinted with permission from (139).

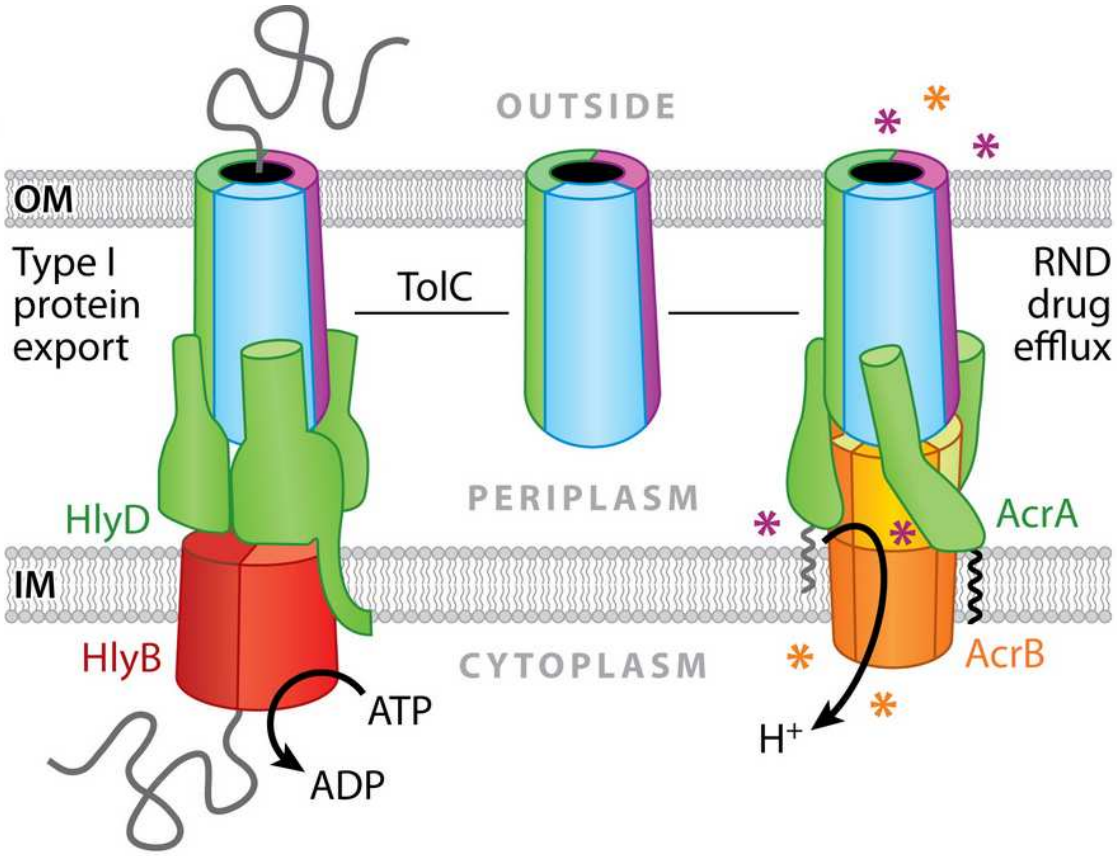

Figure 1.6: Type I protein secretion and multidrug efflux systems. TolC is a periplasm-spanning pore protein embedded in the outer membrane of many Gram-negative bacteria, including *F. tularensis*. TolC is involved in drug efflux and protein secretion via the type I pathway. In the model shown above, *E. coli* HlyA is secreted through TolC following interaction with the inner membrane ATP binding cassette transporter, HlyB, and subsequent HlyD conformational change-dependent channel formation. The drug efflux system is analogous to the type I secretion system, in that it relies on TolC interaction with two inner membrane adapter proteins, shown here as AcrA and AcrB, to form a contiguous channel for efflux. Figure is reprinted with permission from (130).

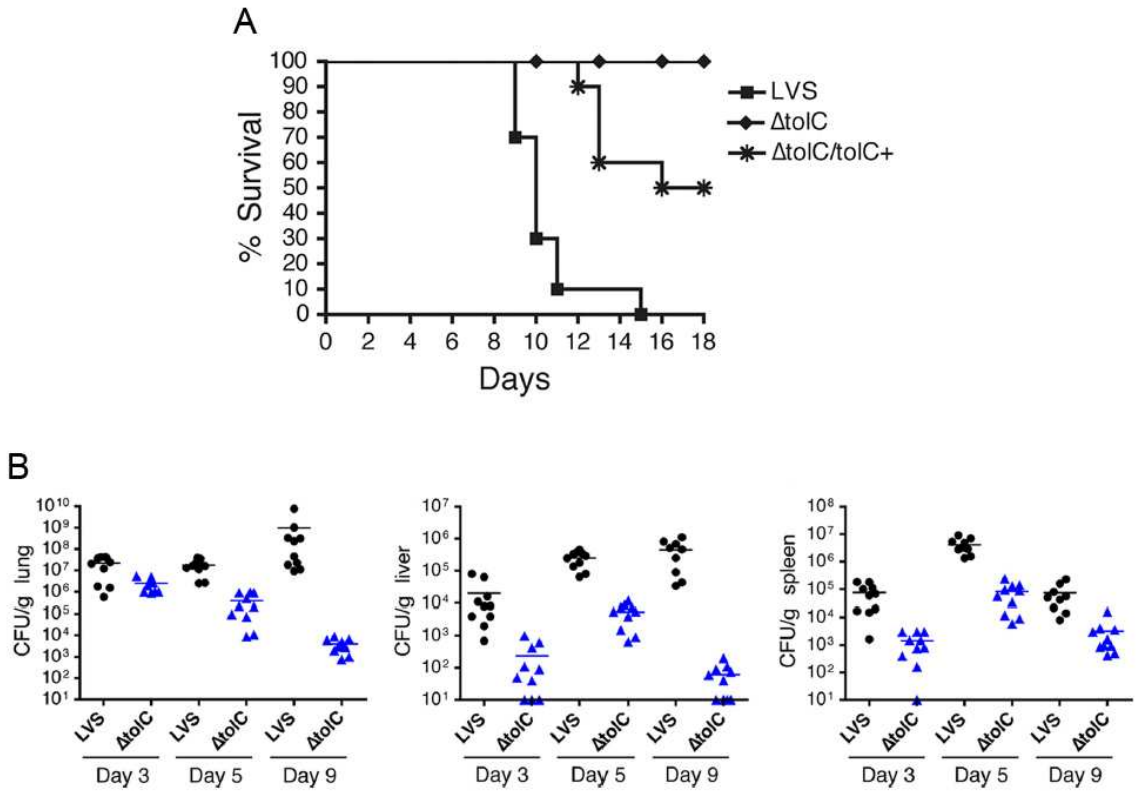

Figure 1.7: The LVS Δ*tolC* mutant is attenuated for virulence in mice and colonizes organs to lower levels than the WT. (A) Mice were infected intranasally with 1 x 10^5 CFU of the WT LVS, Δ*tolC* mutant, or Δ*tolC*/*tolC*+ complemented strain. Mice were monitored for survival for 18 days post-infection. **(B)** Mice were infected intranasally with 5 x 10^3 CFU of the WT LVS or Δ*tolC* mutant. At the indicated times post-infection, lungs, livers, and spleens were harvested and analyzed for bacterial burden. Burdens are shown in CFU/g tissue. Figures are reprinted with permission from (136).

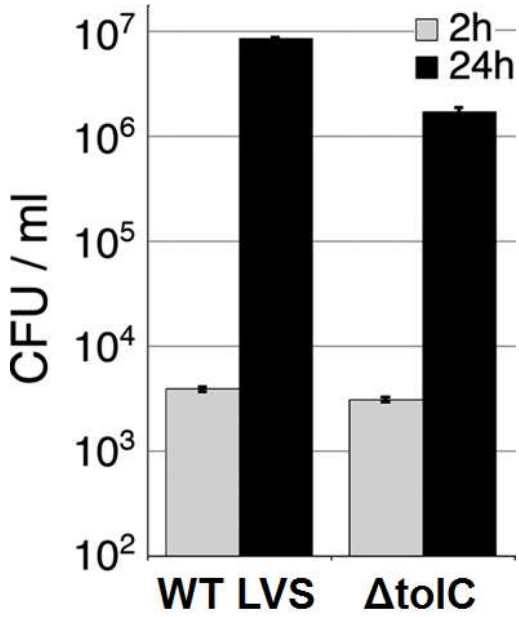

Figure 1.8: The LVS Δ*tolC* mutant replicates to lower levels within BMDM compared to the WT. BMDM were infected with the WT LVS or the Δ*tolC* mutant an MOI of 50. Intracellular bacteria were quantified 2 or 24 hours post-infection and are expressed in CFU/ml. Error bars indicate standard deviations of triplicate samples. The Δ*tolC* mutant consistently showed a slight replication defect at 24 hours compared to the WT LVS ($P < 0.01$; unpaired analysis of variance and Tukey–Kramer multiple comparison post-test). Figure is reprinted with permission from (114).

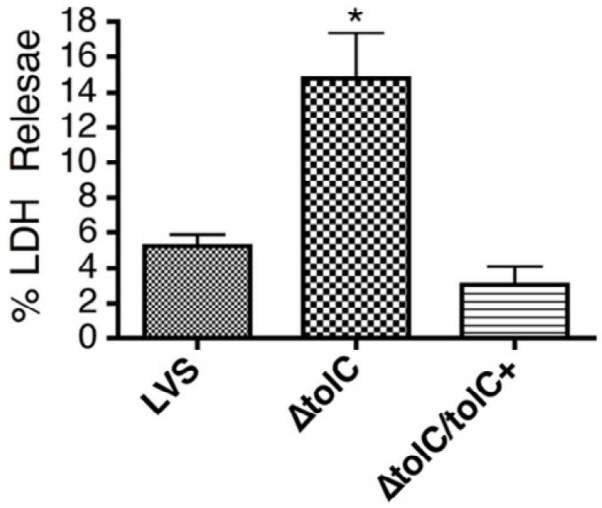

Figure 1.9: The LVS Δ*tolC* mutant is hypercytotoxic to BMDM compared to the WT. BMDM were infected with the WT LVS, Δ*tolC* mutant, or Δ*tolC*/*tolC*+ complemented strain at an MOI of 50. Cytotoxicity to BMDM was determined via LDH release 24 hours post-infection. Bars represent means ± SEM of three independent experiments. The Δ*tolC* mutant caused significantly increased LDH release compared to that of the wild-type LVS ($P < 0.05$). Figure is reprinted with permission from (136).

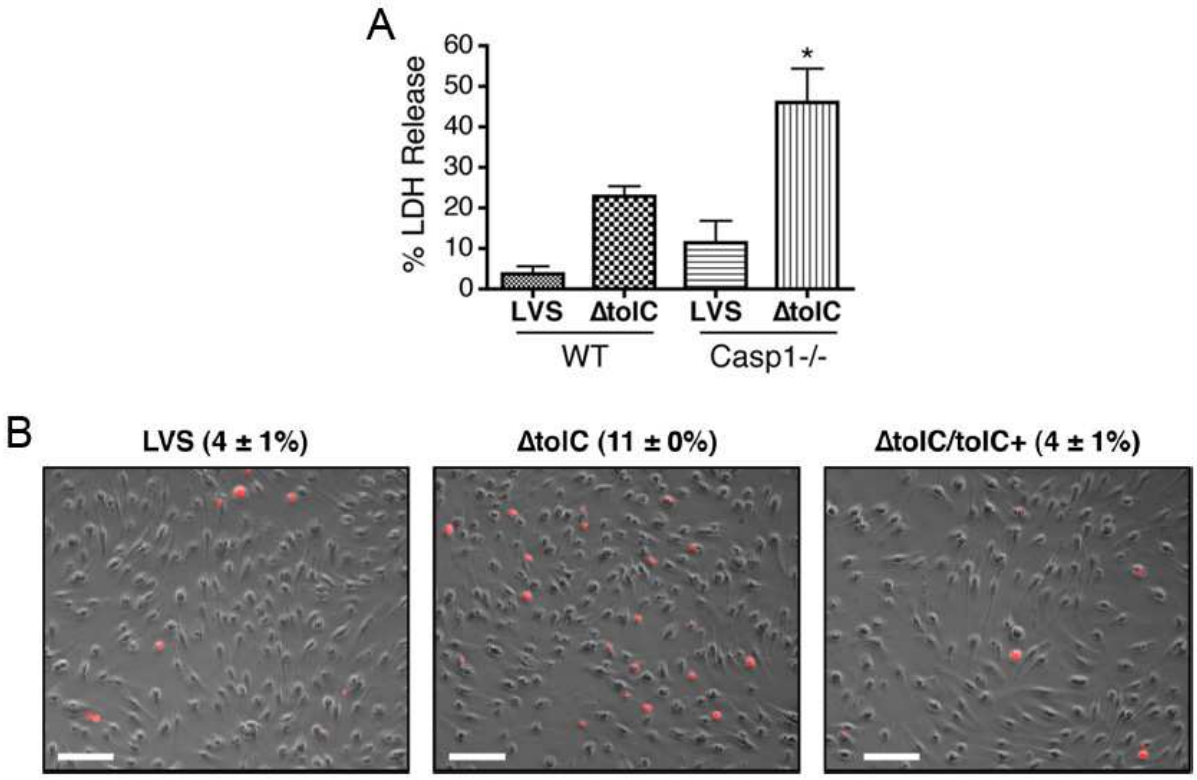

Figure 1.10: Hypercytotoxicity of the LVS Δ*tolC* mutant to BMDM is independent of caspases-1/11 and is associated with increased caspase-3 activation compared to the WT. (A) BMDM from WT or caspase-1/11$^{-/-}$ mice were infected with the WT LVS or Δ*tolC* mutant at an MOI of 50. Cytotoxicity to BMDM was determined via LDH release 24 hours post-infection. A representative experiment is shown. **(B)** BMDM were infected with the WT LVS or Δ*tolC* mutant at an MOI of 50. 17 hours post-infection, cells were fixed and labeled with an anti-cleaved caspase-3 antibody, and visualized with a TRITC-conjugated secondary antibody. Images show overlays of caspase-3-positive cells (red) and corresponding phase-contrast images. The percentages of caspase-3-positive cells ± SEM were calculated from 10 separate fields and represent the averages from three independent experiments. The Δ*tolC* mutant caused significantly increased staining compared to that of the wild-type LVS ($P < 0.05$). Bars = 50 µm. Figures are reprinted with permission from (136).

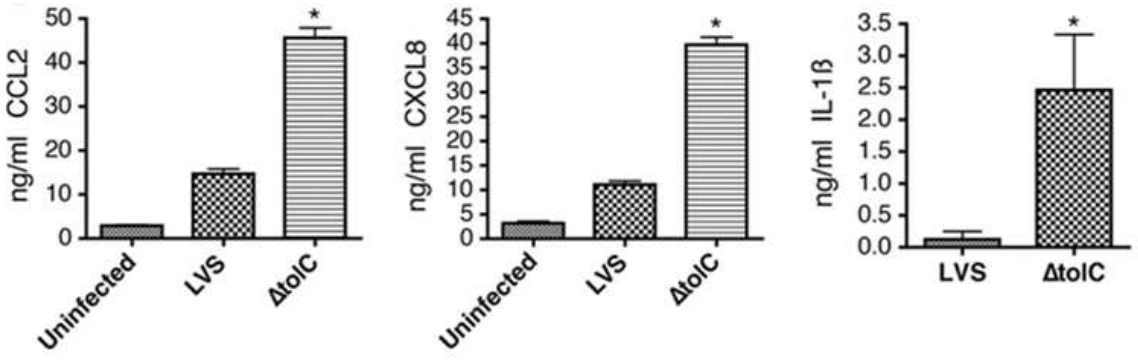

Figure 1.11: The LVS Δ*tolC* mutant elicits increased secretion of proinflammatory cytokines from human MDM compared to the WT. Human MDM were infected with the WT LVS or the Δ*tolC* mutant at an MOI of 25. 24 hours post-infection, the amounts of CCL2, CXCL8, and IL-1B in cell culture supernatants were quantified by ELISA. Bars represent means ± SEM from two experiments with three replicate samples each. The Δ*tolC* mutant caused the significantly increased secretion of the proinflammatory chemokines compared to that of the WT (*, $P < 0.05$). Figure is reprinted with permission from (136).

Table 1.1: Characteristics of known T1SS effector proteins.

Function	Protein Name	Organism	Length (aa)	Reference
Hemolysin	Apx1A	*Actinobacillus pleuropneumoniae*	1022	(140)
	HlyA	*Escherichia coli*	1024	(141)
Bacteriolysin	ColV	*Escherichia coli*	103	(142)
Leukotoxin	LktA	*Mannheimia haemolytica*	953	(143)
	LtxA	*Aggregatibacter actinomycetemcomitans*	1055	(144)
Enterotoxin	StiI	*Escherichia coli*	48	(145)
Protease	AprA	*Pseudomonas aeruginosa*	479	(146)
	ZapA	*Proteus mirabilis*	491	(147)
	PrtA	*Serratia marcescens*	472	(148)
	PrtA/B/C/G	*Erwinia chrysanthemi*	472-481	(149)
Lipase	LipA	*Serratia marcescens*	613	(150)
	TliA	*Pseudomonas fluorescens*	476	(151)
RTX/Cytoskeletal disruption	RtxA/MARTX	*Vibrio cholerae*	4558	(152)
RTX/Adhesin	TosA	*Escherichia coli*	1610	(153)
Adhesin	SiiE	*Salmonella enterica*	595	(154)
	LapA	*Pseudomonas fluorescens*	8682	(155)
S-layer protein	RsaA	*Caulobacter crescentus*	1026	(156)
	CsxA	*Campylobacter rectus*	1123	(157)
	SlaA	*Serratia marcescens*	259	(158)
Heme-binding	HasA	*Serratia marcescens*	188	(159)
Adenylate cyclase	CyaA	*Bordetella pertussis*	1737	(160)
Unknown	FrpA	*Neisseria meningitidis*	1115	(161)
	TRP47	*Ehrlichia chaffeensis*	285	(162)
	TRP32	*Ehrlichia chaffeensis*	198	(162)
	TRP120	*Ehrlichia chaffeensis*	548	(162)
	Ank200	*Ehrlichia chaffeensis*	1463	(162)
	RARP-1	*Rickettsia typhi*	586	(163)

CHAPTER 2: Materials and methods.

Bacteria and growth conditions. The *F. tularensis* LVS (ATCC 29684; Dr. Karen Elkins), Schu S4 (BEI Research Resources Repository, Manassas, VA), and derivatives of each strain were grown on Chocolate II agar plates (BD Biosciences) or in modified Mueller-Hinton broth (MHB; Mueller-Hinton broth [BD Biosciences] containing 1% glucose, 0.025% ferric pyrophosphate, and 0.05% L-cysteine HCl) (164), unless otherwise noted. The *F. tularensis* LVS Δ*tolC* strain was described previously (114). All *F. tularensis* Schu S4 mutants and complemented strains are described below. All growth and manipulations of the *F. tularensis* Schu S4 strain were performed under biosafety level 3 (BSL3) conditions.

Genetic manipulation of bacteria. The Schu S4 Δ*tolC*, Δ*ftlC*, and Δ*silC* deletion mutants were made using a two-step allelic exchange protocol developed by LoVullo *et al.* (165). Briefly, PCR products corresponding to regions of chromosomal DNA directly upstream and downstream of *tolC* (FTT1724), *ftlC* (FTT1095c), or *silC* (FTT1258) were amplified, ligated together using GC overlap PCR (166), and cloned into the pMP812 suicide vector to make pMP812-Δ*tolC,* pMP812-Δ*ftlC,* and pMP812-Δ*silC*. The PCR primers used to amplify all upstream and downstream regions are listed in Table 2.2. These pMP812-based plasmids were electroporated into electrocompetent Schu S4, prepared as previously described (68). Transformants were selected on kanamycin (5 µg/ml), grown overnight in the absence of antibiotics, and then plated onto solid media containing 8% sucrose. Sucrose-resistant colonies were screened via colony PCR using the primers listed in Table 2.2 for the presence or absence of the *tolC*, *ftlC*, or *silC* gene.

For unmarked chromosomal complementation of the Δ*tolC* and Δ*ftlC* deletion strains, deleted genes were reinserted into the chromosome at the *att*Tn7 site downstream of the conserved *glmS* gene (165). Briefly, the transposase-encoding shuttle plasmid pMP720 was electroporated into each deletion mutant and transformants were selected on hygromycin (200 µg/ml). The *tolC* and *ftlC* genes were amplified and separately cloned into pMP749 to make pMP749-*tolC*$^{+}$ and pMP749-*ftlC*$^{+}$. These pMP749-based plasmids were electroporated into the corresponding Schu S4 Δ*tolC* or Δ*ftlC* deletion mutants containing pMP720, and transformants were selected on kanamycin. For each gene complementation, a single kan^{R} colony was grown overnight in the absence of antibiotics and then plated onto kanamycin. Kan^{R} colonies were then screened for hygromycin sensitivity via replica plating, indicating loss of pMP720. These

colonies were then screened via colony PCR to confirm insertion of *tolC* or *ftlC* into the chromosome. Finally, the *aphA-1* kanamycin resistance marker was removed from each strain by electroporation of a resolvase-encoding plasmid, pMP672 (hyg^R). The complemented strains containing pMP672 were plated on hygromycin, grown overnight in the absence of antibiotics to cure pMP672, and then plated on kanamycin. Kan^S, hyg^S colonies were screened via colony PCR for the presence of the *tolC*, *ftlC*, or *silC* gene. One kan^S, hyg^S colony was selected for each gene and maintained as the Schu S4 Δ*tolC/tolC*$^+$, Δ*ftlC/ftlC*$^+$, or Δ*silC/silC*$^+$ complemented strains. The WT Schu S4, Δ*tolC* mutant, Δ*ftlC* mutant, and their complemented strains were examined for TolC and FtlC protein expression by immunoblot analysis using anti-TolC and anti-FtlC antibodies and compared for growth in MHB, brain-heart infusion broth (BHI, pH 6.8; BD Biosciences), and Chamberlain's defined medium (CDM) (167).

Perparation of macrophages. BMDM were isolated from the femurs of 6-8 week old female C3H/HeN mice as previously described (136). Bone marrow-derived cells were cultured for 6 days in bone marrow medium (BMM; DMEM with GlutaMax [Gibco] supplemented with 30% L929 cell supernatant, 20% fetal bovine serum [FBS; Hyclone], and 1 mM sodium pyruvate). For cytotoxicity and intracellular replication experiments, BMDM were seeded in 24-well plates at a concentration of 1.5 x10^5 cells/well in 1 ml BMM. For immunoblotting experiments, BMDM were seeded in 6-well plates at a concentration of 1 x 10^6 cells/well in 3 ml BMM. BMDM were allowed to adhere to plates overnight, and then were washed with PBS prior to infection with the indicated *F. tularensis* strains resuspended in bone marrow infection medium (BMIM; DMEM with GlutaMax (Gibco) supplemented with 15% L929 cell supernatant, 10% FBS, and 1 mM sodium pyruvate).

BMDM infections. For LVS single strain cytotoxicity, intracellular replication, and immunoblotting experiments, BMDM were seeded as described above and infected at a multiplicity of infection (MOI) of 50. Plates were centrifuged for 5 min at 500 x g to facilitate bacterial contact with host cells. For co-infection cytotoxicity experiments, BMDM were seeded and infected as above with the WT or Δ*tolC* LVS alone at MOI of 50, or with a mixture of the Δ*tolC* mutant (MOI = 50) and WT LVS (MOI = 10, 20, 40 or 50). For additional co-infection experiments, BMDM were pre-infected with the Δ*tolC* mutant (MOI = 50), and then co-infected with the WT LVS (MOI = 50) 0, 3, or 6 hours following infection with the Δ*tolC* mutant. For Schu S4 intracellular replication and cytotoxicity assays, BMDM were seeded as described above and infected with WT Schu S4 or the Δ*tolC*, Δ*ftlC*, or Δ*silC* mutants or complemented strains at an

MOI of 500. Plates were not centrifuged following the addition of Schu S4 bacteria, necessitating the high MOI. Unless otherwise indicated, BMDM were incubated with the bacteria for 2 hours, washed with PBS, and incubated for an additional 1 hour with gentamicin (10 µg/ml) to kill extracellular bacteria. After gentamicin treatment, cells were washed with PBS and then incubated with fresh BMIM (lacking gentamicin) until the desired time points. For macrophage activation experiments, 50 ng/ml of purified LPS was added to the BMDM 18 hours prior to infection with bacteria.

Cytotoxicity assays. BMDM were cultured and infected as described above. For some experiments, 125 nM staurosporine (STS) in BMIM was added to cells after the 1 hour gentamicin treatment. For some experiments, bacteria were grown in BHI instead of MHB. At the desired times post-infection, supernatants from infected BMDM were collected and analyzed for the presence of LDH using the CytoTox 96 Non-Radioactive Cytotoxicity Assay (Promega) according to the manufacturer's protocol. Background LDH release was quantified by examining supernatants from uninfected BMDM, and maximum LDH release was quantified from cells that were lysed via a single -80℃/54℃ freeze-thaw cycle. Percent LDH release was calculated by subtracting background LDH release from all experimental sample values, dividing by the maximum LDH release minus background LDH release, and multiplying by 100.

Intracellular replication assays. BMDM were cultured and infected as described above. For some experiments, following the 2 hours infection and 1 hour gentamicin treatment, the fresh BMIM added contained 10 µg/ml gentamicin. At the desired times post-infection, cells were washed with PBS and lysed in DMEM + 0.1% deoxycholate for 10 min at room temperature (168). Lysates were diluted, plated, and incubated for 3 days prior to enumeration of colony-forming units (CFU).

Immunoblotting. For immunoblot analysis of apoptosis during infection, BMDM were cultured and infected as described above. For positive apoptosis controls, cells were treated with 10 ng/ml of recombinant TNFα (Invitrogen) for 12 h. At the desired times post-infection, cells were scraped and supernatant/cell mixtures were collected. Cells were pelleted, washed once with PBS, and then lysed in RIPA buffer. Twenty µg of each protein sample was separated via 12% SDS-PAGE. After separation, proteins were transferred to nitrocellulose membranes at 110 volts for 90 min. Membranes were blocked with 5% milk in TBST (TBS with 0.5% Tween-20) at room temperature for 2 h. Membranes were then incubated with primary polyclonal antibodies

recognizing PARP (Cell Signaling #9542; 1:1000 dilution), tubulin (Sigma T4026; 1:10,000 dilution), caspase-8 (R&D Systems AF1650; 1:1,000 dilution), cleaved caspase-3 (Cell Signaling #9661; 1:1000 dilution), or caspase-9 (Cell Signaling #9504; 1:1,000 dilution) overnight at 4℃. Membranes were washed with TBST four times and incubated with a horseradish peroxidase-conjugated mouse anti-rabbit IgG secondary antibody (Cell Signaling #7074, 1:1000 dilution) for 1 hour at room temperature. Membranes were washed and bands were visualized by enhanced chemiluminescence (Pierce).

For immunoblot analysis of antioxidant enzyme secretion, the WT LVS or Δ*tolC* mutant were grown overnight in MHB, diluted to an OD_{600} of 0.05, and grown for 0, 4, 12, or 24 hours. At each timepoint, 1 ml of culture was collected. Bacteria were removed from samples via centrifugation, and supernatants were filtered through a 0.22 µm syringe filter. Sterility was confirmed by plating for CFU following filtration. All supernatants were concentrated to a volume of ~100 µl using a speedvac concentrator (Savant). Supernatants and bacterial pellets were separated via SDS-PAGE, transferred to PVDF membranes and blocked as described above. Membranes were subsequently incubated with monoclonal antibodies to KatG and SodB (169) at room temperature for 1 hour. Membranes were then washed as described above and incubated with a horseradish peroxidase-conjugated rabbit anti-mouse IgG secondary antibody (Cell Signaling #7076, 1:1000 dilution) for 1 hour at room temperature. Membranes were washed and bands were visualized by enhanced chemiluminescence (Pierce).

Disc diffusion assays. For LVS disc diffusion assays, lawns of the WT or Δ*tolC* mutant were plated from frozen stocks. Prior to incubation of the plates, solutions of the following drugs were diluted in sterile water: polymyxin B (stock concentration = 9.1 M), peroxynitrite (stock concentration = 85 mM), H_2O_2 (stock concentration = 8.8 M), and tBh (stock concentration = 7.8 M). To examine sensitivity to the drugs listed above, a 15 µl aliquot of each desired dilution was added to 6 mm paper discs (BD Biosciences), and saturated discs were placed onto the bacterial lawns. For Schu S4 disc diffusion assays, lawns of the WT, Δ*tolC*, Δ*ftlC*, Δ*silC*, Δ*tolC*/*tolC*$^+$, or Δ*ftlC*/*ftlC*$^+$ strains were plated from frozen stocks. Prior to incubation of Schu S4 plates, 15 µl of the following drugs were added to paper discs and placed onto bacterial lawns: SDS (stock concentration = 44 mM), streptomycin (stock concentration = 290 µM), chloramphenicol (stock concentration = 260 µM), erythromycin (stock concentration = 460 µM),

ampicillin (stock concentration = 480 µM), CCCP (stock concentration = 3.25 mM), nalidixic acid (stock concentration = 1.45 mM), or silver nitrate (stock concentration = 196 mM). Following incubation for 72 hours, zones of growth inhibition were measured and recorded as diameters (mm), including the 6 mm disc.

Serum sensitivity of bacteria. To obtain mouse serum, whole blood was collected from mice via cardiac puncture and then centrifuged in Serum Gel Z/1.1 microfuge tubes (Sarstedt) for 10 minutes at 2,500 x g, 4℃ to remove red blood cells. To obtain human serum, whole blood was collected from non-immune donors and then centrifuged as above to remove red blood cells. Approximately 1 x 10^6 CFU of the WT or Δ*tolC* LVS were incubated at 37° C for 1 hour in the presence of normal or heat-inactivated (54ºC for 45 min) serum. *E. coli* strain DH5α was used as a complement-sensitive control strain. Viable bacterial numbers were determined before and after serum incubation by dilution and plating for CFU.

Transmission electron microscopy. Overnight cultures of the WT and Δ*tolC* LVS grown in MHB were diluted to an OD_{600} of 0.05 and then grown to an OD_{600} of 0.2–0.3 or ~1.0. Bacteria were pelleted, washed with PBS, and adsorbed onto polyvinyl formal-carbon-coated grids (Electron Microscopy Sciences) for 2 min. Bacteria were then fixed with 1% glutaraldehyde for 1 min, washed twice in PBS and twice in water, and then negatively stained with 0.5% phosphotungstic acid (Ted Pella) for 30 seconds. All samples were viewed with an FEI Tecnai12 BioTwinG^2 electron microscope at an 80 kV accelerating voltage, and images were obtained using an AMT XR-60 charge-coupled device digital camera system.

Outer membrane protein profiles. Outer membrane protein fractions were isolated as previously described (114). 50 ml cultures of the WT or Δ*tolC* LVS were grown to an OD_{600} of 0.2–0.4 in MHB. Bacteria were pelleted via centrifugation and resuspended in 100 µl of 20 mM Tris HCl (pH 8) containing Complete Protease Inhibitor mixture (Roche), and lysed by sonication. Lysates were centrifuged for 10 min at 7,500 g to pellet unbroken cells, and sarkosyl was added to supernatants to a final concentration of 0.5% to solubilize inner membranes. After incubation for 5 min, supernatants were centrifuged at 100,000 x g for 1 hour. Outer membrane pellets were then mixed with SDS sample buffer, boiled, and separated via SDS-PAGE before Coomassie blue staining.

Sytox green labeling. Overnight cultures of the WT or Δ*tolC* LVS grown in MHB were diluted to an OD_{600} of 0.05 and then grown to an OD_{600} of 0.2–0.4 or ~1.0. Bacteria were pelleted, washed twice with PBS, and resuspended in 50 µl PBS. As a positive control for loss of membrane integrity, ethanol was added to a final concentration of 50%. Sytox green (Invitrogen) was added to a final concentration of 10%, bacteria were incubated for 30 min at 37℃, and then aliquots were mounted on glass slides. Phase-contrast and epifluorescence images were captured using a Spot camera (Diagnostic Instruments).

Infection of mice. For all LVS infections and vaccinations, bacterial inoculums were prepared by growing lawns of the strains for 60 hours on solid media. Bacteria were scraped from the plates, washed with PBS, and resuspended in MHB supplemented with 10% sucrose (MHB/sucrose). Inoculums were diluted in MHB/sucrose and frozen at -80℃ until use. Intranasal infections of mice were performed by administering a 10 µl inoculum into each naris (20 µl total). Female C3H/HeN mice (6-8 weeks old; Charles River Labs) were used for all infections. Actual infectious doses were determined by retrospective CFU counts.

For all Schu S4 mouse infections, inoculums were prepared by growing bacteria for 72 hours on plates, inoculating overnight cultures, and then diluting the cultures to the desired concentrations. Intranasal infections were performed by administering a 10 µl inoculum into each naris (20 µl total). Intradermal infections were performed by injecting a 50 µl inoculum into the pinnae. Female C3H/HeN mice (6-8 weeks old; Charles River Labs) were used for all infections. Actual infectious doses were determined by retrospective CFU counts. All mouse infections with the *F. tularensis* Schu S4 strain were performed at the Rutgers Regional Biocontainment Laboratory under animal-BSL3 conditions.

Immunohistochemistry. Groups of 6 mice were inoculated with PBS or infected as described above with 5 x 10^3 CFU of the WT or Δ*tolC* LVS. At days 2, 3, and 4 post-infection, 2 mice from each group were sacrificed via CO_2 asphyxiation, and spleens were harvested and bisected. One half of each spleen was fixed in 10% formalin and embedded in paraffin wax, while remaining halves were examined for bacterial CFU as described below. Embedded spleens were cut into 5 µm thick sections and stained for the presence of cleaved caspase-3. Endogenous peroxidase activity was quenched by incubation in 0.5% H_2O_2 in methanol, and epitope retrieval was performed by heating in a decloaking chamber (Biocare Medical) for 1 hour at 60℃ in 10 mM sodium citrate buffer (pH 6.0). Slides were incubated for 1 hour at room

temperature with a primary mouse monoclonal antibody to cleaved caspase-3 (Cell Signaling #9661) at a dilution of 1:1500. After incubation with the primary antibody, slides were processed by an indirect avidin-biotin-based immunoperoxidase procedure using a biotinylated horse anti-mouse antibody (Vectastain Elite ABC kit; Vector Laboratories). Slides were incubated overnight at 4℃ in TBS with 0.25% Triton X-100, developed with 3, 3′-diaminobenzidine (DakoCytomation), and counterstained with hematoxylin. To quantitate apoptotic splenocytes, two separate sections per spleen per time point were stained, and ten fields per section were examined for cells positive for cleaved caspase-3. Caspase-3-positive splenocytes in each field were classified as early apoptotic (cytoplasmic localization of cleaved caspase-3) or late apoptotic (cleaved caspase-3 localized to condensed, fragmented nuclei). Two independent experiments were performed for a total of 4 mice per infecting strain on day 2 post-infection, and three independent experiments were performed for a total of 6 mice per infecting strain on days 3 and 4 post-infection.

Vaccinations. For survival experiments, groups of 3 mice were inoculated with PBS or infected intranasally as described above with 1 x 10^3 CFU WT or Δ*tolC* LVS. Six weeks post-vaccination, all mice were intranasally challenged with 1 x 10^8 CFU of the WT LVS and monitored for survival for three weeks. For organ burden analysis, groups of 3–4 mice were vaccinated and challenged as above. The mice were sacrificed on days 3, 5, and 9 post-challenge and lungs, livers, and spleens were harvested. Bacterial organ burdens were determined as described below. Three independent experiments were performed for a total of 10 mice per vaccinating strain per time point. Mice that did not survive challenge infections were excluded from organ burden analysis.

Organ burden analysis. Organs from mice infected as described above were weighed in 1 ml PBS. Organs were manually homogenized in Whirl-Pak bags (Nasco), and undiluted and serial dilutions of the homogenates were plated to determine CFU. Bacterial burdens were calculated as CFU per gram of tissue.

Conditioned media BMDM experiments. To generate WT LVS- or Δ*tolC*-conditioned media for cell culture experiments, bacteria were grown, in the absence of host cells, in BMM at 37° C for 24 hours with shaking at 100 rpm. Bacteria were removed via centrifugation, supernatants were filtered through a 0.22 μm filter, and sterility was confirmed by CFU plating. For all experiments, BMDM were seeded overnight in normal BMM or conditioned BMM prepared as

described above. The following day (16-18 hours later), BMDM were washed and left uninfected or infected with the WT LVS or Δ*tolC* mutant at an MOI of 50. For some experiments, cytotoxicity was examined 21 hours post-infection via LDH release. In parallel experiments, IL-1β release was examined via ELISA (R&D Systems) following 6 hours of treatment with 50 ng/ml *E. coli* LPS.

Flow cytometric analysis of leukocyte recruitment. Groups of four C3H/HeN mice were left uninfected or infected intranasally with 5 x 10^3 CFU of the WT LVS or Δ*tolC* mutant. Two or four days post-infection, mice were sacrificed and spleens were harvested. Single cell suspensions of spleens were prepared by manual passage of spleens through 70 µm mesh screens (BD Falcon). Cells were incubated for 3 minutes in ACK lysis buffer (Gibco), washed two times with PBS, and resuspended in FACS buffer (BioLegend). 1 x 10^6 cells were transferred to single wells of a 96-well plate, blocked with an anti-CD16/CD32 antibody (BioLegend #101301) for 15 minutes on ice, and labeled with the following fluorophore-conjugated cell surface marker antibodies: CD11b-BV510, F4/80-PE, CD11c-PE-Cy7, and Ly6G-AF700 (BioLegend #101245, #123109, #117317, and #127621, respectively) for 10 minutes on ice followed by 10 minutes at room temperature. Labeled cells were washed, transferred to 5 ml tubes, and examined via flow cytometry. Cells were gated on live populations and analyzed using FloJo software.

Table 2.1: Relevant strains and plasmids used in these studies.

Strain/Plasmid	Characteristics	Source
F. tularensis LVS	WT LVS	ATCC
F. tularensis LVS Δ*tolC*	Deletion *of* the *tolC* ORF (FTL1865) in the LVS	(114)
F. tularensis Schu S4	WT Schu S4	BEI
F. tularensis Schu S4 Δ*tolC*	Deletion *of* the *tolC* ORF (FTT1724) in Schu S4	This study
F. tularensis Schu S4 Δ*ftlC*	Deletion *of* the *ftlC* ORF (FTT1095) in Schu S4	This study
F. tularensis Schu S4 Δ*silC*	Deletion *of* the *silC* ORF (FTT1258) in Schu S4	This study
F. tularensis Schu S4 Δ*tolC*/*tolC*+	Chromosomal complementation of *tolC* at the attTn7 site of the Δ*tolC* mutant	This study
F. tularensis Schu S4 Δ*ftlC*/*ftlC*+	Chromosomal complementation of *ftlC* at the attTn7 site of the Δ*ftlC* mutant	This study
pMP672	Hyg^R; resolvase	(164)
pMP720	Hyg^R; transposase	(164)
pMP749	Amp^R/Kan^R; attTn7 integration sites	(164)
pMP812	Kan^R; sacB-based suicide vector	(164)

Table 2.2: Relevant primers used in these studies.

Primer Name	Sequence (5'-3')	Description
tolC USR-F	TTAGCCGTAGCAAGGCGTC	Forward primer for amplification of DNA upstream of *tolC* ORF for allelic exchange
tolC USR-GC-R*	GGGGGCCCCCGGGGGGCTAAAGCTAGACAAAACCC	Reverse primer with GC overlap for amplification of DNA upstream of *tolC* ORF for allelic exchange
tolC DSR-GC-F	CCCCCGGGGGCCCCCCGGAGTAATTAGTTTGATGCC	Forward primer with GC overlap for amplification of DNA downstream of *tolC* ORF for allelic exchange
tolC DSR-R	GCACCACTCAAGCCTTTAGC	Reverse primer for amplification of DNA downstream of *tolC* ORF for allelic exchange
ftlC USR-F	TGTGGTGGTACTCATGTTGCCT	Forward primer for amplification of DNA upstream of *ftlC* ORF for allelic exchange
ftlC USR-GC-R	GGGGGCCCCCGGGGGCGCACTACTTTCAAGCCACC	Reverse primer with GC overlap for amplification of DNA upstream of *ftlC* ORF for allelic exchange
ftlC DSR-GC-F	CCCCCGGGGGCCCCCGACGTGGAGCTATAAAGATG	Forward primer with GC overlap for amplification of DNA downstream of *ftlC* ORF for allelic exchange
ftlC DSR-R	TAGCAATATCAGCTGGCCCC	Reverse primer for amplification of DNA downstream of *ftlC* ORF for allelic exchange
silC USR-F	GGTGCAGCCAAACTAAGCTA	Forward primer for amplification of DNA upstream of *silC* ORF for allelic exchange
silC USR-GC-R	GGGGGCCCCCGGGGGCGTATCATTGTTGTGACCTA	Reverse primer with GC overlap for amplification of DNA upstream of *silC* ORF for allelic exchange
silC DSR-GC-F	CCCCCGGGGGCCCCCTCCTCATTATGATAACCCAGCT	Forward primer with GC overlap for amplification of DNA downstream of *silC* ORF for allelic exchange
silC DSR-R	GCAGCCCCATCACCGAATTT	Reverse primer for amplification of DNA downstream of *silC* ORF for allelic exchange
tolC-F	AAGTAAAGAGTGCTATGAAG	*tolC* ORF forward primer for complementation
tolC-R	TTACTCCGTTGCAATCTGCG	*tolC* ORF reverse primer for complementation
ftlC-F	GGTGGCTTGAAAGTAGTGCG	*ftlC* ORF forward primer for complementation
ftlC-R	ACATCTTTATAGCTCCACG	*ftlC* ORF reverse primer for complementation

* GGGGGCCCCCGGGGG overlap ligation sequences are underlined

CHAPTER 3: TolC-dependent modulation of host cell death by the *Francisella tularensis* Live Vaccine Strain.

I. Introduction.

F. tularensis is a facultative intracellular pathogen that is able to invade and replicate within a variety of host cells, including macrophages, dendritic cells, neutrophils, hepatocytes, and pneumocytes (68-73). Following uptake by macrophages, *F. tularensis* prevents maturation of the phagosome, and within ~1-4 hours escapes into the host cell cytosol where bacterial replication occurs (90, 170, 171). Escape into the cytoplasm depends on the function of genes located in the FPI; FPI mutants that are defective for phagosomal escape are unable to replicate in host cells and are avirulent (83, 172, 173). The bacteria replicate to large numbers in the cytoplasm, eventually triggering lysis of the host cell to release bacteria for additional rounds of infection and spread throughout the host.

A hallmark of *F. tularensis* is its ability to evade host defense mechanisms and subvert innate immune responses. This is evident in murine models of tularemia, where robust proinflammatory responses are not observed during the first 48–72 hours of infection (51-56). *F. tularensis* also dampens host programmed cell death responses during infection (51, 136, 174-179). Death of *F. tularensis*-infected cells occurs via two primary mechanisms: caspase-1-mediated pyroptosis and caspase-3-mediated apoptosis (174, 180). During infection of activated macrophages, DNA from lysed intracellular *Francisella* bacteria is sensed in the cytoplasm by AIM2, caspase-1 is activated, and pyroptotic cell death occurs (102, 110). In addition, *F. tularensis* infection of a variety of host cell types, as well as in the mouse model of tularemia, results in caspase-3 activation and apoptotic cell death (99, 107, 180, 181). Notably, infection of mice with fully virulent type A *F. tularensis* results in extensive activation of caspase-3, but minimal activation of caspase-1, suggesting a central role for apoptosis in the pathogenesis of tularemia (99, 107). Although *F. tularensis* infection eventually leads to activation of host programmed cell death pathways, the bacteria interfere with this response. *F. tularensis* has been shown to delay induction of apoptosis during infection of both macrophages and neutrophils (104-106). The ability of *F. tularensis* to dampen and delay host responses during infection likely provides time for the bacteria to gain an advantage within the host and

cause disease. However, identification and characterization of the precise molecular mechanisms behind the immunomodulatory capacity of *F. tularensis* remain incomplete.

We previously identified the TolC protein as a virulence factor of the LVS that is important for the host suppressive activities of *F. tularensis* (114, 136). The *Francisella* genome encodes three TolC orthologs: TolC (FTT1724), FtlC (FTT1095), and SilC (FTT1258). Both FtlC and TolC have been shown to function in multidrug efflux, but only TolC is required for virulence (114). This suggests a distinct function for TolC, presumably in protein secretion. A Δ*tolC* mutant of the LVS is highly attenuated for virulence in mice, despite being able to disseminate from the site of infection and colonize the liver, spleen and lungs (136). The LVS Δ*tolC* mutant maintains the ability to replicate intracellularly, although the bacteria reach levels in infected organs and cultured host cells that are consistently 1–2 logs lower than for the WT LVS (114, 136). Compared to the WT strain, the LVS Δ*tolC* mutant causes 2–3 fold more cytotoxicity to both murine and human macrophages (136). This hypercytotoxicity is a result of increased apoptosis via a mechanism involving caspase-3 (136). In addition to causing hypercytotoxicity, the LVS Δ*tolC* mutant elicits increased release of proinflammatory chemokines from human macrophages compared to infection with the WT strain (136). Based on these data, we hypothesized that effector proteins secreted via TolC function to subvert innate immune pathways of the host, and that the attenuation in virulence of the LVS Δ*tolC* mutant is due to a combination of hypercytotoxicity, leading to premature loss of the intracellular replication niche, and increased proinflammatory responses, leading to improved recruitment of immune cells to sites of infection and more effective bacterial clearance.

Here, we examined the kinetics of *F. tularensis*-induced inhibition of macrophage cell death and the specific host pathways involved. Our results demonstrate that TolC is required to delay activation of the intrinsic apoptotic pathway during the first ~24–36 hours of infection, and that this delay maximizes intracellular replication of the bacteria. We present evidence that the TolC-dependent delay of apoptosis is an active process, and that the hypercytotoxicity of the LVS Δ*tolC* mutant is not due to compromised structural integrity of the mutant bacteria. Using the mouse model of tularemia, we show that TolC is required for *F. tularensis* to delay caspase-3-mediated apoptosis during infection of host tissues. In addition, we present evidence that the altered responses of the host to primary infection with the Δ*tolC* mutant lead to altered establishment of adaptive immunity. These findings suggest that *Francisella* Δ*tolC* mutants could function as safer and more effective live vaccine strains.

II. Results

***F. tularensis* delays death of infected macrophages in a TolC-dependent manner.** Intracellular replication of *F. tularensis* leads to induction of host cell death pathways (174, 180). We examined the kinetics of cell death during infection of BMDM with either the WT or Δ*tolC* LVS. Significantly increased cytotoxicity, measured by LDH release, was observed for the Δ*tolC* mutant compared to the WT strain as early as 7 hours post-infection (Figure 3.1). The hypercytotoxicity of the LVS Δ*tolC* mutant persisted through 36 hours post-infection. By 48 hours post-infection, WT LVS-infected macrophages exhibited similar levels of cell death as Δ*tolC*-infected cells (Figure 3.1). Thus, *F. tularensis* delays host cell death in a TolC-dependent manner.

The LVS Δ*tolC* mutant is able to invade and replicate within various host cells similar to WT *F. tularensis*, but the Δ*tolC* mutant reaches CFU levels ~1–2 logs lower than the WT strain by 24 hours post-infection (114, 136). This growth defect is observed during infection of mouse organs as well as in cell culture (Figure 1.7 and 1.8) (136). To determine if the diminished replication of the Δ*tolC* mutant correlates with its increased cytotoxicity, we quantified intracellular CFU over time in BMDM infected with either the WT or Δ*tolC* LVS. Matching the kinetics of cytotoxicity, we observed no significant differences in intracellular CFU between the WT and Δ*tolC* LVS at early time points post-infection (up to 8 hours; Figure 3.2A). However, at later times post-infection (16–24 h), intracellular CFU recovered from macrophages infected with the Δ*tolC* mutant were significantly lower than CFU recovered from WT-infected cells (Figure 3.2A). These results support the hypothesis that the growth defect observed for the LVS Δ*tolC* mutant is related to the inability of the mutant to delay host cell death.

In our standard *Francisella* infection assay, we use gentamicin to kill extracellular bacteria following the initial infection period, but then perform the remainder of the assay in gentamicin-free medium (there is minimal *F. tularensis* replication in the macrophage infection medium). If the replication defect of the LVS Δ*tolC* mutant is indeed due to premature lysis of host cells and loss of the intracellular replication niche, then we should see an enhancement of this defect in the continuous presence of extracellular gentamicin, as the gentamicin will gain access to the intracellular bacteria upon host cell lysis. As shown in Figure 3.2B, CFU recovered at 24 hours post-infection from BMDM infected with the Δ*tolC* mutant in the continuous presence of extracellular gentamicin were significantly lower than CFU recovered under our standard

infection conditions. In contrast, the continuous presence of extracellular gentamicin had no significant effect on CFU recovered following infection with the WT LVS (Figure 3.2B). Taken together, these results demonstrate that *F. tularensis* prolongs viability of infected host cells in a TolC-dependent manner, allowing for greater bacterial replication in the protected intracellular niche.

TolC is required for *F. tularensis* to delay induction of the intrinsic apoptotic pathway. Previous work from our laboratory demonstrated that the hypercytotoxicity of the LVS Δ*tolC* mutant correlated with increased activation of caspase-3 and apoptosis (Figure 1.10) (136). Cleavage and activation of caspase-3 is triggered during apoptosis by both extrinsic and intrinsic pathways that are dependent on caspase-8 and -9, respectively (Figure 1.3) (182). Upon activation, caspase-3 translocates to the nucleus, where it facilitates many apoptotic processes, including PARP cleavage, chromatin condensation, DNA fragmentation, and nuclear disruption (182-185). By immunoblot analysis, we detected proteolytic cleavage of caspase-3 and -9 in BMDM infected with the LVS Δ*tolC* mutant as early 6 hours post-infection, whereas macrophages infected with the WT LVS showed little-to-no cleavage of these caspases (Figure 3.3). Cleavage of PARP, an indication of caspase-3/7 activation, was observed by 6 hours post-infection for Δ*tolC* mutant-infected macrophages, but not for WT LVS-infected macrophages. Increased cleavage of PARP and caspases-3 and -9 was observed at 12 and 36 hours post-infection for Δ*tolC*-infected cells, whereas BMDM infected with the WT LVS showed strong cleavage of caspases-3, -9, and PARP only after 36 hours of infection (Figure 3.3). In contrast, cleavage of caspase-8 was not apparent at any time point during infection with either the WT or Δ*tolC* LVS (Figure 3.3). As a positive control, caspase-8 cleavage was detected in cells treated with TNFα (Figure 3.3). These results demonstrate that *F. tularensis* delays induction of the intrinsic apoptotic host cell response in a TolC-dependent manner.

The hypercytotoxicity of the LVS Δ*tolC* mutant is not due to compromised bacterial integrity. Several *Francisella* genes in addition to *tolC* have been identified that, when mutated, result in a hypercytotoxic phenotype (110, 177, 186, 187). Investigation of these mutants revealed that the structural integrity of the bacteria is compromised, rendering the mutants more susceptible to lysis following uptake by macrophages. In activated macrophages, DNA released by lysed intracellular *F. tularensis* is detected by AIM2, which induces inflammasome assembly and leads to pyroptotic cell death characterized by activation of caspase-1 and secretion of IL-1β and IL-18 (102, 110). We demonstrated previously that the

hypercytotoxicity of the LVS Δ*tolC* mutant toward BMDM is caspase-1 independent (Figure 1.10) (136), suggesting that detection of DNA from lysed bacteria is not the basis for the phenotype. To determine if the activation state of the macrophage impacts hypercytotoxicity of the LVS Δ*tolC* mutant, we compared infection of untreated BMDM (our standard infection condition) with LPS-stimulated BMDM. Infection with the Δ*tolC* mutant resulted in increased toxicity compared to infection with the WT LVS regardless of the activation state of the macrophages (Figure 3.4A). Growth of *F. tularensis* in BHI versus MHB results in bacteria more closely resembling organisms isolated from infected macrophages (188). These different growth conditions have been shown to affect structural integrity of *F. tularensis* and cytotoxicity toward host cells (189). We found that the LVS Δ*tolC* mutant was hypercytotoxic to BMDM compared to the WT strain regardless of bacterial growth medium used (Figure 3.4B).

We next conducted a series of experiments to compare directly the structural integrity of the Δ*tolC* mutant with the WT LVS. *Francisella* mutants that are structurally compromised exhibit increased sensitivity to ROS and RNS, and are susceptible to the bactericidal action of complement (186, 190, 191). We observed no differences between the WT and Δ*tolC* LVS in sensitivity to ROS- or RNS-inducing compounds, including H_2O_2, tert-butyl hydroperoxide, and peroxynitrite (Figures 3.5 and 3.6). We also saw no difference between the WT LVS and Δ*tolC* mutant in the ability to secrete *F. tularensis* antioxidant enzymes (Figure 3.7). Additionally, we detected no difference between the WT and Δ*tolC* LVS in resistance to the membrane-active antimicrobial peptide polymyxin B (Figure 3.8), indicating that the Δ*tolC* mutant does not have gross alterations in its envelope. In support of this, the protein profiles of outer membrane fractions isolated from the WT and Δ*tolC* LVS were indistinguishable, as determined by SDS-PAGE (Figure 3.9). In addition, the WT and mutant bacteria exhibited similar resistance to both mouse and human serum (Figure 3.10), indicating no change in complement sensitivity and suggesting that the exopolysaccharide capsule of the Δ*tolC* mutant is not altered (190). To test further the integrity of the bacteria, we assessed permeability to Sytox green, a DNA binding stain normally excluded by the bacterial envelope, and examined the ultrastructure of the bacteria by electron microscopy. These studies revealed no differences between the WT and Δ*tolC* LVS (Figures 3.11 and 3.12). Taken together, these results demonstrate that the LVS Δ*tolC* mutant is not structurally compromised and that the hypercytotoxicity of the Δ*tolC* mutant is not due to increased bacterial lysis.

***F. tularensis* actively delays death of infected macrophages.** If the hypercytotoxicity of the LVS Δ*tolC* mutant is not due to compromised bacterial integrity, this suggests that *F. tularensis* may actively inhibit host cell death pathways in a TolC-dependent manner. Treatment of host cells with STS activates caspase-3 and induces apoptotic cell death (192). To test if *F. tularensis* is capable of interfering with cell death caused by proapoptotic stimuli, we examined STS-treated or untreated BMDM left uninfected or infected with the WT or Δ*tolC* LVS. Treatment of uninfected BMDM with 125 nM STS induced approximately 12% cytotoxicity after 21 hours of treatment (Figure 3.13). Infection with WT bacteria blocked this STS-induced cell death early during infection (6 and 21 hours post-infection), whereas infection with the Δ*tolC* mutant did not (Figure 3.13). At a later time point (45 hours post-infection), suppression of STS-induced cell death in WT LVS-infected cells was no longer apparent (Figure 3.13), consistent with *F. tularensis* initially delaying, but ultimately inducing, host cell death. Thus, *F. tularensis* is able to inhibit cell death induced by proapoptotic stimuli in a TolC-dependent manner. This result is not compatible with the hypercytotoxicity of the Δ*tolC* mutant being due to a passive structural defect.

If the TolC-dependent activity of *F. tularensis* in delaying host cell death is an active process due to factors secreted via TolC, then co-infection of WT with Δ*tolC* mutant bacteria should rescue the premature cell death induced by the mutant bacteria. To test this, we infected BMDM with either the WT or Δ*tolC* LVS alone (MOI = 50), or performed experiments in which the Δ*tolC* mutant (MOI = 50) was added together with increasing amounts of the WT LVS (MOI = 10–50). The single strain control infections showed that the Δ*tolC* mutant was hypercytotoxic to the macrophages compared to the WT LVS (Figure 3.14), as seen previously. However, co-infection of BMDM with the Δ*tolC* mutant and the WT strain led to a dose-dependent decrease in cytotoxicity, reaching a level indistinguishable from infection with the WT LVS alone (Figure 3.14). Additional experiments indicated that death of BMDM pre-infected with the Δ*tolC* mutant could be inhibited by the addition of WT LVS up to 3 hours after infection with the Δ*tolC* mutant (Figure 3.15). These results support a model in which *F. tularensis* secretes effectors via TolC that function to interfere with activation of host cell death pathways during early stages of infection of BMDM.

***F. tularensis* delays apoptosis in mice in a TolC-dependent manner.** To determine if *F. tularensis* interferes with host cell death pathways during infection in vivo, we inoculated mice intranasally with the WT or Δ*tolC* LVS and examined bacterial burdens and caspase-3 activation

in spleens at early times post-infection (days 2, 3 and 4). As observed previously (Figure 1.7) (136), organ burden analysis showed that CFU levels in spleens from mice infected with the Δ*tolC* mutant were lower by ~1–2 logs at each time point compared to mice infected with the WT LVS (Figure 3.16A). Despite this decreased bacterial burden, examination by immunohistochemistry using an anti-cleaved caspase-3 antibody revealed that overall levels of caspase-3 cleavage in Δ*tolC* LVS-infected spleens were similar to levels in WT LVS-infected spleens at each time point (Figure 3.16B). All spleens examined from PBS-inoculated control mice were negative for cleaved caspase-3 at all time points. These results indicate that the Δ*tolC* mutant is hypercytotoxic compared to the WT LVS during infection of host tissues. The immunohistochemical analysis revealed that cleaved caspase-3 was localized to two distinct subcellular compartments: the cytoplasm, indicative of early stages of apoptosis; or condensed, fragmented nuclei, indicative of late stages of apoptosis (Figure 3.16C) (184, 185, 193). Notably, at each time point, the proportion of cleaved caspase-3-positive cells undergoing late stage apoptosis was significantly higher for mice infected with the Δ*tolC* mutant compared to mice infected with the WT LVS (Figure 3.16D). This difference was particularly stark at day 3 post-infection, where only 8% of cleaved caspase-3-positive splenocytes were late apoptotic for the WT LVS, but 80% of cleaved caspase-3-positive splenocytes were late apoptotic for the Δ*tolC* mutant (Figure 3.16D). Thus, *F. tularensis* suppresses and delays caspase-3-mediated host cell death in vivo by a mechanism dependent on TolC.

Mice vaccinated with the Δ*tolC* mutant clear challenge doses more efficiently than mice vaccinated with the WT LVS. The defect of the LVS Δ*tolC* mutant in delaying apoptosis during infection in vivo should result in premature exposure of the bacteria to the extracellular environment due to loss of the intracellular replication niche. We hypothesized that this premature exposure of the Δ*tolC* mutant could lead to altered innate immune responses and more efficient adaptive immune responses compared to infection with the WT LVS. In addition, the attenuation in virulence and lower organ burden levels of the Δ*tolC* mutant could make it a safer vaccine strain compared to the WT LVS. To test this, we immunized mice via the intranasal route with a sublethal dose (10^3 CFU) of the WT or Δ*tolC* LVS. We hypothesized that this vaccinating dose was safe and effective, as the majority of mice infected with 5 x 10^3 CFU of the WT LVS or Δ*tolC* mutant survived vaccinations and were protected from lethal challenge (Table 3.1). Six weeks following vaccination, mice were challenged intranasally with a lethal dose (10^8 CFU) of the WT LVS and monitored for survival over 21 days. All mock-vaccinated control mice died 5–15 days post-challenge, whereas the majority of mice vaccinated with WT

LVS (73%) or the Δ*tolC* mutant (82%) survived the lethal challenge (Figure 3.17). Therefore, vaccination with the LVS Δ*tolC* mutant protects mice from lethal challenge at least as well as the WT LVS, despite the fact that it colonizes host organs to lower levels (Figures 1.7 and 3.16A).

In parallel experiments, we vaccinated mice intranasally with 10^3 CFU of the WT or Δ*tolC* LVS, or mock vaccinated with PBS as a control, and challenged with 10^8 CFU of WT LVS as above. We then quantified bacterial burdens in the lungs, livers, and spleens on days 3, 5 and 9 post-challenge. Consistent with the protection conferred by immunization with either strain, organ burdens for mock-vaccinated mice were significantly higher compared to the WT and Δ*tolC* LVS-vaccinated mice, and all mock-vaccinated mice died by day 9 post-challenge (Figure 3.18). Notably, a difference in organ burden patterns between mice vaccinated with the WT or Δ*tolC* LVS emerged from these studies. On day 3 post-challenge, WT LVS-vaccinated mice had significantly lower bacterial burdens in all organs analyzed compared to Δ*tolC* LVS-vaccinated mice (Figure 3.19). In contrast, on day 5 post-challenge, similar organ burdens were obtained for both the WT and Δ*tolC*-vaccinated mice. This change was due to an increase in bacterial burdens from days 3 to 5 for mice vaccinated with the WT LVS, whereas levels remained similar or decreased in mice vaccinated with the Δ*tolC* mutant (Figure 3.19). Moreover, greater numbers of Δ*tolC* LVS-vaccinated mice had undetectable challenge doses in their organs on day 5 compared to day 3, indicating clearance of the bacteria by the host. This increased clearance was not observed for WT LVS-vaccinated mice (Figure 3.19). By day 9 post-challenge, organ burdens for all mice decreased compared to day 5. However, bacterial levels in the liver were significantly lower for mice vaccinated with the Δ*tolC* mutant compared to mice vaccinated with the WT LVS, reversing the pattern seen on day 3 (Figure 3.19). In addition, all mice vaccinated with the Δ*tolC* mutant had completely cleared challenge doses from the liver and spleen by day 9, whereas bacteria were still detected in organs from mice vaccinated with the WT LVS (Figure 3.19). These data demonstrate that the kinetics of challenge dose clearance are different between the WT and Δ*tolC* LVS-vaccinated mice, with mice immunized with the Δ*tolC* mutant able to clear challenge doses more efficiently. Taken together, these findings support our hypothesis that primary infection with the Δ*tolC* mutant leads to altered and more effective adaptive immune responses.

III. Discussion

F. tularensis is a highly virulent human pathogen. A key feature of *F. tularensis* virulence is its ability during early stages of infection to evade and subvert host innate immune responses, including induction of programmed cell death pathways. The ability of *F. tularensis* to dampen host responses during infection likely provides time for the bacteria to replicate and spread within the host, contributing to the morbidity and mortality associated with tularemia. However, the molecular mechanisms underlying the immunomodulatory capacity of *F. tularensis* are not well understood. Previously, we identified TolC as critical for the virulence of the *F. tularensis* LVS. TolC is an outer membrane channel protein required for secretion by the type I secretion pathway. We show here that TolC is necessary for *F. tularensis* to delay induction of the intrinsic apoptotic pathway during infection of macrophages, and that loss of TolC function results in premature loss of the intracellular replicative niche. We also demonstrate that *F. tularensis* delays induction of apoptosis during infection of mice in a TolC-dependent manner. Despite the virulence attenuation and replication defect of the LVS Δ*tolC* mutant, immunization of mice with this strain provides protection against lethal challenge with WT LVS. Moreover, mice immunized with the Δ*tolC* mutant clear challenge bacteria more effectively than mice immunized with the WT LVS. Taken together, our results demonstrate that TolC is a critical *F. tularensis* virulence determinant that may modulate host innate and adaptive immune responses during pathogenesis.

Although *Francisella* has a detectable extracellular phase in the host, the bacteria are thought to replicate primarily within the intracellular niche during infection (70, 194). *F. tularensis* mutants that are unable to survive within host cells, such as FPI mutants that are defective for phagosomal escape, are severely attenuated for virulence (83, 172, 173). The LVS Δ*tolC* mutant has a distinct phenotype, in that it replicates intracellularly, but reaches numbers consistently lower compared to the WT strain. We found that the LVS Δ*tolC* mutant replicates similarly to the WT LVS in macrophages during the first ~8 hours post-infection (Figure 3.2). Given that *F. tularensis* escapes from the phagosome within ~1-4 hours after uptake by macrophages (90, 170, 171), this observation indicates that TolC is not required for phagosomal escape or initiation of replication within the cytoplasm. After this initial period, the LVS Δ*tolC* mutant exhibits a replication defect compared to the WT strain (Figure 3.2). This timing parallels the kinetics of macrophage cell death induced by the Δ*tolC* mutant (Figure 3.1). Our results support a model in which *F. tularensis* delays induction of host cell death by a TolC-

dependent mechanism. This delay in cell death allows *F. tularensis* to preserve its intracellular replicative niche and maximize bacterial growth. The LVS Δ*tolC* mutant also exhibits decreased replication compared to the WT strain during infection of host organs (Figures 1.7 and 3.16A), demonstrating that TolC function is required to preserve the bacterial replicative niche in vivo.

We previously showed that the hypercytotoxicity of the LVS Δ*tolC* mutant in BMDM was associated with increased activation of caspase-3 and apoptosis, and independent of caspase-1 activity (Figure 1.10) (136). We show here that TolC is required for the LVS to delay activation of the intrinsic pathway of apoptosis, as evidenced by earlier cleavage of caspase-3, caspase-9 and PARP during infection of macrophages with the Δ*tolC* mutant compared to WT bacteria, and the absence of caspase-8 cleavage (Figure 3.3). Our results are in contrast to analyses of several other *Francisella* mutants that exhibit hypercytotoxicity toward host cells (110, 177, 186, 187, 195). The hypercytotoxicity of these other mutants was correlated with compromised structural integrity of the bacteria leading to release of bacterial DNA, activation of caspase-1, and pyroptotic, rather than apoptotic, cell death.

We directly confirmed through a number of tests that the structural integrity of the LVS Δ*tolC* mutant is not compromised compared to the WT LVS. Moreover, we present two separate lines of evidence that the TolC-dependent delay in apoptosis during *F. tularensis* infection is an active process. We show that co-infection of WT bacteria with the Δ*tolC* mutant reduces cytotoxicity back to levels observed upon infection with the WT alone, and that the LVS suppresses STS-induced activation of apoptosis in a TolC-dependent manner. While the reasons underlying the lack of additive cytotoxicity of the Δ*tolC* mutant towards STS-treated BMDM are unclear, our data may suggest that STS and the LVS Δ*tolC* mutant induce cytotoxicity via a similar mechanism. Together, these results are incompatible with the hypercytotoxicity of the LVS Δ*tolC* mutant being due to a structural or some other passive defect. Instead, they support a model wherein *F. tularensis* secretes effector proteins via TolC that actively interfere with the innate cell death responses of macrophages.

Using the mouse model of tularemia, we found that *F. tularensis* delays induction of caspase-3-mediated apoptosis in a TolC-dependent manner in infected host tissues. The inability of the Δ*tolC* mutant to delay apoptosis in vivo could result in premature loss of the intracellular replicative niche and greater exposure of the Δ*tolC* mutant to host immune surveillance mechanisms in the extracellular environment. We previously observed that the LVS Δ*tolC*

mutant elicits increased proinflammatory responses from human macrophages compared to the WT strain (Figure 1.11). Taking these possibilities together, the greater exposure of the Δ*tolC* mutant bacteria to the extracellular environment and increased proinflammatory responses may in turn affect the development of adaptive immune responses. Consistent with this hypothesis, we found that mice immunized with the Δ*tolC* mutant cleared challenge doses of the WT LVS more efficiently than mice immunized with the WT strain (Figure 3.19). Future studies are needed to determine the basis for the differences in initial colonization levels and kinetics of challenge dose clearance between the WT and Δ*tolC* LVS-vaccinated mice. Nevertheless, our results demonstrate a role for TolC during primary *F. tularensis* infection that impacts the adaptive immune response.

Taken together, the work presented here demonstrates that TolC is a major *F. tularensis* virulence factor that inhibits the intrinsic apoptotic pathway during infection and facilitates preservation of intracellular replicative niches. The *F. tularensis* Δ*tolC* mutant exhibits a 1–2 log replication defect and 2–3 fold increase in cytotoxicity compared to the WT bacteria. Yet, the attenuation in virulence of the *F. tularensis* Δ*tolC* mutants is highly significant. Our work highlights how shifts in the dynamics and kinetics of host-pathogen interactions may dramatically affect the outcome of disease.

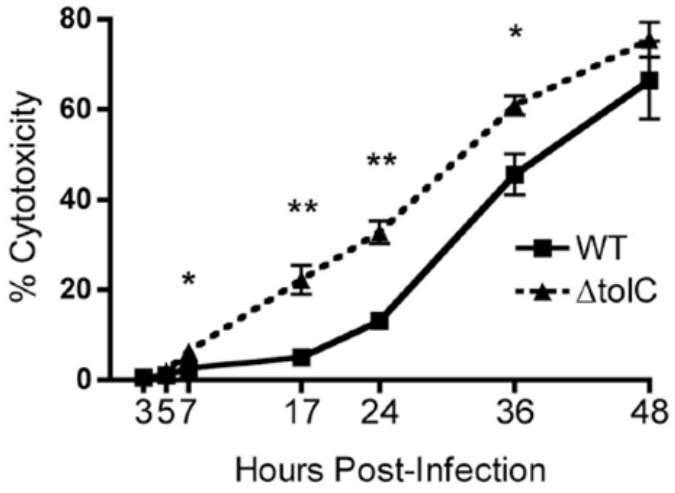

Figure 3.1: TolC is required for the ability of the LVS to delay host cell death during infection. BMDM were infected with the WT LVS or Δ*tolC* mutant at an MOI of 50. At the indicated times post-infection, cytotoxicity was quantified via LDH release. Data represent means ± SEM of three independent experiments. *, $P < 0.05$; **, $P < 0.01$; calculated by one-way ANOVA and Tukey's post-test.

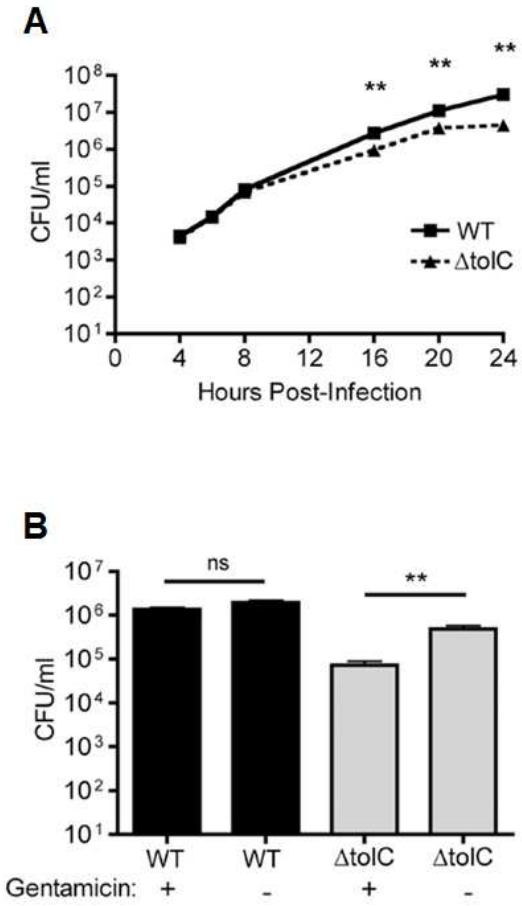

Figure 3.2: TolC is required for optimal LVS replication within host cells. BMDM were infected with the WT LVS or Δ*tolC* mutant at an MOI of 50 for 2 hours, treated with gentamicin for 1 hour to kill extracellular bacteria, and incubated in gentamicin-free media. **(A)** Intracellular replication was quantified by lysing infected BMDM and plating for CFU at the indicated times post-infection. **(B)** BMDM were infected as described above. Following the 1 hour gentamicin treatment step, BMDM were either incubated in gentamicin-free (-) or gentamicin-containing (+) media. Intracellular replication was quantified 24 hours post-infection. Data represent means ± SEM of three independent experiments. **, $P < 0.01$, calculated by one-way ANOVA and Tukey's post-test.

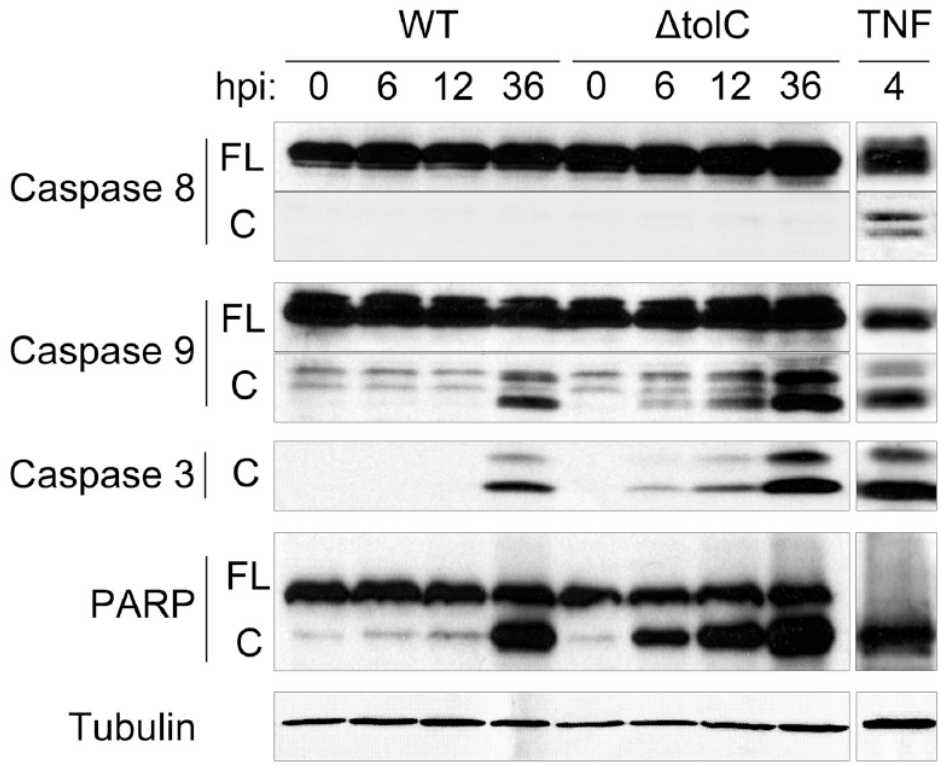

Figure 3.3: The LVS delays induction of the intrinsic apoptotic pathway during infection in a TolC-dependent manner. BMDM were infected with the WT LVS or Δ*tolC* mutant at an MOI of 50. At the times indicated post-infection, cell lysates were collected and examined for the presence of the indicated proteins via SDS-PAGE and immunoblotting. Analysis of BMDM treated with TNFα served as a positive apoptosis control. Sizes of full length (FL) and cleaved **(C)** proteins are as follows. Caspase-8: FL, 57 kDa; C, 43 kDa. Caspase-9: FL, 49 kDa; C, 39 and 37 kDa. Caspase-3: C, 19 and 17 kDa. PARP: FL, 116 kDa; C = 89 kDa. α-tubulin = 52 kDa. Results are representative of at least 2 independent experiments per time point.

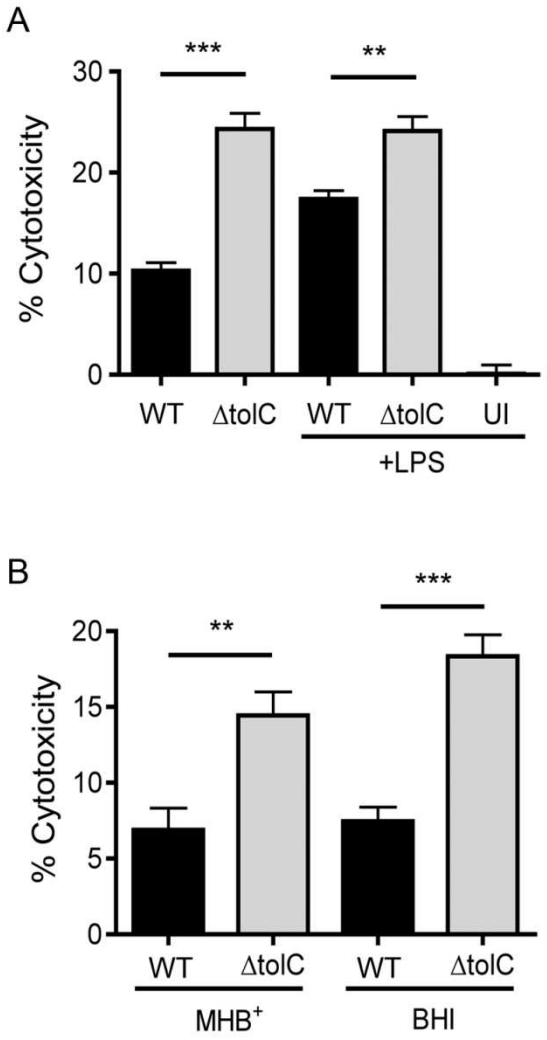

Figure 3.4: The hypercytotoxicity of the LVS Δ*tolC* mutant is not dependent on macrophage activation state or bacterial growth media. (A) BMDM were seeded overnight with or without 50 ng/ml *E. coli* LPS prior to infection with the WT or Δ*tolC* LVS at MOI of 50. Some LPS-activated macrophages were left uninfected (UI). Cytotoxicity was measured 24 hours post-infection by quantitating LDH release. **(B)** The WT and Δ*tolC* LVS were grown in MHB or BHI and then used to infect BMDM at MOI of 50. Cytotoxicity was measured 24 hours post-infection by quantitating LDH release. Bars represent means ± SEM of 3 independent experiments. **P < 0.01, ***P < 0.001; calculated by Student's t test.

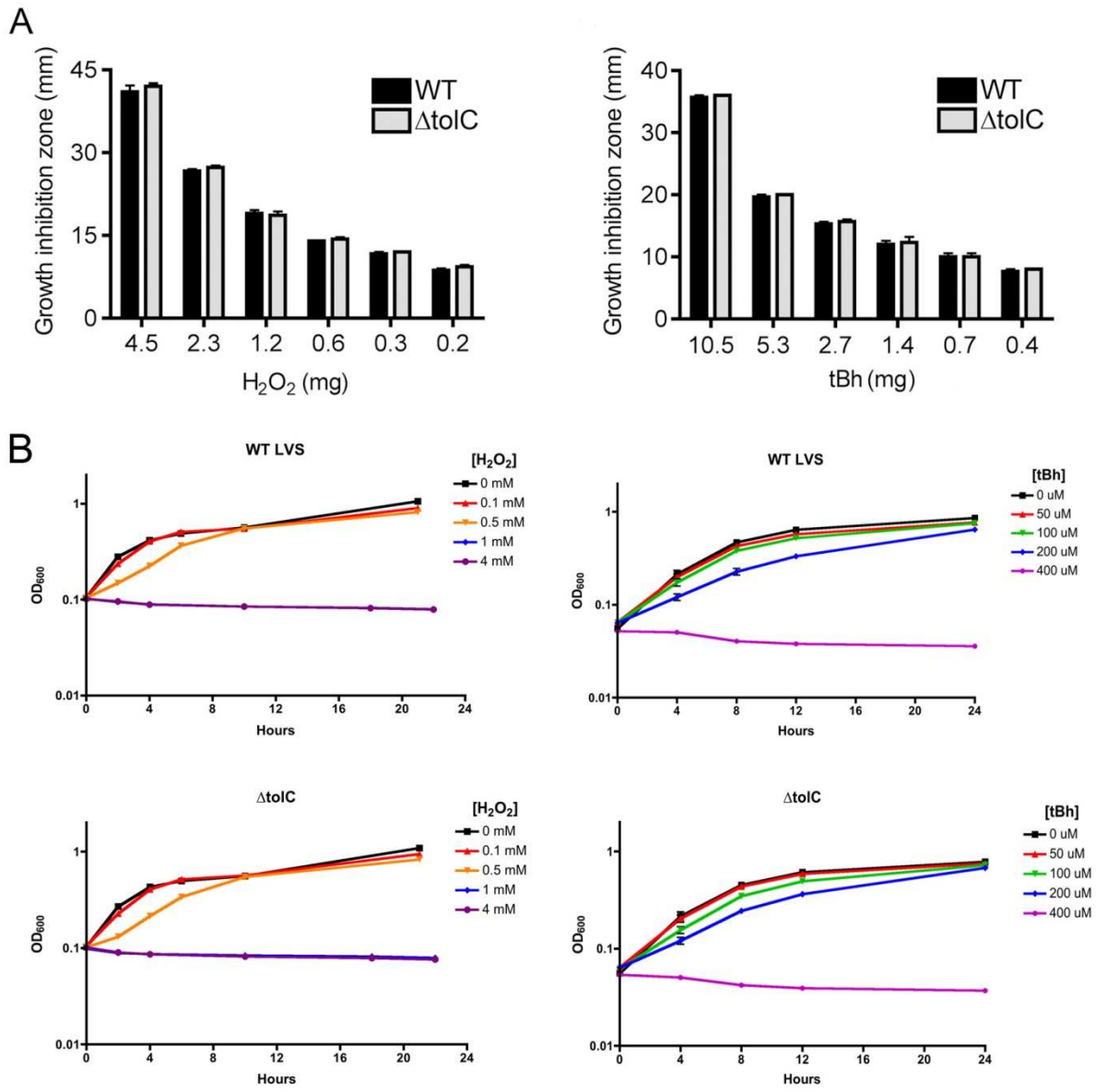

Figure 3.5: Sensitivity of the WT LVS and Δ*tolC* mutant to ROS. (A) 6 mm paper discs containing the indicated amounts of hydrogen peroxide (H_2O_2) or tert-butyl-hydroperoxide (tBh) were placed on freshly plated lawns of the WT LVS or Δ*tolC* mutant. Diameters of growth inhibition, including the 6 mm paper disc, were measured after 72 hours of incubation. **(B)** Overnight cultures of the WT LVS or Δ*tolC* mutant were diluted to starting OD_{600} of 0.05-0.10, and grown in the presence of the indicated amounts of H_2O_2 or tBh. OD_{600} values were determined as a measure of bacterial growth. Data represent means ± standard deviation **(A)**, or SEM **(B)**, from three independent experiments.

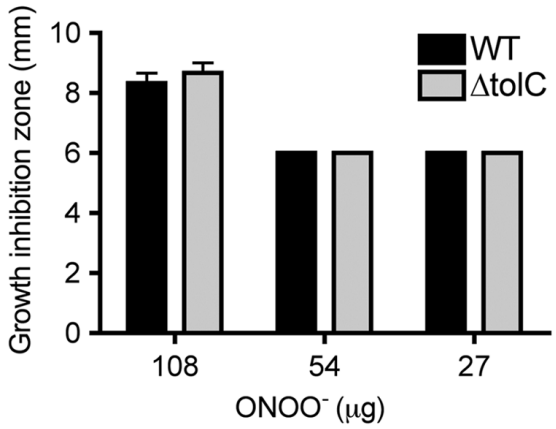

Figure 3.6: Sensitivity of the WT LVS and Δ*tolC* mutant to peroxynitrite. 6 mm paper discs containing the indicated amounts of peroxynitrite ($ONOO^-$) were placed on freshly plated lawns of the WT LVS or Δ*tolC* mutant. Diameters of growth inhibition, including the 6 mm paper disc, were measured after 72 hours of incubation. Data represent means ± standard deviation from three independent experiments.

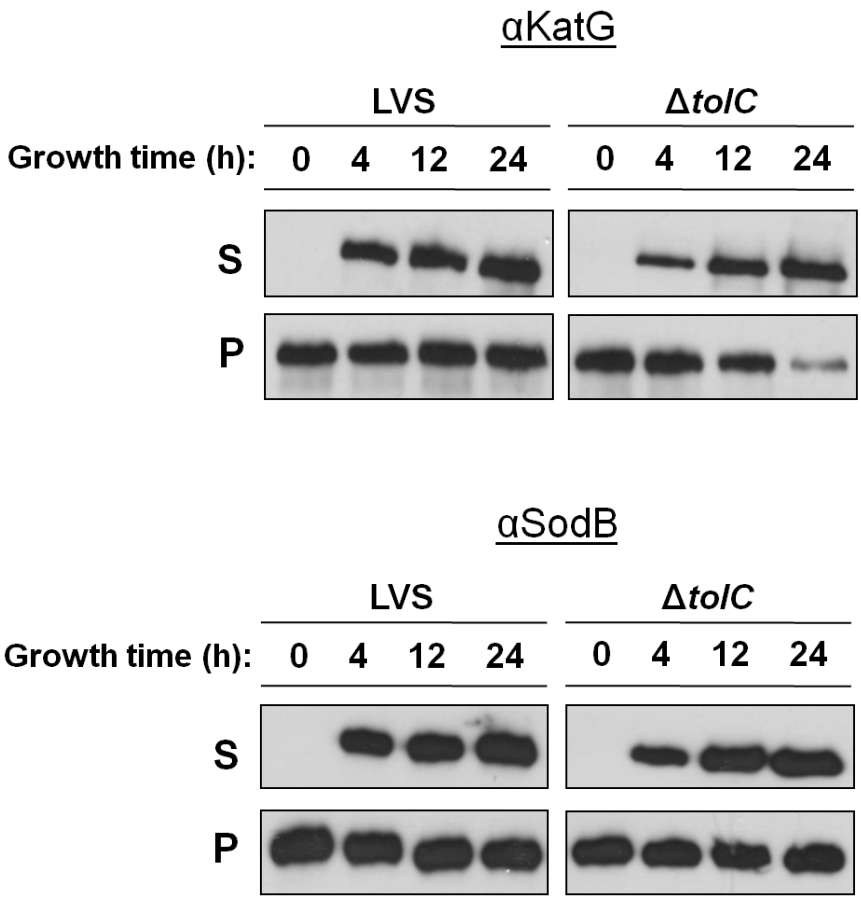

Figure 3.7: The LVS Δ*tolC* mutant is not defective for secretion of antioxidant enzymes. The WT LVS or Δ*tolC* mutant were grown overnight in MHB. Overnight cultures were diluted to a starting OD_{600} of ~0.05. Then, at the times indicated, cell-free supernatants (S) and bacterial pellets (P) were analyzed for the presence of SodB and KatG via immunoblotting. Images are representative of two independent experiments.

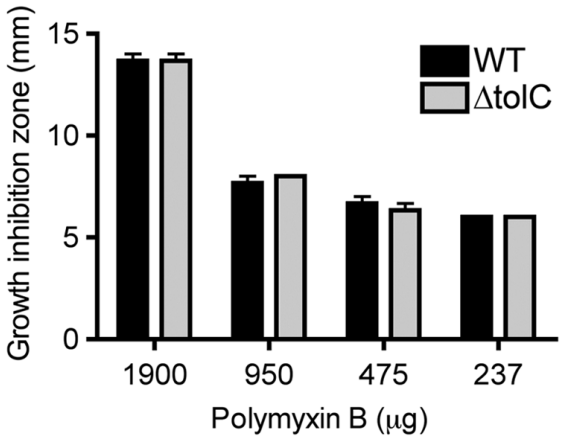

Figure 3.8: Sensitivity of the WT LVS and Δ*tolC* mutant to polymyxin B. 6 mm paper discs containing the indicated amounts of polymyxin B were placed on freshly plated lawns of the WT LVS or Δ*tolC* mutant. Diameters of growth inhibition, including the 6 mm paper disc, were measured after 72 hours of incubation. Data represent means ± standard deviation from three independent experiments.

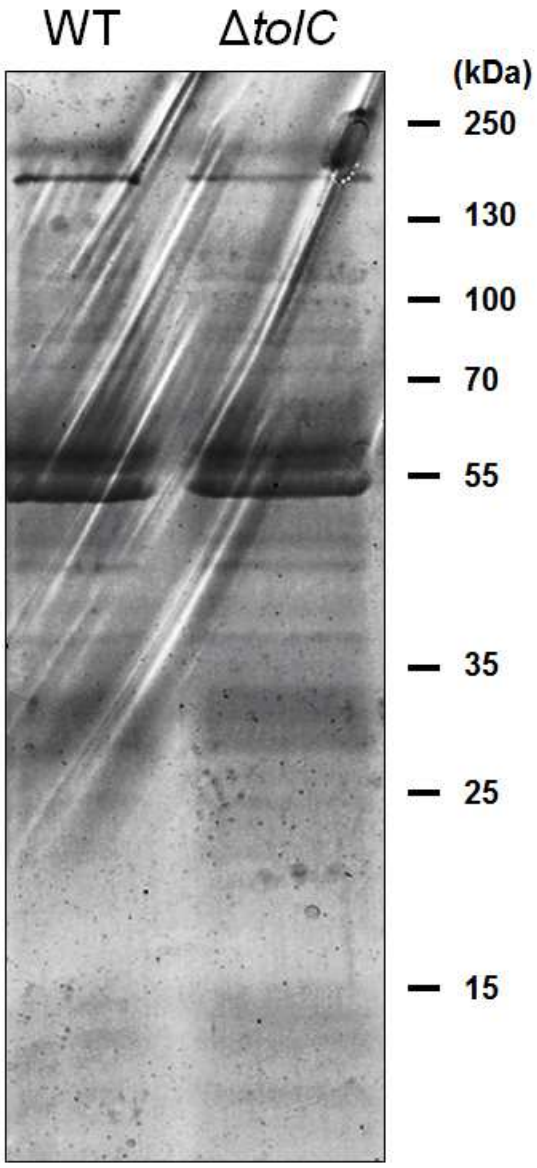

Figure 3.9: Outer membrane protein profiles from the WT LVS and Δ*tolC* mutant. The WT LVS or Δ*tolC* mutant was grown to an OD_{600} of 0.2-0.4 in MHB. Bacteria were collected, lysed via sonication, and outer membranes were isolated. Outer membrane proteins were separated via SDS-PAGE and stained with Coomassie blue. Results are representative of two independent experiments.

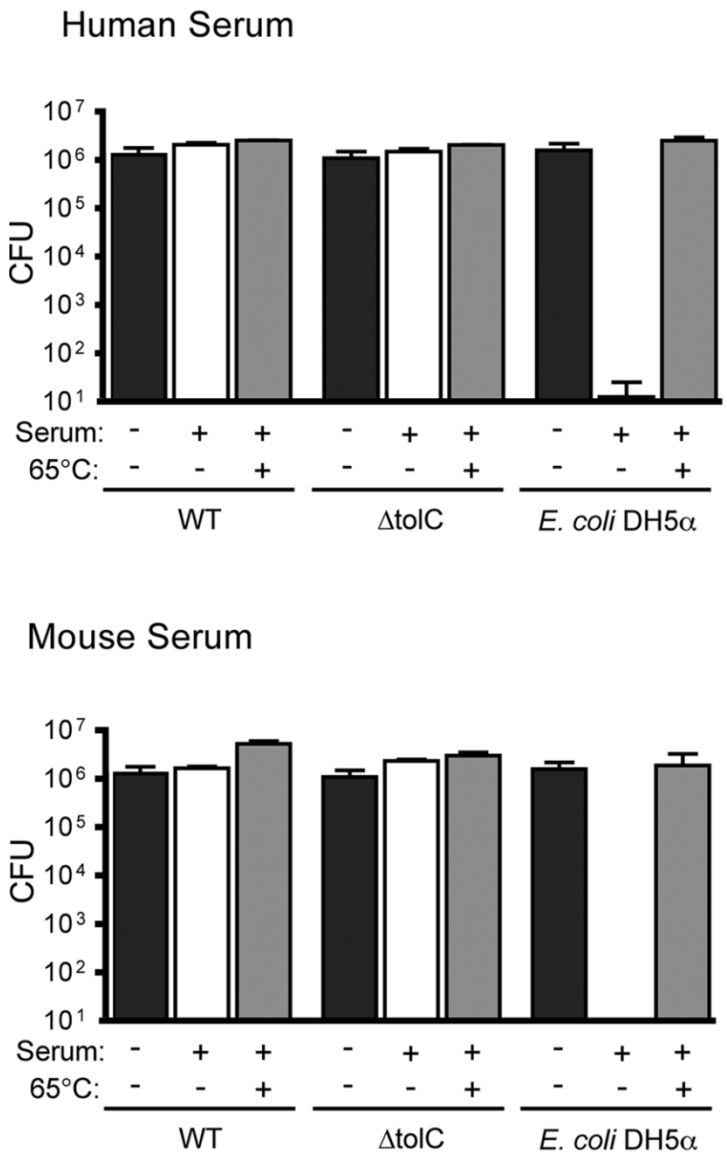

Figure 3.10: The LVS Δ*tolC* mutant is resistant to human and mouse serum-mediated killing. Approximately 10^6 CFU of the WT LVS or Δ*tolC* mutant were incubated with normal or heat-inactivated (65℃) human or mouse serum for 1 hour at 37℃. *E. coli* DH5α was used as a complement-sensitive control strain. Serum sensitivity was determined by quantifying CFU before and after serum incubation. Bars represent means ± SEM of 3 independent experiments.

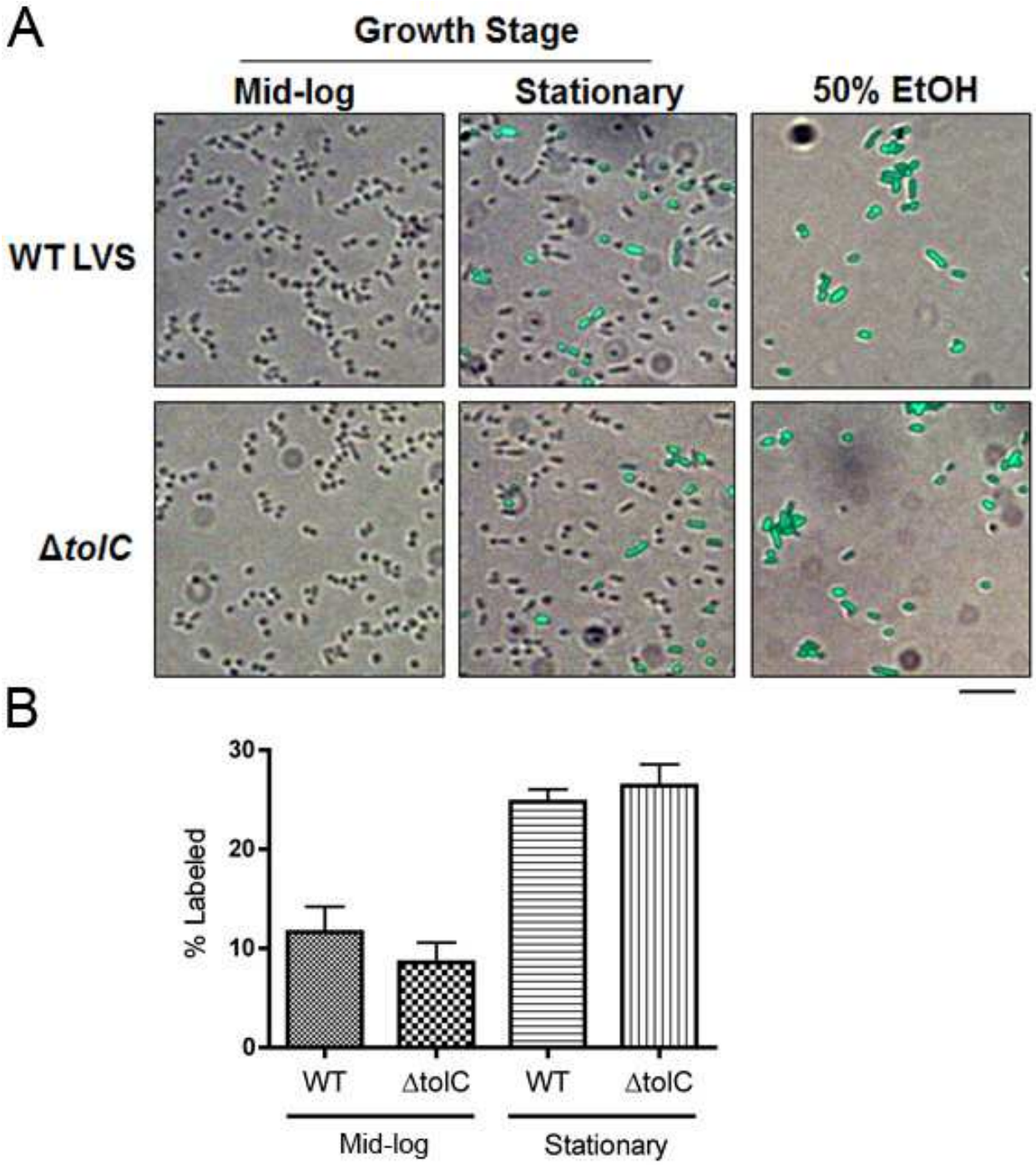

Figure 3.11: The envelope integrity of the LVS Δ*tolC* mutant is not compromised compared to the WT. The WT LVS and Δ*tolC* mutant were grown in liquid media overnight. Cultures were diluted to a starting OD_{600} of ~0.05, and grown to mid-log (OD_{600} = 0.20) or stationary growth phase (OD_{600} = 1.00). Following growth, bacteria were collected via centrifugation, washed once in PBS, and incubated with Sytox green at a final concentration of 0.5 µM for 10 minutes. As a positive control, bacteria were incubated with 50% ethanol in PBS for 10 minutes prior to Sytox labeling. Following labeling, bacteria were washed in PBS and viewed via phase-contrast and fluorescence microscopy. **(A)** Fluorescence images overlaid

onto corresponding phase-contrast images. Images are representative of two independent experiments. Scale bar = 5 µm. **(B)** Sytox green-positive bacteria per field were counted. The percentages of labeled bacteria were determined by dividing Sytox green-positive bacteria by the total number bacteria per field and multiplying by 100. Results are from two fields from two independent experiments, with >200 bacteria/field.

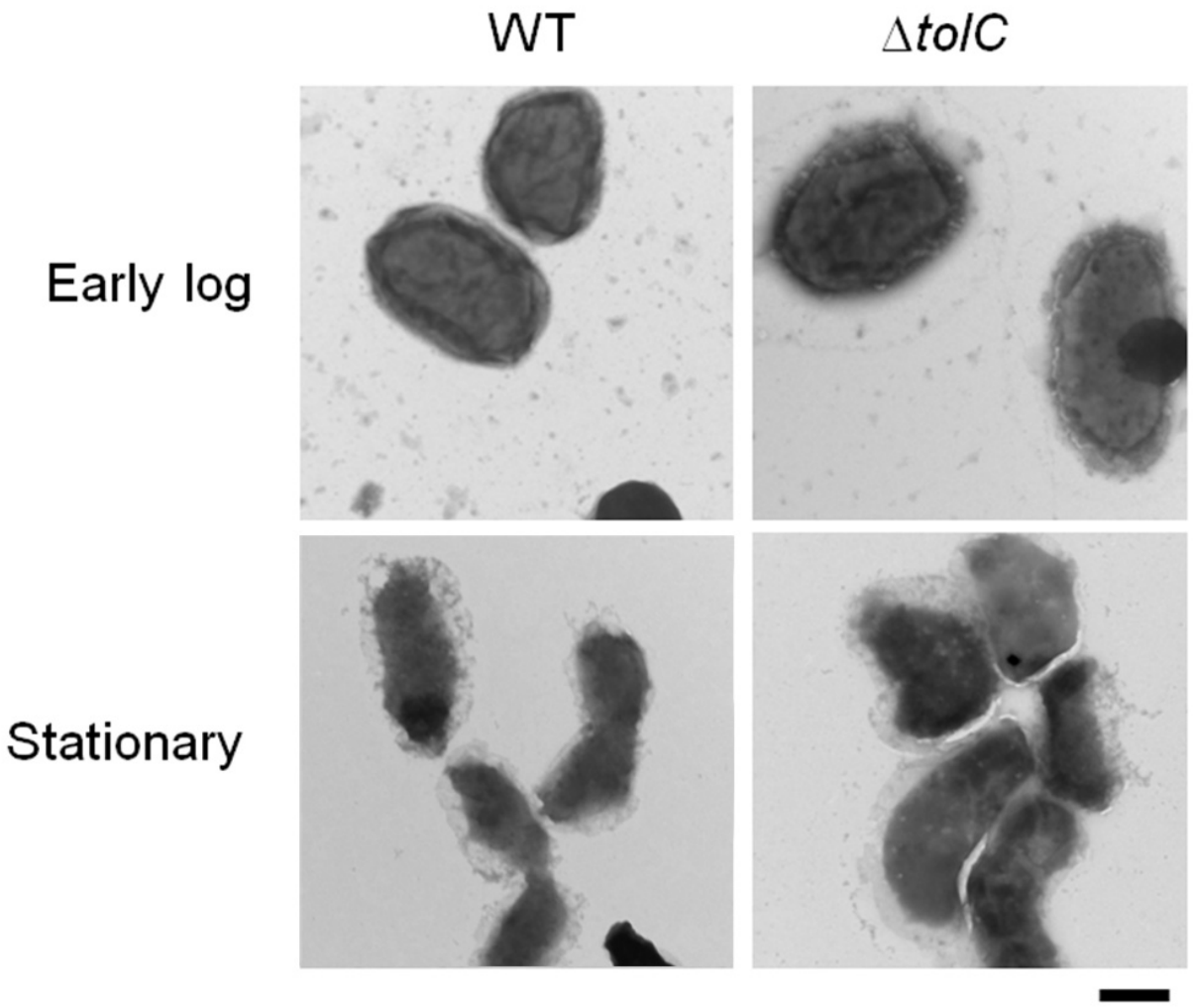

Figure 3.12: Ultrastructure of the WT LVS and Δ*tolC* mutant. The WT LVS and Δ*tolC* mutant were grown in MHB overnight. Cultures were then diluted to a starting OD_{600} of ~0.05, and grown to early-log (OD_{600} = 0.10–0.20) or stationary phase (OD_{600} >1.00). Following growth, bacteria were washed, fixed, stained with phosphotungstic acid, and viewed via electron microscopy. Scale bar = 500 nm.

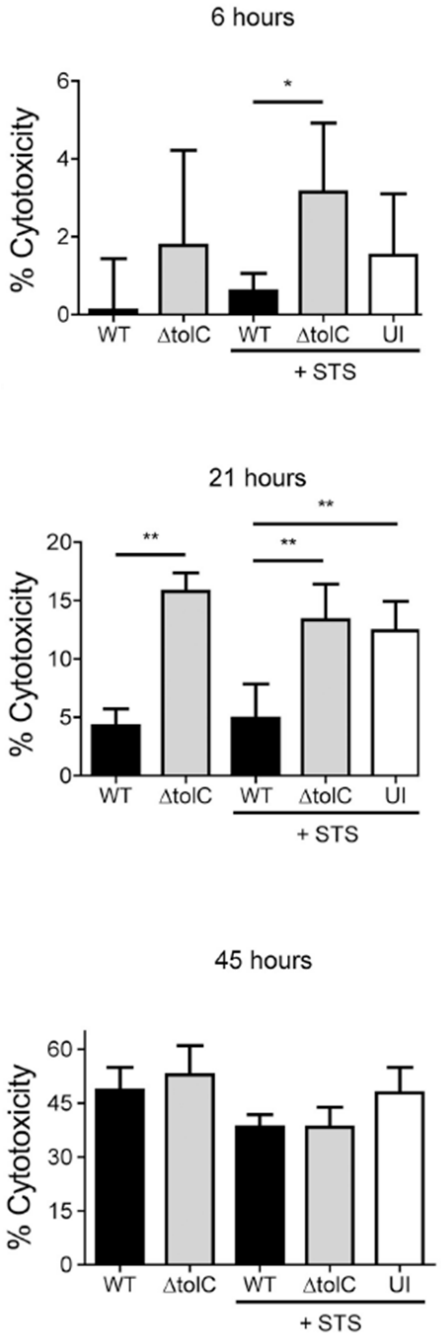

Figure 3.13: The LVS inhibits proapoptotic death stimuli in a TolC-dependent manner. BMDM were infected with the WT or Δ*tolC* LVS at MOI of 50. 3 hours post-infection, BMDM were left untreated or treated with staurosporine (125 ng/ml) to trigger apoptotic cell death. Cytotoxicity was determined by measuring LDH release at the indicated times post-infection. Note the differences in scale of the y-axis at each timepoint. Bars represent means ± SEM of three independent experiments. *P<0.05, **P < 0.01; calculated by one-way ANOVA and Tukey's post-test for the indicated comparisons.

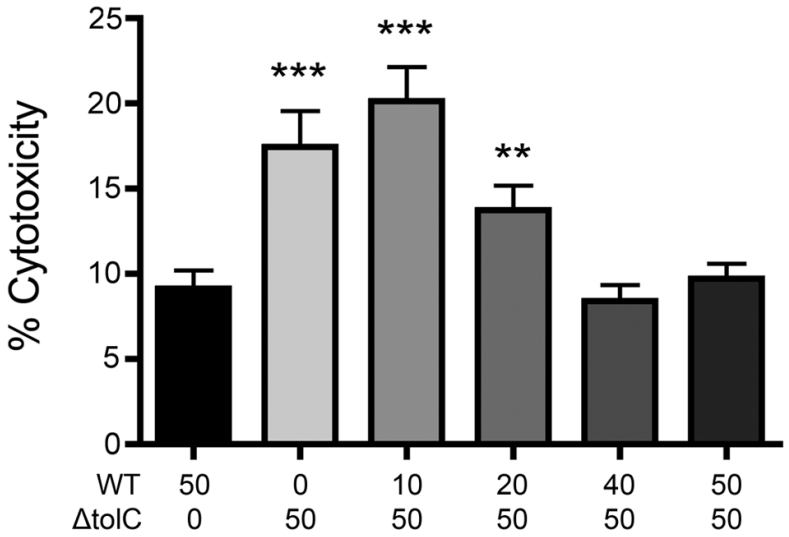

Figure 3.14: Co-infection of BMDM with the WT LVS and Δ*tolC* mutant rescues the hypercytotoxic phenotype of the Δ*tolC* mutant. BMDM were infected with the WT or Δ*tolC* LVS alone at MOI of 50, or co-infected with the WT and Δ*tolC* LVS at the indicated MOI. Cytotoxicity was quantified by measuring LDH release 24 hours post-infection. Bars represent means ± SEM of three independent experiments. **P < 0.01, ***P<0.001; calculated by one-way ANOVA and Tukey's post-test for comparison to infection with WT LVS alone.

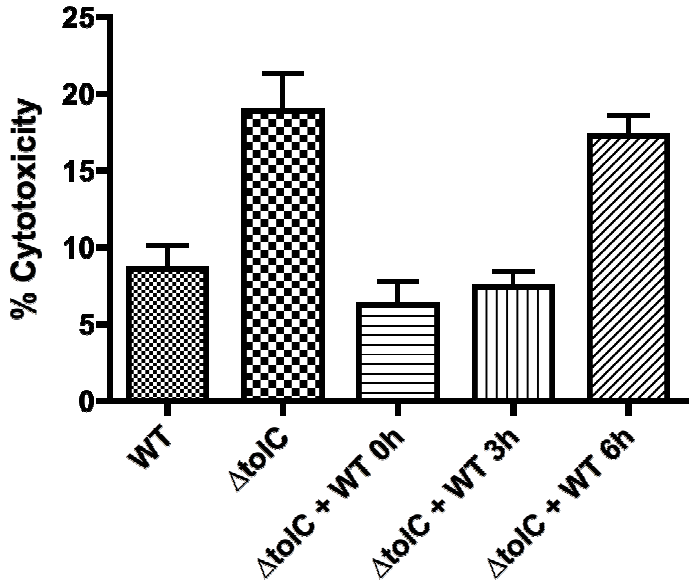

Figure 3.15: The WT LVS can suppress death of BMDM pre-infected with the Δ*tolC* mutant. BMDM were infected with the LVS Δ*tolC* mutant at an MOI of 50. At the indicated times following Δ*tolC* infection, BMDM were infected with the WT LVS. Cytotoxicity was quantified via LDH release 21 hour following the initial infection. Single strain infection controls (MOI = 50) are shown in the first two bars. Bars represent means ± SEM from two independent experiments.

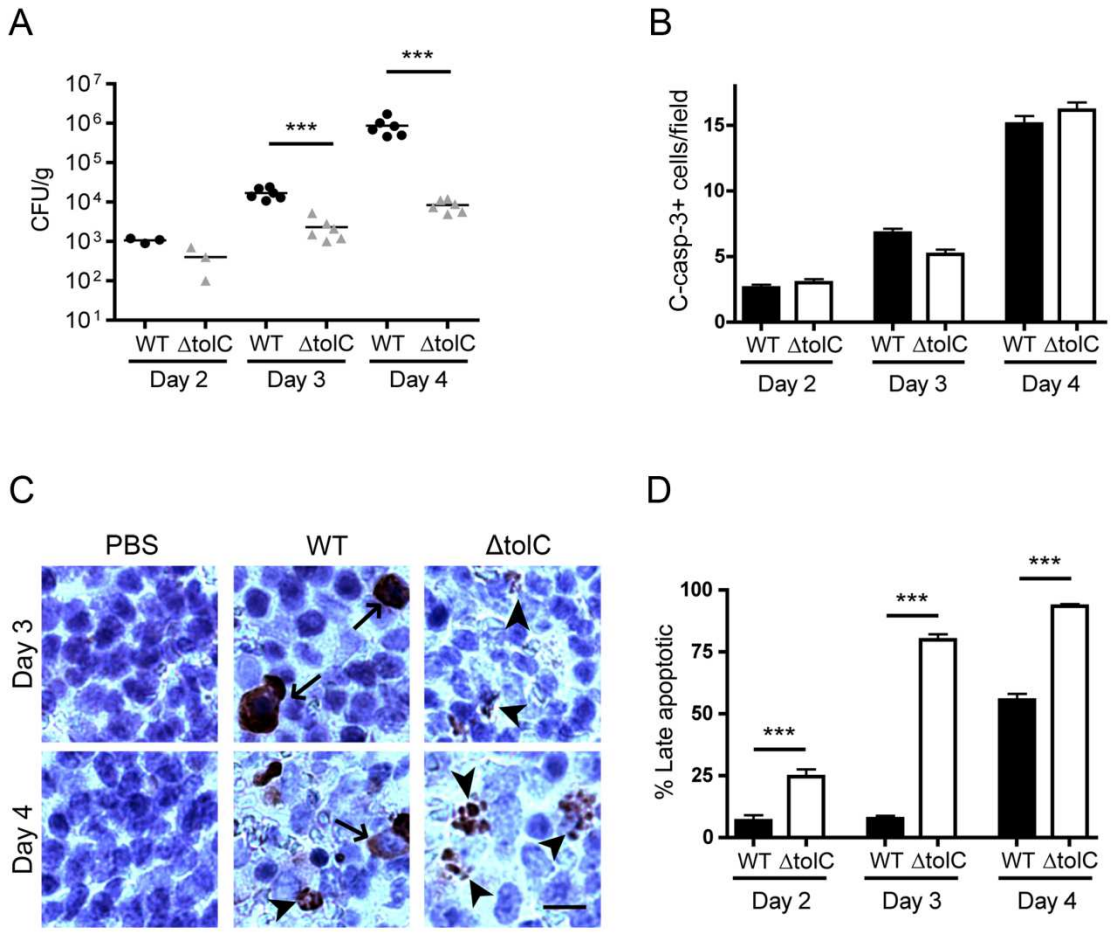

Figure 3.16: The LVS delays induction of apoptosis during infection of mice in a TolC-dependent manner. C3H/HeN mice were intranasally infected with a sublethal dose (5 x 10^3 CFU) of the WT LVS or Δ*tolC* mutant. **(A)** Bacterial burdens in the spleen on days 2, 3, and 4 post-infection were determined by plating for CFU. **(B)** Spleens harvested on days 2, 3 and 4 post-infection were sectioned and labeled using an anti-cleaved caspase-3 antibody. Cleaved caspase-3-positive cells were quantified based on two sections per spleen and ten fields per section. **(C)** Representative immunohistochemistry analysis of infected spleens. Arrows indicate intact cells expressing cleaved caspase-3 in the cytoplasm. Arrowheads indicate fragmented apoptotic nuclei containing cleaved caspase-3. Scale bar = 10 μm. **(D)** Caspase-3-positive cells from panel **B** were characterized as early or late apoptotic based on cleaved caspase-3 localization and nuclear fragmentation. The percentage of total caspase-3-positive cells undergoing late stage apoptosis was calculated for each time point. Bars represent means ± SEM of 2–3 independent experiments (total n = 4–6 mice per strain per time point). ***P <0.001; calculated by Student's t-test.

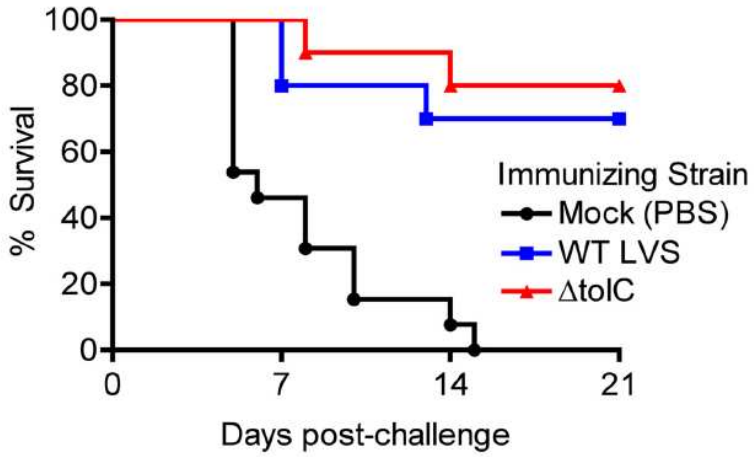

Figure 3.17: Mice vaccinated with the LVS Δ*tolC* mutant are protected from lethal LVS challenge. Mice were intranasally vaccinated with PBS (mock) or with 1 x 10^3 CFU of the WT LVS or Δ*tolC* mutant. All mice were intranasally challenged with 1 x 10^8 CFU of the WT LVS six weeks post-vaccination. Mice were monitored for survival for 21 days following challenge. Data represent three independent experiments (total n = 9-12 mice per vaccinating strain).

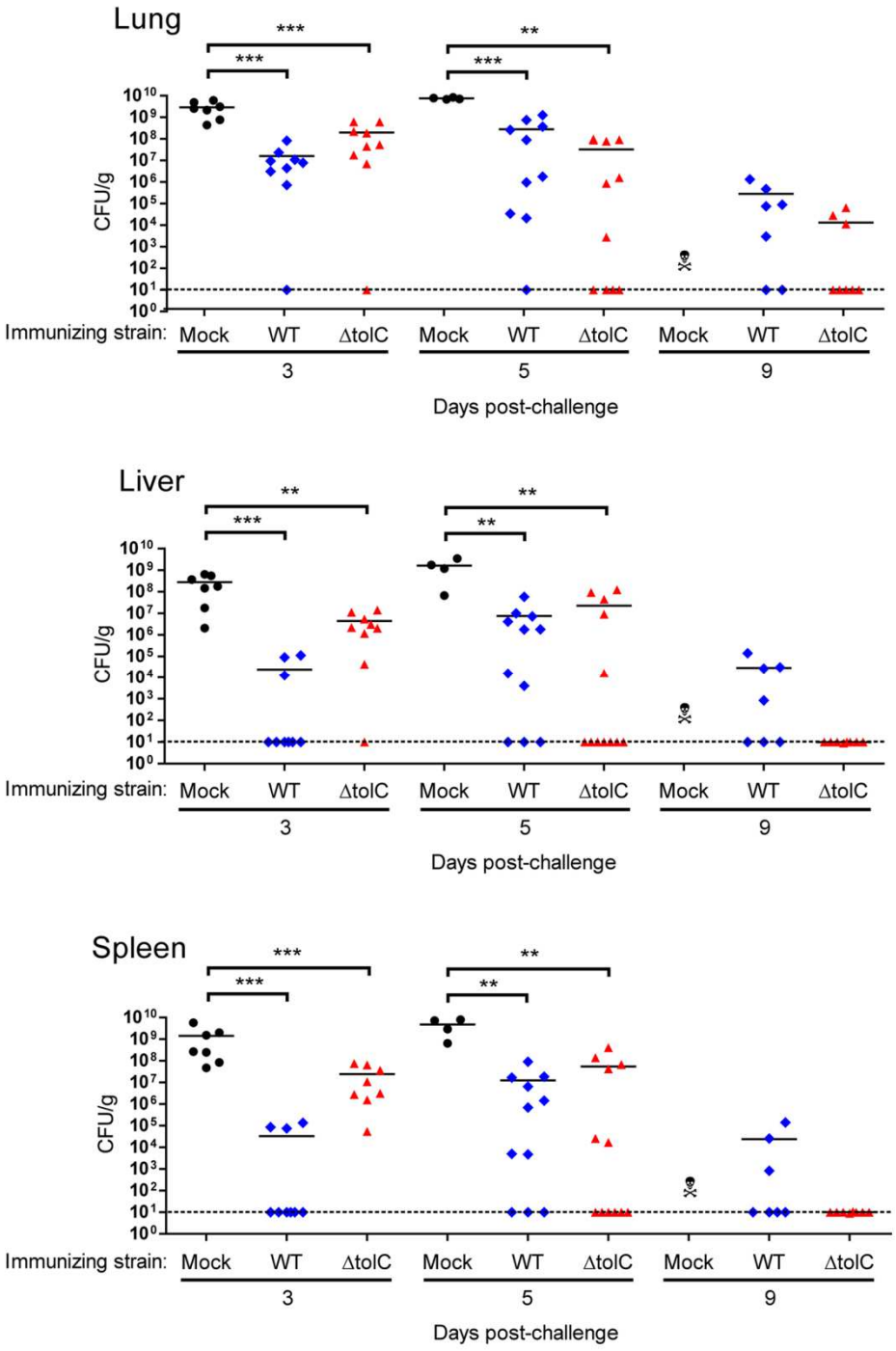

Figure 3.18. Comparison of organ burdens in mock-vaccinated mice with WT LVS- and Δ*tolC*-vaccinated mice. Mice were intranasally vaccinated with PBS (mock) or with 5 x 10^3 CFU of the WT or Δ*tolC* LVS. All mice were intranasally challenged with 1 x 10^8 CFU of the WT LVS six weeks post-vaccination, and then sacrificed at days 3, 5, or 9 post-challenge. Bacterial burdens in the lungs, liver, and spleen were determined by plating for CFU and are expressed as CFU/g tissue. The limit of detection was 10 CFU. Results represent three independent experiments (total n= 10 mice per vaccinating strain per time point). All PBS-vaccinated mice

died by day 9 post-challenge. **P < 0.01, ***P < 0.001; calculated by the Mann-Whitney test for nonparametric data.

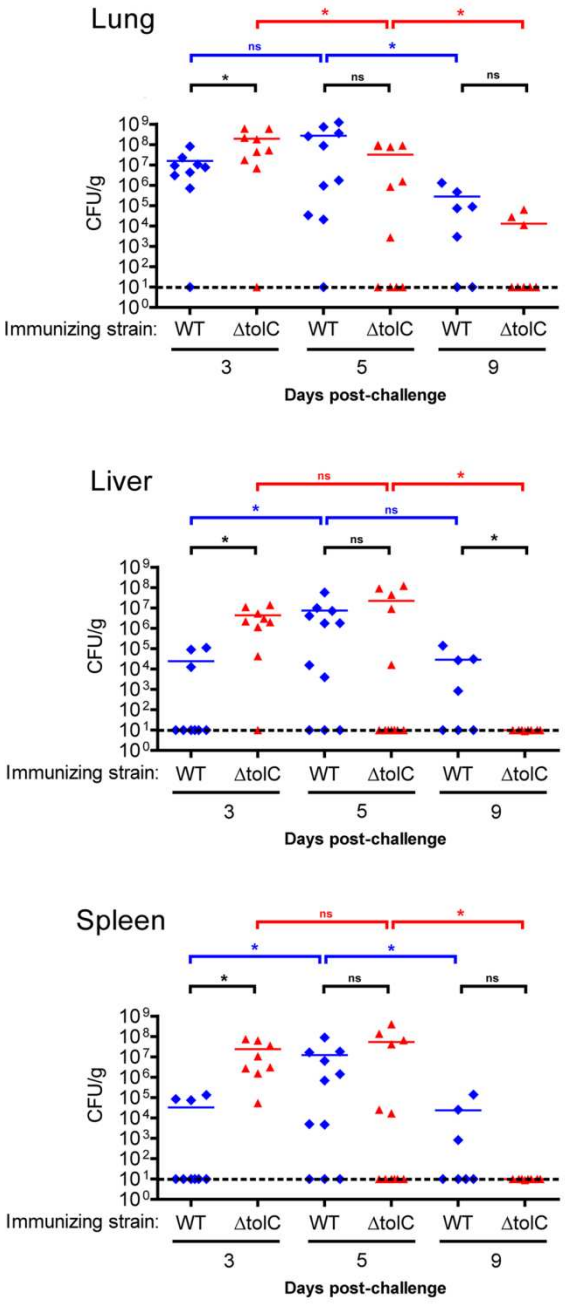

Figure 3.19: Mice vaccinated with the LVS Δ*tolC* mutant clear WT challenge doses faster than mice vaccinated with the WT LVS. Mice were intranasally vaccinated with 1 x 10^3 CFU of the WT LVS or Δ*tolC* mutant. All mice were intranasally challenged with 1 x 10^8 CFU of the WT LVS six weeks post-vaccination, and then sacrificed at days 3, 5, or 9 post-challenge. Bacterial burdens in the lungs, liver, and spleen were determined by plating for CFU and are expressed in CFU/g tissue. The limit of detection was 10 CFU. Results represent three independent experiments (total n = 10 mice per vaccinating strain per time point). *P < 0.05; ns, not significant; calculated by the Mann-Whitney test for nonparametric data.

Table 3.1: Survival of mice following vaccination with the WT LVS or Δ*tolC* mutant and challenge with the WT LVS.

Vaccinating strain	Vaccinating dose (CFU)	Survival	Challenge strain	Challenge dose (CFU)	Survival*
WT	$5x10^2$	3/3	WT	$1x10^8$	3/3
WT	$5x10^3$	2/3	WT	$1x10^8$	2/2
WT	$5x10^4$	1/3	WT	$1x10^8$	1/1
Δ*tolC*	$5x10^2$	3/3	WT	$1x10^8$	2/3
Δ*tolC*	$5x10^3$	3/3	WT	$1x10^8$	3/3
Δ*tolC*	$5x10^4$	3/3	WT	$1x10^8$	3/3

* All mice that survived vaccinations were challenged with $1x10^8$ CFU of WT LVS.

CHAPTER 4: Contribution of TolC to the virulence of *Francisella tularensis* Schu S4.

I. Introduction.

Francisella tularensis is a highly virulent, Gram-negative human pathogen and the causative agent of tularemia. The most lethal form of tularemia occurs following pneumonic exposure; inhalation of as few as ten bacteria are sufficient to cause severe disease in humans (196). There are two clinically relevant subspecies of *F. tularensis*: subsp. *tularensis* (Type A), and subsp. *holarctica* (Type B) (197). The *tularensis* subspecies is highly virulent and causes the most severe form of tularemia, while the *holarctica* subspecies is comparably less virulent and causes a milder disease. While strains exhibiting low virulence to humans have proven useful for preliminary characterization of *F. tularensis* virulence in mice, experimentation with human pathogenic, Type A *F. tularensis* strains is critical for a more complete understanding of *F. tularensis* pathogenesis.

We previously identified a role for the TolC protein in the virulence and host suppressive activities of the LVS (Chapter 3) (114, 136). We demonstrated that TolC is necessary for the ability of the LVS to delay induction of host cell apoptosis and enable optimal bacterial replication within host cells and during organ colonization in mice (Figure 3.3) (136). The *F. tularensis* genome encodes three proteins orthologous to the *E. coli* TolC protein: TolC (FTT1724), FtlC (FTT1095), and SilC (FTT1258). In previous studies, TolC and FtlC were shown to participate in LVS multidrug efflux, while only TolC contributed to virulence (114). The contribution of SilC to virulence and/or multidrug efflux has not been examined for any *F. tularensis* strain. Given that phenotypes obtained with attenuated or less virulent *F. tularensis* strains, such as the LVS, are not always reproduced in fully virulent strains, we sought to characterize the role of TolC, FtlC, and SilC in the virulence of the human pathogenic Schu S4 strain.

Here, we constructed deletion mutants of the *tolC*, *ftlC*, and *silC* genes in the human pathogenic *F. tularensis* Schu S4 strain. We determined the contributions of TolC, FtlC, and SilC to Schu S4 multidrug resistance, and found that all three proteins participate in multidrug resistance. In

contrast to these results, only the Schu S4 Δ*tolC* mutant exhibited hypercytotoxicity towards host cells and suboptimal intracellular replication compared to the WT. Finally, we performed intranasal and intradermal mouse infection experiments with each deletion mutant, and found that the Schu S4 Δ*tolC* mutant was attenuated for virulence via both infection routes, while the Δ*ftlC* and Δ*silC* mutants exhibited less severe virulence defects. Taken together, the results reported here demonstrate that TolC is a critical Schu S4 virulence factor, and lay the groundwork for future work to define TolC's contributions to the virulence of human pathogenic *F. tularensis* strains.

II. Results.

Construction of Schu S4 deletion mutants. TolC is the prototypical OM component of the T1SS used by Gram-negative bacteria to secrete proteins from the cytoplasm directly to the extracellular milieu in a single, ATP-dependent step. Previous bioinformatic analysis of the Schu S4 genome identified two open reading frames predicted to encode proteins orthologous to the well-characterized *E. coli* TolC protein: *tolC* (FTT1724), and *ftlC* (FTT1095c) (Figure 4.1) (114). Subsequent analysis identified a third ortholog with lower homology to *E. coli* TolC but with significant homology to a similar *E. coli* outer membrane protein, SilC. This protein was previously characterized as an outer membrane protein of the Schu S4 strain and annotated as SilC (198). To begin to investigate the role of each protein in Schu S4 pathogenesis, we constructed unmarked chromosomal deletion mutants using an allelic exchange protocol (164). Additionally, we constructed unmarked chromosomal complementation strains for the Δ*tolC* and Δ*ftlC* deletion mutants by reintroducing the *tolC* or *ftlC* open reading frames downstream of the highly conserved *glmS* gene (164). Presence or absence of the *tolC*, *ftlC*, and *silC* genes was verified by PCR (Figure 4.2A and C). Using polyclonal antibodies raised against the TolC and FtlC proteins from the LVS, we confirmed loss of TolC and FtlC protein expression in the Schu S4 Δ*tolC* and Δ*ftlC* deletion mutants, and recovery in the complemented strains (Figure 4.2B and D). In vitro analysis of each mutant demonstrated that neither the Δ*tolC*, Δ*ftlC*, nor Δ*silC* mutants exhibited growth defects in a variety of media commonly used for *Francisella* cultivation (Figure 4.3).

TolC, FtlC, and SilC contribute to Schu S4 multidrug resistance. In addition to participating in the active secretion of proteins across the Gram-negative double membrane via the T1SS, TolC is the OM component of multidrug efflux systems that export a wide variety of antibiotics, drugs, and other toxic compounds from the cell (117). Previous work from our lab identified TolC and FtlC as being important for multidrug resistance in the LVS, while SilC has not been studied to date (114, 136). To investigate the contributions of TolC, FtlC, and SilC to Schu S4 multidrug resistance, we tested each mutant strain for susceptibility to a variety of drugs and antibiotics via growth inhibition assays (Table 4.1). Our results show that loss of TolC, FtlC, or SilC led to increased susceptibility to a broad range of drugs tested compared to the WT Schu S4 strain, indicating that TolC, FtlC, and SilC are all components of Schu S4 multidrug resistance machineries. In line with our previous bioinformatic analysis, the Schu S4 TolC and FtlC proteins appear to have overlapping substrate specificities, while SilC facilitated the efflux

of CCCP, nalidixic acid, and silver nitrate, three compounds known to be exported by *E. coli* SilC/CusC proteins (Table 4.1).

The Schu S4 Δ*tolC* mutant replicates to lower levels than the WT within BMDM. *F. tularensis* is a facultative intracellular pathogen. A defining feature of *F. tularensis* during infection is its ability to escape the phagosome, enter the cytoplasm, and multiply to high levels prior to host cell death and bacterial release (79, 97). To determine the function of TolC, FtlC, and SilC in the ability of Schu S4 to invade and replicate within host cells, we performed intracellular replication experiments. At early times post-infection (3 hours), intracellular CFU of the Δ*tolC*, Δ*ftlC*, and Δ*silC* mutant strains were similar to WT Schu S4, indicating that none of the three TolC paralogs play a significant role in initial infection of BMDM or escape from the phagosome (Figure 4.4A). At later stages of infection (24 hours), however, intracellular CFU from Δ*tolC*-infected cells were lower than the WT Schu S4, while the Δ*ftlC* and Δ*silC* mutants showed no differences compared to the WT (Figure 4.4B-C). These results indicate that, even though the Schu S4 Δ*tolC* mutant is able to replicate to high levels within host cells, TolC is required for maximal intracellular replication of the Schu S4 strain following initial infection.

The Schu S4 Δ*tolC* mutant is hypercytotoxic to host cells compared to the WT. Based on the observation that the Schu S4 Δ*tolC* mutant exhibited an intracellular replication defect compared to the WT, we hypothesized that the Δ*tolC* mutant may trigger increased lysis of host cells, which would result in loss of replicative niches and account for the decreased replication. This was shown previously in studies using the LVS; an LVS Δ*tolC* mutant triggered premature apoptosis of host cells during infection compared to the WT LVS, resulting in reduced intracellular replication (Figures 3.2 and 3.3). We sought to determine if the Schu S4 Δ*tolC*, Δ*ftlC*, or Δ*silC* mutant strains triggered increased host cell death compared to the WT via LDH release assays. The Δ*tolC* mutant strain exhibited hypercytotoxicity to BMDM compared to the WT Schu S4 (Figure 4.5A). In contrast, the Δ*ftlC* and Δ*silC* mutants induced similar levels of cytotoxicity as the WT Schu S4 (Figure 4.5B-C). Complementation of the Schu S4 Δ*tolC* mutant reduced cytotoxicity back to WT levels (Figure 4.5A). These data indicate that the Schu S4 Δ*tolC* mutant is hypercytotoxic to BMDM compared to the WT, and further suggest that the function of TolC in Schu S4 is distinct from the roles of FtlC and SilC.

TolC, FtlC, and SilC contribute to Schu S4 virulence in mice. Previous work from our lab showed that TolC and, to a lesser degree, FtlC, contribute to LVS virulence in mice (114).

However, the contributions of TolC, FtlC, and SilC to the virulence of fully pathogenic *Francisella* strains have not been investigated. Using intranasal and intradermal mouse infection models, we investigated the contributions of each protein to Schu S4 virulence. C3H/HeN mice were infected with 10 CFU of the WT Schu S4 strain or 10-100 CFU of the Δ*silC* mutant, 10-1,000 CFU of the Δ*ftlC* mutant, or 10-10,000 CFU of the Δ*tolC* mutant. In agreement with the high virulence of the Schu S4 strain, all mice infected with 10 CFU of the WT died within 5 days post-infection regardless of infection route (Figures 4.6 and 4.7). Mice infected via the intranasal route with 10 CFU of the Schu S4 Δ*ftlC* and Δ*silC* mutants survived longer than WT-infected mice, but succumbed to infection with 100 CFU of the Δ*ftlC* or Δ*silC* mutants (Figure 4.6B-C). In contrast, mice infected intranasally with up to 1,000 CFU of the Δ*tolC* mutant survived longer than WT-infected mice (Figure 4.6A). Similar experiments using the intradermal route of infection revealed a loss of virulence for the Δ*tolC* and Δ*ftlC* mutants, as mice infected with up to 1,000 CFU of the Δ*ftlC* mutant, or up to 10,000 CFU of the Δ*tolC* mutant, survived the infections (Figure 4.7A-B). In contrast, the Δ*silC* mutant was just as virulent as the WT Schu S4 strain via the intradermal infection route, as mice infected with 10 CFU of the Δ*silC* mutant succumbed to the infection (Figure 4.7C). Using the results from these infection experiments, we estimated the 50% lethal doses (LD_{50}) for each deletion mutant (Table 4.2). These estimations indicated that, of the Schu S4 Δ*tolC*, Δ*ftlC*, and Δ*silC* mutants, the Δ*tolC* mutant is the most severely attenuated for virulence in mice. These results, together with the multidrug sensitivity and cell culture results presented above, suggest that TolC's function in virulence is not simply due to impaired multidrug efflux ability, as the Δ*ftlC* and Δ*silC* mutants exhibit sensitivity to several antibiotics but are not hypercytotoxic to host cells, exhibit no replication defects, and are not as attenuated as the Δ*tolC* mutant for Schu S4 virulence.

III. Discussion.

F. tularensis is a highly virulent Gram-negative human pathogen. A hallmark of *F. tularensis* infection is its ability to interfere with host immune responses during infection, but many bacterial factors responsible for immune evasion remain uncharacterized. We previously described a role for the TolC protein in the virulence of the LVS and the ability of the LVS to delay host cell death during infection (Figures 3.1 and 3.3) (136). TolC is the canonical OM pore protein involved in type I protein secretion and multidrug efflux from Gram-negative bacteria. Genomic analysis of the *F. tularensis* Schu S4 genome identified three proteins with high homology to the *E. coli* TolC protein: FtlC, SilC, and TolC. Here, we constructed Δ*tolC,* Δ*ftlC*, and Δ*silC* deletion mutants and determined the contributions of each protein to multidrug efflux, interactions with host cells, and virulence in the human pathogenic *F. tularensis* Schu S4 strain. Our results demonstrate that TolC, FtlC and SilC all contribute to Schu S4 multidrug efflux. Importantly, we show that only the Δ*tolC* mutant is hypercytotoxic to BMDM and has a reduced ability to replicate intracellularly. Finally, we evaluated the relative importance of TolC, FtlC, and SilC for Schu S4 virulence, and show that while SilC has a negligible role for virulence in mice, FtlC and, to a much greater degree, TolC, contribute to the virulence of *F. tularensis* Schu S4.

Bacterial pathogens have evolved many ways to counteract the harmful effects of antibiotics and other deleterious compounds, including the use of multidrug efflux systems. Multidrug efflux systems reliant on TolC and its orthologs are conserved across bacteria and often are critical mediators of bacterial virulence (199-202). Previous work from our lab identified roles for TolC and FtlC in the ability of the LVS to resist a variety of antibiotics and other toxic chemicals (114). Here, we characterize a role for TolC, FtlC, and an additional ortholog, SilC, in the ability of the Schu S4 strain to resist antibiotics and other small molecules. Our experiments suggest that SilC function in multidrug efflux is distinct from the functions of TolC and FtlC (Table 4.1). Genomic analysis indicated that the Schu S4 SilC protein is more similar to SilC/CusC proteins than to the *E. coli* TolC homolog involved in protein secretion via the type I pathway. In *E. coli*, SilC/CusC proteins participate in the efflux of cationic molecules including CCCP, nalidixic acid, and silver nitrate (203-205). In agreement with the Schu S4 *silC* gene encoding a protein functionally analogous to the *E. coli* SilC protein, the Schu S4 Δ*silC* mutant was hypersensitive to CCCP, nalidixic acid, and silver nitrate compared to the WT. Additional studies are needed to

determine the involvement of TolC and FtlC in the efflux of CCCP, nalidixic acid, and silver nitrate.

Multidrug efflux and type I protein secretion both rely on the TolC family of OM pore proteins for the passage of small molecules and proteins across the periplasm and into the extracellular milieu. While our drug sensitivity experiments indicated that TolC, FtlC, and SilC all participate in multidrug efflux (Table 4.1), our mouse infection experiments revealed that each OM pore protein examined contributes to Schu S4 virulence to varying degrees (Figures 4.6 and 4.7; Table 4.2). Together, these results suggest that the contribution of TolC to Schu S4 virulence is independent of multidrug efflux, as the Δ*tolC* mutant was highly attenuated compared to the Δ*ftlC* and Δ*silC* mutants, despite similar roles in multidrug efflux. To investigate possible mechanistic reasons for the high level of attenuation observed for the Δ*tolC* mutant, we conducted a series of cell culture experiments. Previous work from our group using the LVS demonstrated that the LVS Δ*tolC* mutant is attenuated for virulence due to its inability to suppress host cell apoptosis during infection (Figures 3.3 and 3.16) (114, 136). As a result, the LVS Δ*tolC* mutant does not replicate within host cells as well as the WT. Our experiments here show a similar role for TolC during Schu S4 infection of macrophages, as the Schu S4 Δ*tolC* mutant is hypercytotoxic to BMDM during infection and replicates to lower levels within host cells compared to the WT (Figures 4.4A and 4.5A). Importantly, the Δ*ftlC* or Δ*silC* mutants were not hypercytotoxic to BMDM, and both replicated within cells to similar levels as the WT. Together, these cell culture experiments reinforce the hypothesis that the contribution of TolC to Schu S4 virulence is not solely due to its role in multidrug efflux and reinforce the hypothesis that TolC facilitates the secretion of proteins aimed at interfering with host immune responses. In other bacteria, loss of TolC leads to a reduced ability to efflux antibiotics and other harmful compounds, and thus leads to defects in bacterial survival and virulence. We do not believe this to be the case with our Schu S4 Δ*tolC* mutant, as TolC's function in Schu S4 virulence appears to be distinct from its role in multidrug efflux. We hypothesize that any virulence defects of the Δ*tolC* mutant caused the decreased ability for multidrug efflux are sufficiently compensated for by FtlC and SilC during Schu S4 infection of BMDM and mice.

Taken together, the work presented here indicates that the *F. tularensis* Schu S4 genome encodes three TolC orthologs that contribute to multidrug efflux and/or bacterial virulence in the mouse model of tularemia. While TolC, FtlC, and SilC all function in multidrug efflux, our results

indicate that loss of TolC has the most severe impact on Schu S4 virulence. The data presented here reinforce the hypothesis that TolC functions in the secretion of virulence factors aimed at disabling host responses during *F. tularensis* infection and lay the groundwork for future studies aimed at investigating TolC and TolC-secreted effector proteins by virulent *F. tularensis* strains.

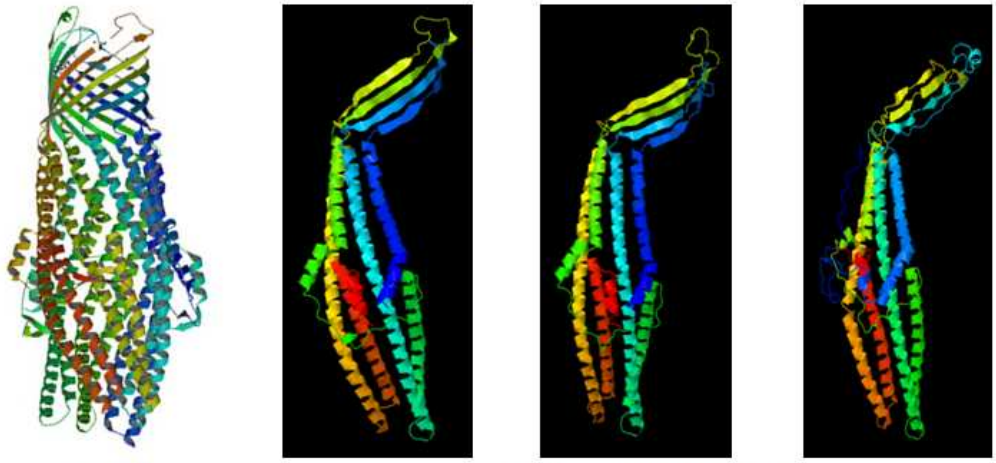

	E. coli	*F. tularensis* Schu S4		
	TolC	**TolC**	**FtlC**	**SilC**
Length (aa):	493	509	460	490
Identity:	100%	27%	18%	13%
Similarity:	100%	47%	45%	38%

Figure 4.1: *F. tularensis* Schu S4 encodes three *E. coli* TolC orthologs. Each Schu S4 protein was compared to the *E. coli* TolC protein via CLUSTALW alignment. Protein sequence length, percent identity, and percent similarity to *E. coli* TolC are shown. Hypothetical *F. tularensis* Schu S4 TolC, FtlC, and SilC monomeric protein structures were derived from Phyre analysis (206) using solved crystal structures as templates. TolC and FtlC were modeled to the *E. coli* TolC protein, while SilC was modeled to the *E. coli* CusC/SilC protein.

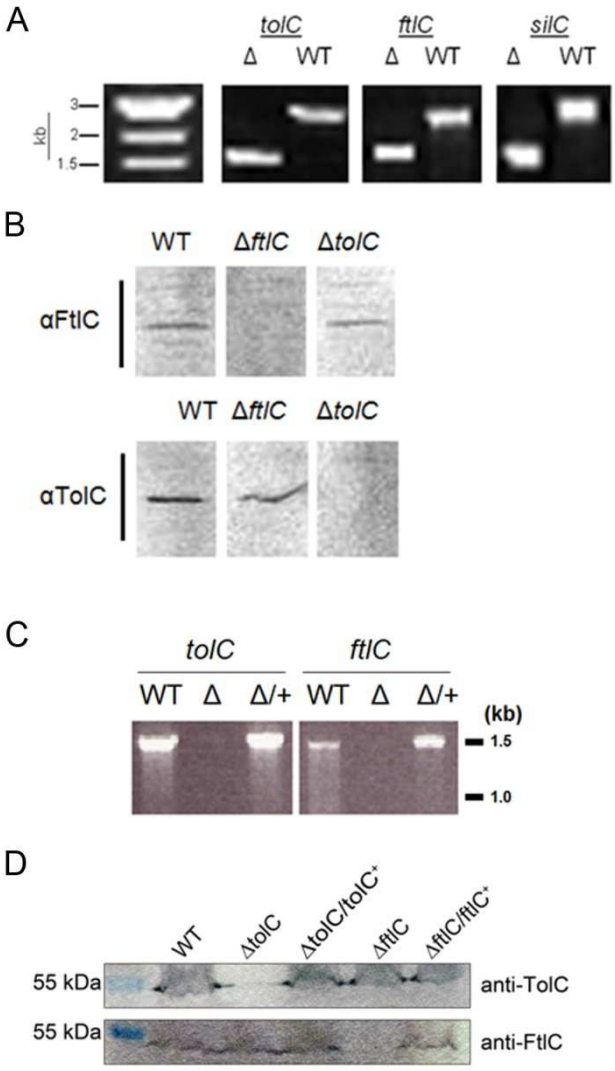

Figure 4.2: PCR and Western blot analysis of Schu S4 deletion mutants and complemented strains. (A) Absence of the *tolC*, *ftlC*, and *silC* genes in the indicated deletion strains was confirmed via PCR using primers upstream and downstream of the indicated ORF. **(B)** Bacterial lysates from equivalent amounts of the WT Schu S4 or the indicated deletion strains were separated via SDS-PAGE. Loss of TolC or FtlC expression was confirmed via Western blot. **(C)** Absence of the *tolC or ftlC* genes in the indicated deletion or complemented strains was determined via PCR using primers to the coding region of the indicated ORF. **(D)** Bacterial lysates from equivalent amounts of the indicated strains were separated via SDS-PAGE. TolC or FtlC expression was examined via Western blot.

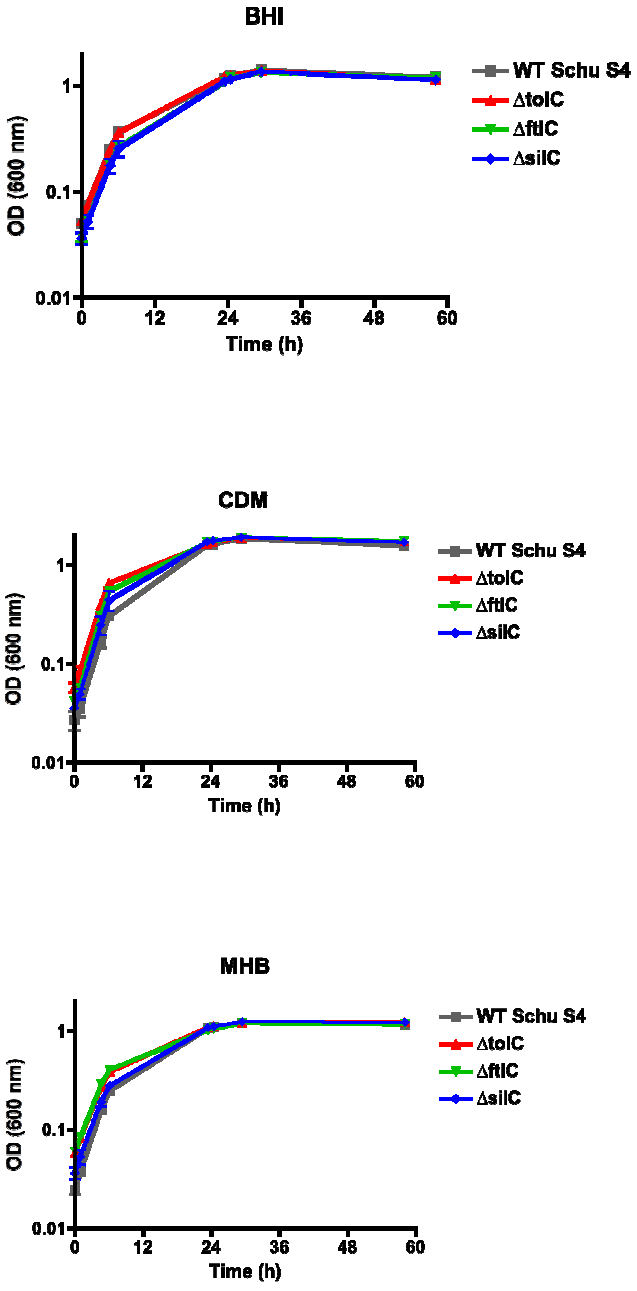

Figure 4.3: Growth of Schu S4 mutant strains in BHI, CDM, and MHB. The indicated strains were grown overnight BHI, MHB or CDM, diluted to an OD_{600} of ~0.05 the following day, and grown for the times indicated. Data represent means ± SEM from three independent experiments.

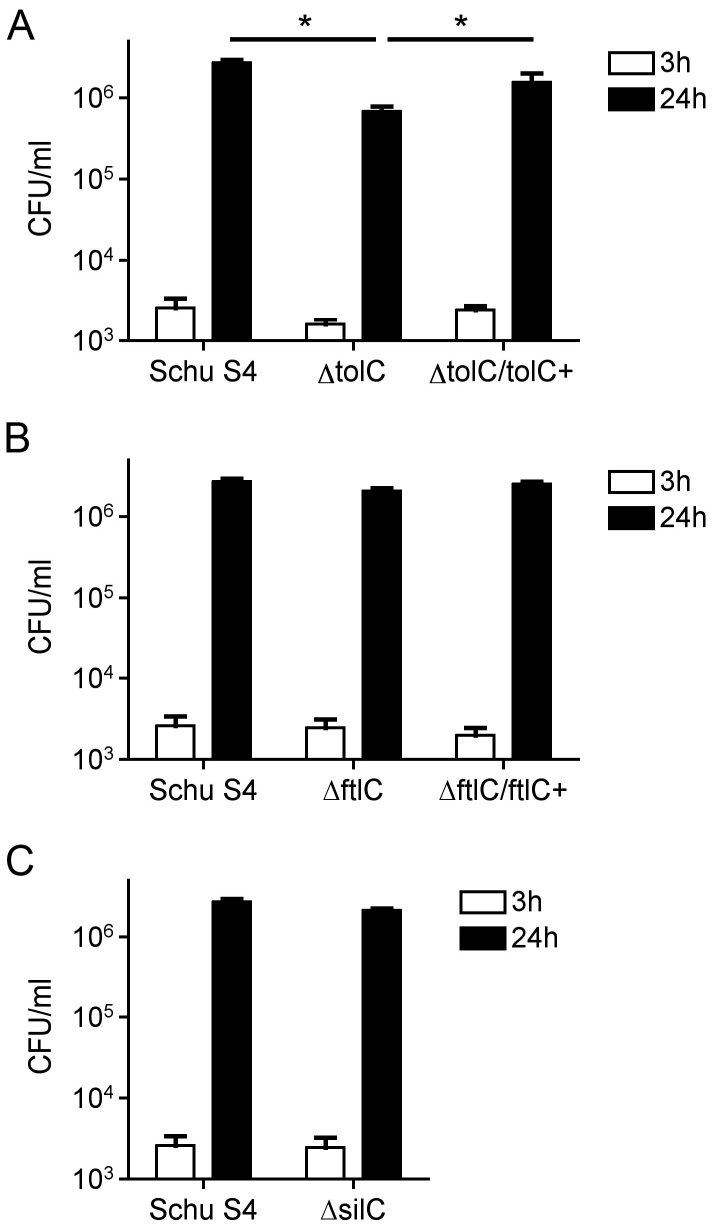

Figure 4.4: The Schu S4 Δ*tolC* mutant replicates to lower levels within BMDM compared to WT Schu S4. BMDM were infected with **(A)** WT Schu S4, the Δ*tolC,* or Δ*tolC*/*tolC*+ strains; **(B)** WT Schu S4, the Δ*ftlC*, or Δ*ftlC*/*ftlC*+ strains; and **(C)** the WT Schu S4 or Δ*silC* mutant strain, all at an MOI of 500. Intracellular replication was quantified by lysing infected BMDM and plating for CFU at 3 and 24 hours post-infection. Data represent means ± SEM of three independent experiments. *, $P < 0.05$, calculated by one-way ANOVA and Tukey's post-test.

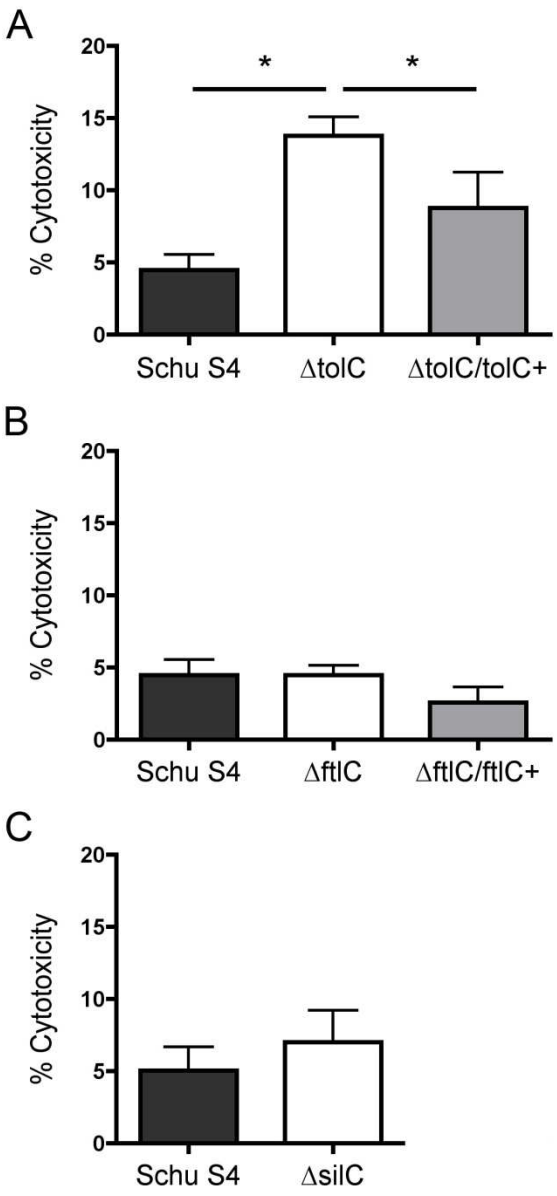

Figure 4.5: The Schu S4 Δ*tolC* mutant is hypercytotoxic to BMDM compared to the WT. BMDM were infected with the WT Schu S4, the Δ*tolC*, Δ*ftlC*, or Δ*silC* mutants, or the Δ*tolC*/*tolC*+ or Δ*ftlC*/*ftlC*+ complemented strains at an MOI of 50. 24 hours post-infection, cytotoxicity was quantified via LDH release. Data represent means ± SEM of three independent experiments. *, $P < 0.05$; calculated by one-way ANOVA and Tukey's post-test.

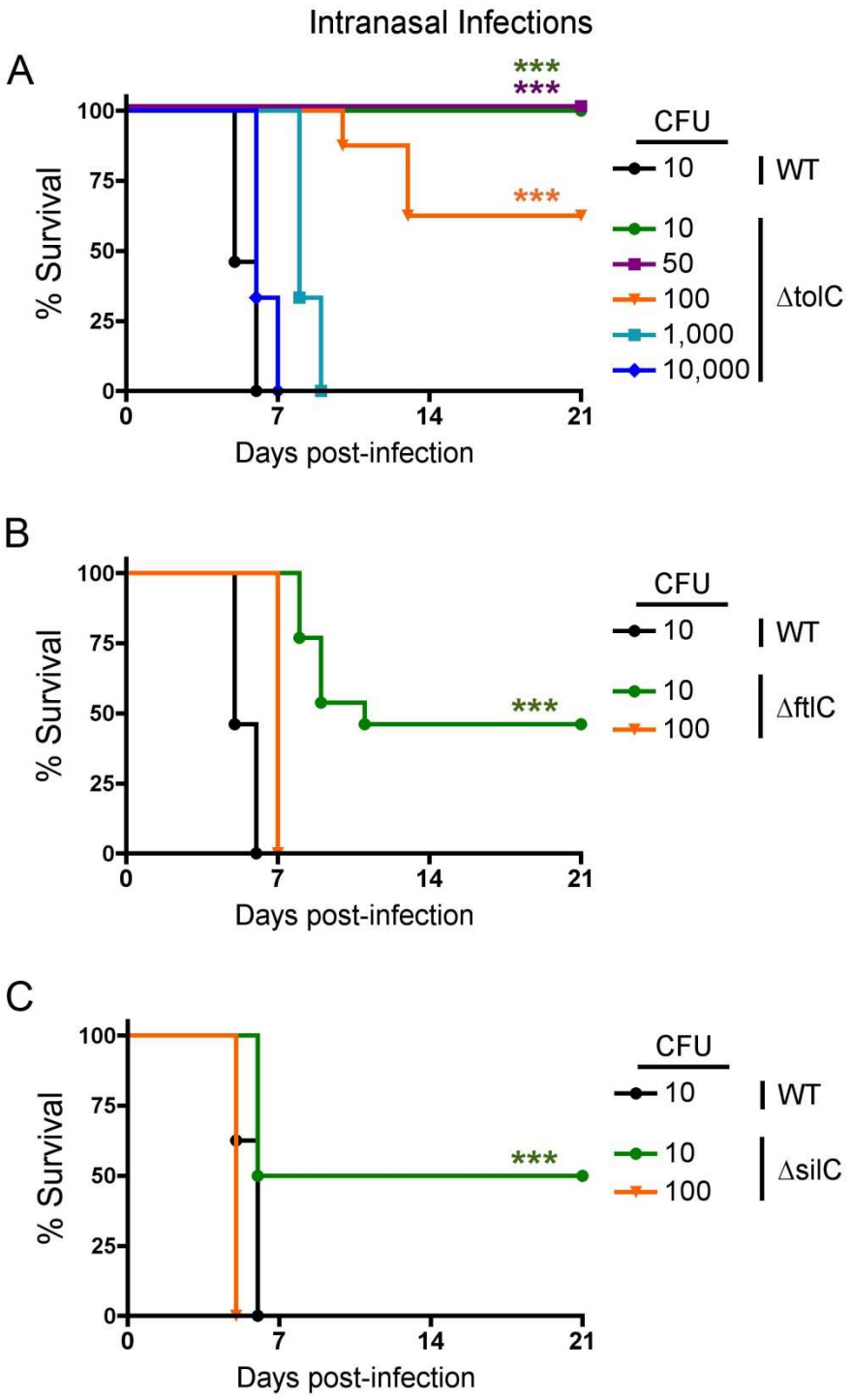

Figure 4.6: The Schu S4 Δ*tolC* mutant is attenuated for virulence in mice via the intranasal route of infection. C3H/HeN mice were infected intranasally with 10 CFU of WT Schu S4 or the indicated doses of the **(A)** Δ*tolC,* **(B)** Δ*ftlC, or* **(C)** Δ*silC* mutants. Mice were monitored for survival for 21 days. For all infections with 10 CFU, total n = 10-13 mice per strain. For infections with 50 or 100 CFU of the Δ*tolC* mutant, n = 5 and 8 mice, respectively.

For all other infections, n = 3 mice. Wherever n ≥ 5 mice, statistical analysis was performed. ***, $p < 0.001$ by the log-rank test, for comparison to infection with 10 CFU of the WT strain.

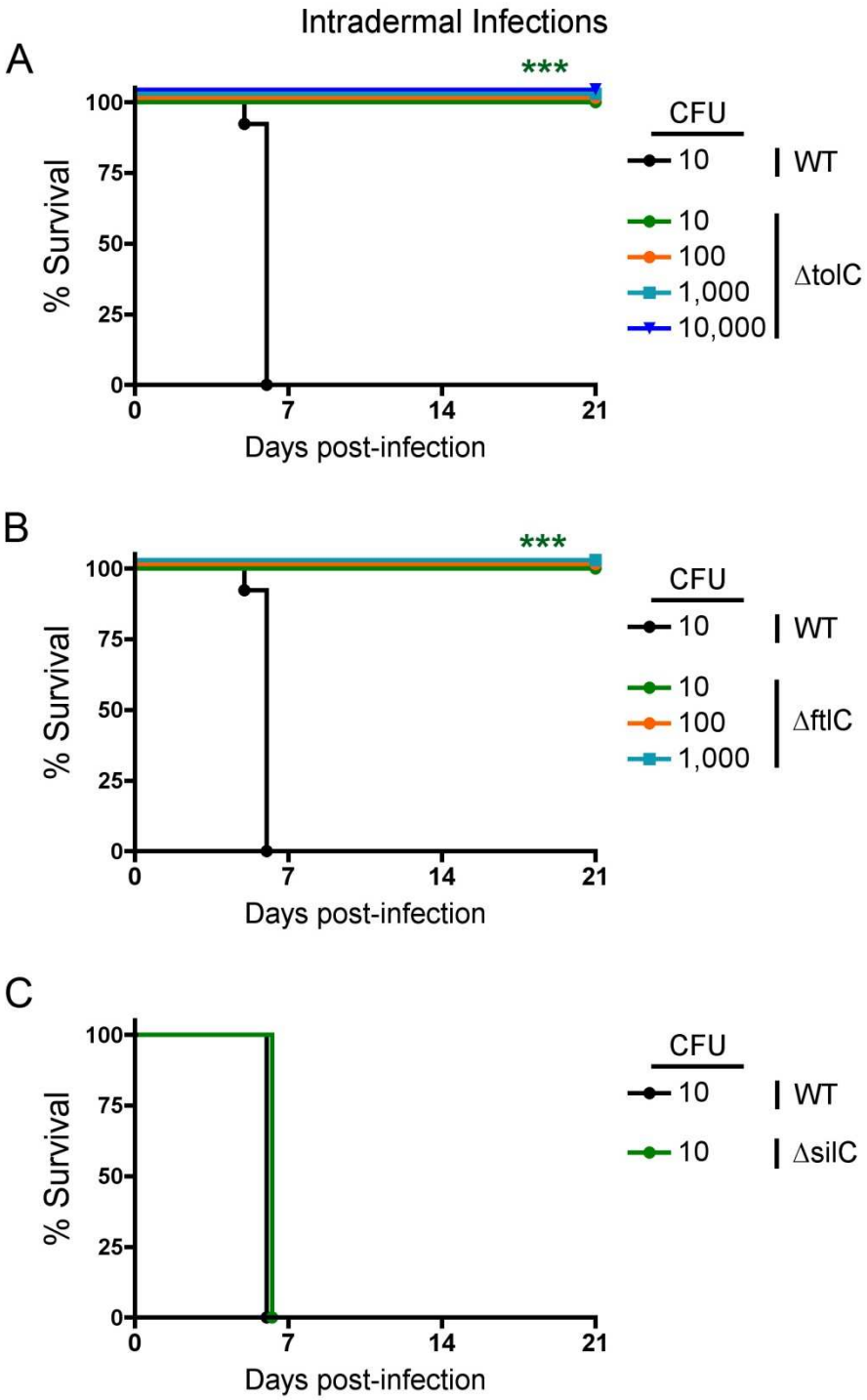

Figure 4.7: The Schu S4 Δ*tolC* and Δ*ftlC* mutants are attenuated for virulence in mice via the intradermal route of infection. C3H/HeN mice were infected intradermally with 10 CFU of WT Schu S4 or the indicated doses of the **(A)** Δ*tolC,* **(B)** Δ*ftlC, or* **(C)** Δ*silC* mutants. Mice were monitored for survival for 21 days. For all WT, Δ*tolC*, and Δ*ftlC* infections with 10 CFU, total n = 10 mice per strain; for all Δ*silC* infections, n=5. For all other infections, n = 3 mice. Wherever n

≥ 5 mice, statistical analysis was performed. ***, $p < 0.001$ by the log-rank test, for comparison to infection with 10 CFU of the WT strain.

Table 4.1: TolC, FtlC, and SilC contribute to Schu S4 multidrug resistance.

Drug Name	µg/disc*	WT	Δ*tolC*	Δ*ftlC*	Δ*silC*
SDS	188	7 ± 1°	13 ± 1	13 ± 0	10 ± 1
Streptomycin	2.5	15 ± 1	15 ± 3	14 ± 2	17 ± 1
Chloramphenicol	1.25	15 ± 2	20 ± 2	18 ± 2	15 ± 2
Erythromycin	5	29 ± 1	39 ± 2	33 ± 1	29 ± 1
Ampicillin	2.5	6 ± 0	6 ± 0	6 ± 0	6 ± 0
CCCP	10	9 ± 0	n.d.	n.d.	13 ± 1
Nalidixic acid	5	20 ± 1	n.d.	n.d.	26 ± 1
Silver nitrate	500	6 ± 0	n.d.	n.d.	11 ± 1

Drug Name^	µg/disc	WT	Δ*tolC*	Δ*ftlC*	*tolC*$^{+}$	*ftlC*$^{+}$
SDS	188	9 ± 1	15 ± 0	15 ± 1	12 ± 1	12 ± 0
Erythromycin	5	34 ± 3	47 ± 0	56 ± 4	34 ± 4	35 ± 4
Chloramphenicol	1.25	18 ± 2	31 ± 1	28 ± 3	28 ± 3	17 ± 2

* The indicated amounts of drugs were added to 6 mm paper discs in 15 µl volumes. n.d., not determined.

$^{\Psi}$ Zones of growth inhibition are shown in mm ± standard deviation from three independent experiments. Values shown in red are significantly different ($P < 0.05$) from the corresponding WT values by Student's t-test.

^ Drug sensitivities of complemented strains were tested in a single experiment.

Table 4.2: Estimated LD_{50} values for Schu S4 mutant strains.

Strain	Intranasal LD_{50} (CFU)*	Intradermal LD_{50} (CFU)
WT Schu S4	<10	<10
Δ*tolC*	200	>10,000
Δ*ftlC*	10	>1,000
Δ*silC*	10	<10

* LD50 estimates were calculated using the method of Reed and Muench as previously described (207).

CHAPTER 5: Open questions and future directions.

The identity of TolC-secreted effectors. A major outstanding question surrounding our data is the identity of TolC-secreted effectors. At this point, we believe that we have ample evidence that the immunomodulatory effects attributable to TolC are, in fact, due to a secreted protein, and not due to TolC itself or structural differences between the WT and Δ*tolC* mutant strains. In addition to the data that support a role for TolC in protein secretion discussed in this dissertation, our lab has evidence demonstrating that *F. novicida* secretes a hemolysin in a TolC-dependent manner (Platz, unpublished data). While this suggests that TolC (>99% identity between *F. novicida* and Schu S4) may participate in type I protein secretion from other *Francisella* species, the *F. novicida* hemolysin protein does not appear to be present in the LVS or virulent strains, as these strains do not exhibit hemolytic activity (208). To this point, conventional approaches taken to identify TolC-secreted effectors have proven fruitless. For example, analysis of supernatants from WT LVS or the Δ*tolC* mutant grown in CDM indicated no differences in secreted protein profiles (McCaig, unpublished data). Therefore, it is possible that TolC-dependent secretion is initiated only upon host cell contact or internalization. This would not be surprising, as activation of the *Brucella* type IV secretion system and *Salmonella* and *Yersinia* type III secretion systems occur upon contact with or internalization into host cells (209-211). Examination of secreted proteins from WT or Δ*tolC* bacteria grown in media designed to mimic intracellular conditions (low Ca^{2+}, low pH, oxidative stress, etc.) could be useful in identifying proteins secreted through TolC following *F. tularensis* interaction with host cells.

The co-infection experiments discussed in Chapter 3 support a model whereby *F. tularensis* secretes effector proteins through TolC to interfere with host cell death pathways prior to the ultimate activation of caspase-3 and apoptosis. If the TolC-secreted effectors responsible for this modulation are soluble and secreted in the absence of host cells, we should be able to suppress host cell death during infection by treating cells with conditioned media from the WT LVS, but not with conditioned media from the Δ*tolC* mutant. Conditioned media were prepared by growing the WT LVS or Δ*tolC* mutant overnight in BMM, collecting cell-free supernatants via centrifugation and subsequent filtration using a 0.22 µm filter. To address the possibility that the TolC-secreted effector proteins responsible for inhibition of cell death are soluble and secreted in the absence of host cells, I seeded BMDM in normal BMM or conditioned BMM from the WT

LVS or Δ*tolC* mutant. I then infected BMDM's with the WT LVS or Δ*tolC* mutant, and quantified cytotoxicity 21 hours post-infection. These experiments revealed that BMDM treated with either WT- or Δ*tolC*-conditioned media were hypersensitive to infection, as cytotoxicity of the WT LVS or Δ*tolC* mutant towards conditioned media-treated BMDM was increased following infection, compared to BMDM cultured in unconditioned media (Figure 5.1). The increases in BMDM death that I observed may be due to an increased propensity of conditioned media-treated BMDM to undergo pyroptosis, as IL-1β release from uninfected BMDM treated with WT- or Δ*tolC*-conditioned media was readily induced following LPS stimulation (Figure 5.2). These results suggest that growth of bacteria in BMM may lead to the release of BMDM-stimulating products, such as DNA, which may lead to inflammasome assembly. If this is the case, death of conditioned media-treated BMDM during infection may be skewed from apoptosis to pyroptosis, thus interfering with our ability to observe any apoptosis-inhibitory effects of proteins found in conditioned media in these experiments. Therefore, the specific effects of WT- and/or Δ*tolC*-conditioned media on apoptotic responses during *F. tularensis* infection of BMDM remain to be determined. Treatment of conditioned media with DNase prior to BMDM treatment, precipitation of proteins from conditioned media, or examination of caspase-3 activation, instead of LDH release, could help lead to the identification of TolC-secreted proteins responsible for inhibiting apoptosis during infection.

As discussed in Chapter 1, T1SS effectors generally contain repeating RTX motifs, have few cysteine residues, and have low isoelectric points. Based on this knowledge, I probed the *F. tularensis* proteome for the presence of proteins containing RTX motifs. My analysis revealed that only one conserved *F. tularensis* protein, GlgB, has a canonical RTX motif. While the role of GlgB in *F. tularensis* has not been examined, it is unlikely that GlgB secretion via TolC accounts for the dramatic phenotypes attributed to TolC in our studies, as GlgB is a metabolic enzyme involved in glycogen synthesis in other organisms and does not appear to be secreted (212-214). In addition to containing RTX motifs, T1SS effectors contain signal sequences that appear to be located in the last ~50 amino acids of the primary structure. To determine if any *F. tularensis* proteins shared sequence homology with known T1SS effectors, I performed a Δ-BLAST analysis (NCBI) comparing whole proteins or the last 60 amino acids of the known T1SS effectors listed in Table 1.1 with *F. tularensis* proteins. This analysis identified no *F. tularensis* proteins with significant C-terminal homology. Thus, it is likely that TolC-secreted effectors of *F.*

tularensis are unique, in that they do not have RTX repeats or share homology with other known T1SS effectors.

Protein secretion via the T1SS relies on the interaction of IM ABC and periplasmic MFP proteins with TolC to form a envelope-spanning channel (Fig 1.6). With this in mind, identification of the proteins that interact with TolC to facilitate secretion in *Francisella* would be extremely useful for biochemical approaches aimed at identifying secreted proteins bound to assembled TolC-MFP-IM ABC complexes. Additionally, many genes encoding T1SS effector proteins in other organisms are genetically arranged adjacent to those encoding the MFP and IM ABC proteins, but distant from the OM pore components such as TolC (116). Accordingly, the identification of the MFP and/or IM ABC proteins that facilitate secretion could be very useful in identifying putative secreted proteins. To begin to investigate the MFP proteins that may be interacting with TolC, we performed Δ-BLAST analysis of the *F. tularensis* genome, using *E. coli* HlyD and AcrA (Figure 1.6) as templates. This analysis revealed five *F. tularensis* proteins (Table 5.1) with high homology to *E. coli* MFP's, all of which have RXXXLXXXXXX[T/S] motifs, characteristic of MFP's that interact with TolC (128), and all of which are highly conserved between low and high virulence *F. tularensis* strains (Table 5.1).

To identify putative IM ABC proteins that may be interacting with TolC, we performed delta-BLAST analysis of the *F. tularensis* genome using *E. coli* HlyB and AcrB as templates. This analysis revealed several proteins with high homology to the *E. coli* IM ABC proteins (Table 5.1). Additionally, several of the putative IM ABC proteins match predicted membrane-associated ABC proteins identified in a recent analysis of the *F. tularensis* genome (215). In order to determine which MFP and IM ABC proteins associate with TolC, and thus identify potential TolC-secreted effector proteins, we could examine MFP and IM ABC mutant strains for the inability to delay host cell apoptosis during infection. Initial studies could take advantage of the *F. novicida* U112 transposon mutant library, and would be aimed at identifying MFP or IM ABC proteins that trigger apoptosis earlier than the WT strain. As a more comprehensive approach at identifying TolC-secreted effectors, we could screen the entire U112 mutant library for mutants that trigger rapid apoptosis compared to the WT strain, followed by phenotypic confirmation in the LVS and/or Schu S4 strains. Upon identifying putative MFP or IM-ABC proteins predicted to be involved in TolC-mediated secretion, we could examine adjacent genes

for expression within host cells. Transcriptional profiling of Schu S4 during infection of macrophages revealed that *tolC* expression did not change during infection (97). This is not unexpected, as TolC is involved in various aspects of cellular physiology in addition to its role in protein secretion (216, 217). However, it would useful to examine transcription and expression of putative effector proteins encoded by genes adjacent MFP's or IM-ABC's that are necessary for inhibition of cell death. Together, these analyses and screening approaches could lead to the successful identification of TolC-associated MFP and IM ABC proteins, and, ultimately, TolC-secreted effectors.

Immune responses elicited by vaccination with the Δ*tolC* mutant. A major aspect of our overarching hypothesis surrounding TolC function in *F. tularensis* is that TolC-secreted effectors interfere with various aspects of host innate immunity, and thus interfere with the development of adaptive immunity. In support of this idea, mice vaccinated with the LVS Δ*tolC* mutant clear lethal challenge bacteria faster than WT-vaccinated mice (Figure 3.19, days 5-9 post-challenge). However, WT-vaccinated mice initially controlled challenge dose replication and/or dissemination from the lung better than Δ*tolC*-vaccinated mice (Figure 3.19, day 3 post-challenge). While we do not yet understand the molecular basis for the altered kinetics of challenge dose clearance, these results are intriguing and raise several possibilities. First, the specific host cell types that are actually infected during primary infection (or vaccination) with the WT LVS or Δ*tolC* mutant are unknown and may differ. Additionally, the identities of host cells undergoing apoptosis during infection of mice are not known. It is possible that differences in the types of infected and/or apoptotic host cells may influence innate immune responses, and in turn, influence the generation, timing, and robustness of adaptive responses. To investigate this possibility, we could infect mice with GFP-expressing bacteria (WT LVS or the Δ*tolC* mutant), and examine infected host cell populations via flow cytometry. Similarly, we could determine the identity of apoptotic cells during infection of mice with the WT LVS or Δ*tolC* mutant by labeling and examining cell surface proteins of caspase-3-positive cells via flow cytometry. Completion of these experiments should allow us to determine if the Δ*tolC* mutant infects different host cell types than the WT and if the Δ*tolC* mutant induces apoptosis of distinct host cell types compared to the WT. Any differences observed in these experiments would help explain the altered kinetics of challenge dose clearance following vaccination with the WT LVS or Δ*tolC* mutant.

Another possible explanation for the altered kinetics of challenge dose clearance observed during our vaccination experiments is that immune cell recruitment to sites of infection following vaccination with the WT LVS or Δ*tolC* mutant are different. However, in preliminary flow cytometry experiments, I observed no differences in the numbers of neutrophils, macrophages, or dendritic cells recruited to the spleen following infection with the WT LVS or Δ*tolC* mutant (Figure 5.3), suggesting that differential immune cell recruitment following vaccination is not the primary basis for the differences in challenge dose clearance kinetics. A possible explanation for the initially better control of challenge doses by WT-vaccinated mice is that vaccination with the WT LVS leads to more effective induction of *F. tularensis*-specific antibody responses. This would make sense, in that the WT LVS is present at higher levels than the Δ*tolC* mutant and persists for longer times following primary infection of mice (136). Additionally, circulating levels of *F. tularensis*-specific antibodies peak approximately 7 weeks post-infection (218), and our challenge experiments were performed 6 weeks post-vaccination. To explore potential differences in the antibody responses to vaccination with the WT LVS or Δ*tolC* mutant, serum from convalescent mice could be probed for reactivity with F. tularensis antigens from heat-killed bacteria. As IgA, IgG1, IgG2a and IgM are the primary *F. tularensis*-specific antibody isotypes generated following primary infection, we could use an ELISA-based approach to determine titers of *F. tularensis*-specific IgA, IgG1, IgG2a, and IgM following vaccination with the WT LVS or Δ*tolC* mutant.

Finally, a possible explanation for faster challenge dose clearance by Δ*tolC*-vaccinated mice is that the Δ*tolC* mutant elicits increased or enhanced T cell responses following vaccination compared to those elicited following WT infection. If this is the case, it could help explain the delayed, but enhanced, responses of Δ*tolC*-vaccinated mice seen during our challenge experiments (Figure 3.19). This also would make sense, as we know that cells infected with the Δ*tolC* mutant undergo rapid apoptosis (Figures 3.3 and 3.16). Apoptotic macrophages (or other Δ*tolC*-infected cells) could be taken up by adjacent phagocytes that then present *F. tularensis* antigen to responding T cells. In support of this possibility, vaccination of mice with apoptotic phagocytes pretreated with live or heat-killed pathogens (*Histoplasma capsulatum*, *Mycobacterium tuberculosis*, and *Toxoplasma gondii*) elicits T cell responses that are protective against subsequent lethal, homologous challenge (219-221). We could characterize the *F.*

tularensis-specific activity of T cells isolated from spleens of mice vaccinated with the WT LVS or Δ*tolC* mutant via ex vivo macrophage co-culture experiments, using a flow cytometric approach with IFN-γ as a readout for T cell activation. Completion of these experiments should elucidate any differences in antibody and T cell responses following vaccination with the WT LVS or Δ*tolC* mutant and may provide a clearer picture of the molecular basis for the differences in kinetics of challenge dose kinetics during vaccination with the WT LVS or Δ*tolC* mutant.

The role of TolC in Schu S4 virulence. My analysis of TolC in the fully virulent Schu S4 strain revealed that, similar to what was seen previously in work with the LVS, the Schu S4 Δ*tolC* mutant is hypercytotoxic to host cells and as a result, is defective for intracellular replication at 24 hours post-infection (Figures 4.4A and 4.5A). The role of TolC in Schu S4-mediated apoptosis has not been examined and should be determined using similar approaches to those using the LVS (Figure 3.3). Additionally, while we expect that the Schu S4 Δ*tolC* mutant is not structurally compromised and that TolC mediates Schu S4 active suppression of host cell death, this must be confirmed by using studies similar to those performed for the LVS (Figures 3.5-3.12). Finally, the Schu S4 data shows that TolC is an important virulence factor in mice, and suggests that the contribution of TolC to virulence in mice is independent of, or in addition to, its role in multidrug efflux, as the Δ*ftlC* and Δ*silC* mutants are not as attenuated as the Δ*tolC* mutant during infection of mice.

Our mouse infection results revealed that both the Schu S4 Δ*tolC* and Δ*ftlC* mutant, but not the Δ*silC* mutant, are attenuated for virulence compared to the WT via the intradermal route of infection (Figure 4.7). Interestingly, the virulence defects observed for the Schu S4 Δ*tolC* and Δ*ftlC* mutants via the intradermal route were several orders of magnitude greater than those seen during intranasal infection experiments (Table 4.2). While WT *F. tularensis* and many *F. tularensis* mutant strains are generally less virulent via the intradermal route compared to the intranasal route (222, 223), our results suggest that the differences we observed are directly attributable to loss of TolC and FtlC, as WT-infected mice showed no difference in survival following infection via either infection route (Figures 4.6 and 4.7). This raises the possibility that TolC and/or FtlC may play a site-specific role during infection that could facilitate dissemination to the lung, a critical step in *F. tularensis* virulence via the intradermal route of infection (223-225). Therefore, analysis of bacterial burdens at sites of infection (skin) and in distal organs

(lungs and spleen) could shed light on the specific role of TolC and TolC-secreted effectors during Schu S4 infection. Finally, the exact degree of attenuation of the Schu S4 Δ*tolC* and Δ*ftlC* mutants during intradermal infections remains to be examined, as all mice survived infection with the highest doses (10,000 and 1,000 CFU, respectively) of each mutant administered (Figure 4.7).

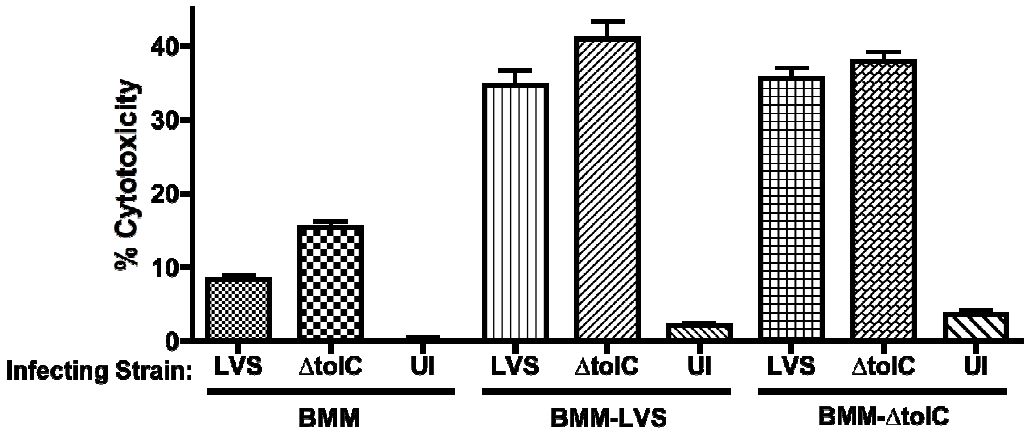

Figure 5.1: Treatment of BMDM with WT LVS- or Δ*tolC*-conditioned media enhances WT- and Δ*tolC*-induced cytotoxicity compared to treatment with normal BMM. BMDM were seeded overnight in normal BMM or conditioned BMM from WT LVS (BMM-LVS) or the Δ*tolC* mutant (BMM-Δ*tolC*). The next day, BMDM were washed and infected with the indicated strains in normal BMM. Cytotoxicity was examined 24 hours post-infection. Results are from two independent experiments with three samples per experiment.

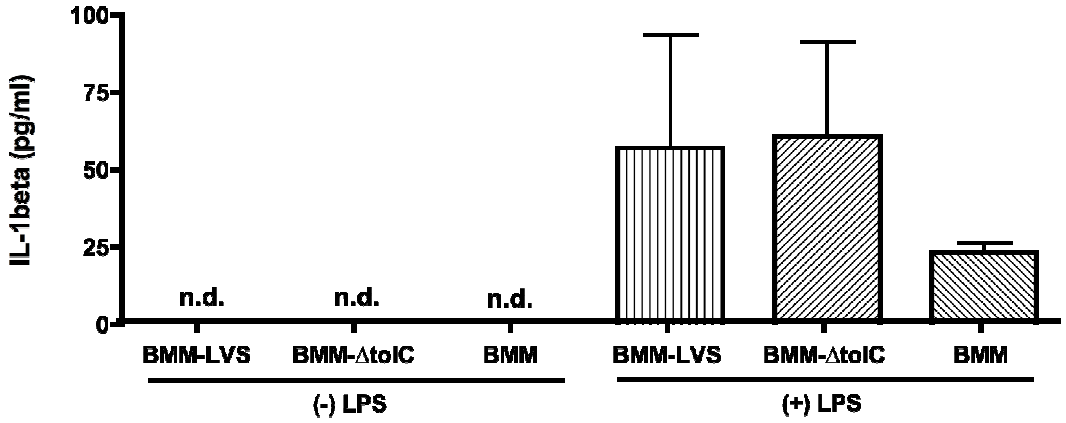

Figure 5.2: Incubation of BMDM with conditioned media from the WT LVS or Δ*tolC* mutant increases IL-1β secretion following LPS stimulation. BMDM were seeded overnight in normal BMM or conditioned BMM from WT LVS (BMM-LVS) or the Δ*tolC* mutant (BMM-Δ*tolC*). The next day, BMDM were washed and incubated with or without 50 ng/ml of *E. coli* LPS diluted in normal BMM. IL-1β release was examined 6 hours post-treatment via ELISA. Results are from two independent experiments with two samples per experiment. n.d., below limit of detection.

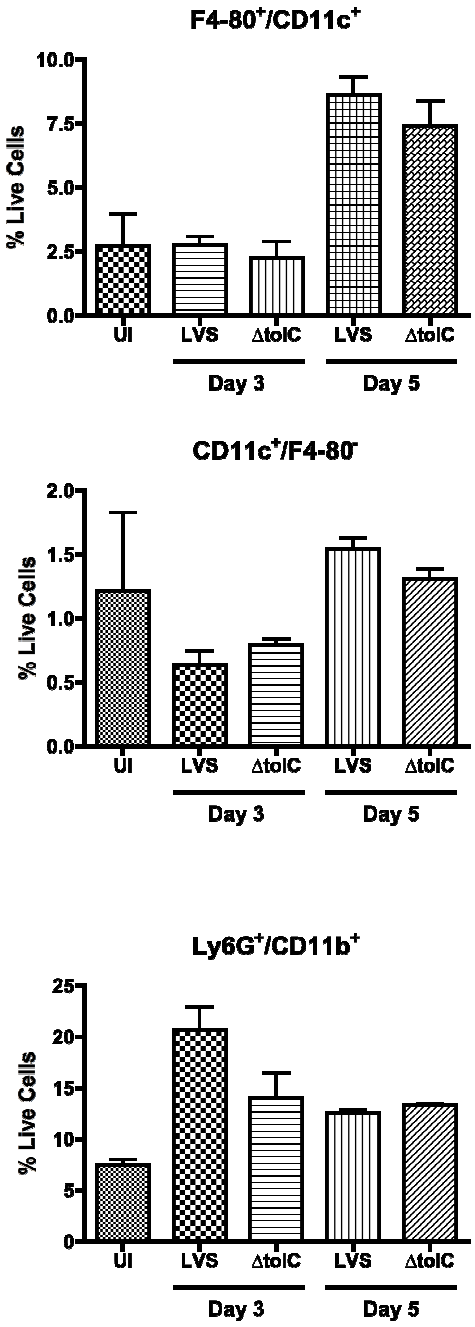

Figure 5.3: Leukocyte recruitment to the spleen is similar following infection of mice with the WT LVS or Δ*tolC* mutant. Groups of two C3H/HeN mice were left uninfected or infected with the WT LVS or Δ*tolC* mutant. At the indicated days post-infection, spleens were harvested from infected mice, and single cell spleen suspensions were labeled with fluorescent antibodies to F4/80, CD11c, CD11b, and Ly6G. The percentage of live cells that were macrophages ($F4/80^+$, $CD11c^+$), dendritic cells ($F4/80^-$, $CD11c^+$), and neutrophils ($Ly6G^+$, $CD11b^+$) were determined via flow cytometry. A representative experiment is shown.

Table 5.1: Putative *F. tularensis* membrane fusion proteins and inner membrane ABC transporters.

Type	Gene[§]	Putative Function	MFP Motif*	% ID[▲]
IM-ABC	FTT0017	Bacteriocin/toxin secretion	-	99
MFP	FTT0018	Membrane fusion protein	RLT	99
IM-ABC	FTT0105	Multidrug efflux	-	99
MFP	FTT0106	Membrane fusion protein	RLS	>99
IM-ABC	FTT0109	LPS biogenesis	-	99
IM-ABC	FTT0110	LPS biogenesis	-	99
IM-ABC	FTT0746	Hydroxybenzoic acid efflux	-	98
MFP	FTT0747	Membrane fusion protein	RLS	97
IM-ABC	FTT0793	LPS biogenesis	-	98
IM-ABC	FTT1256	Cationic drug efflux	-	>99
MFP	FTT1257	Membrane fusion protein	RLS	96
IM-ABC	FTT1335	Met export	-	97
IM-ABC	FTT1336	Met export	-	98
MFP	FTT1654	Membrane fusion protein	RLS/RLT	96
IM-ABC	FTT1655	Unknown	-	97

[§] Gene numbers are from Schu S4 genome annotations (112).
* RLS indicates RXXXLXXXXXS motif on MFP; RLT indicates RXXXLXXXXXT.
[▲] % ID indicates percent identity between proteins from Schu S4 (virulent strain) and *F. novicida* (avirulent strain).

CHAPTER 6: Concluding remarks.

The studies detailed in this dissertation demonstrate that TolC is required for the ability of the LVS to delay induction of apoptosis during infection. TolC thus facilitates optimal LVS replication within host cells and prevents premature exposure of the LVS to extracellular immune responses. The contributions of TolC to immune evasion are evident in our vaccination experiments, where mice vaccinated with the LVS Δ*tolC* mutant appear to develop altered adaptive immune responses and ultimately clear challenge doses faster than mice vaccinated with the WT LVS. Furthermore, this dissertation details my extension of our LVS TolC studies to the fully virulent Schu S4 strain. Using a Schu S4 Δ*tolC* mutant, I showed that TolC is required for Schu S4 virulence. Moreover, my data suggest that the role of TolC in Schu S4 virulence is distinct from its role in multidrug efflux. Taken together, the work detailed here significantly advances our understanding of how TolC functions to facilitate *F. tularensis* pathogenesis.

The results reported here are in contrast to findings in other bacteria, such as *E. coli*, where loss of TolC leads to alterations in various aspects of bacterial physiology, including membrane integrity, sensitivity to ROS, and metabolic defects (216, 217, 226, 227). However, whereas *E. coli* encodes a single TolC protein, the *Francisella* genome encodes three TolC orthologs. We propose that these additional orthologs compensate for any physiological effects that might be caused by loss of TolC in the *F. tularensis* outer membrane. In support of this, none of our Schu S4 deletion mutants exhibited in vitro growth defects or an inability to escape from the phagosome (as evidenced by intracellular CFU 3 hours post-infection; Figure 4.4), where ROS sensitivity would be observed (79, 178). Additionally, TolC, FtlC, and SilC appear to have at least partially overlapping substrate specificities in multidrug efflux experiments (Table 2). Finally, although TolC, FtlC, and SilC were shown to participate in Schu S4 multidrug efflux, only loss of TolC significantly affected virulence during both intranasal and intradermal infections, implicating a specific role for TolC in Schu S4 virulence that is independent of multidrug efflux.

Inhibition of host cell apoptosis appears to be a general strategy employed by intracellular pathogens to combat innate immune responses and facilitate infection. For example: *Ehrlichia, Neisseria*, *Salmonella,* and *Chlamydia* inhibit cytochrome C release from mitochondria (228-

231); *Bartonella*, *Rickettsia*, and enteropathogenic *E. coli* disrupt signaling pathways leading to the induction of apoptosis (232-234); and *Shigella* and *Legionella* modulate the activity of proapoptotic caspases (235, 236). Although a role for multidrug efflux in modulation of host inflammatory responses has been described in *Listeria monocytogenes* (237), none of the anti-apoptotic activities characterized to date for intracellular pathogens has been attributed directly to TolC or the type I secretion system. Thus, *F. tularensis* likely employs unique mechanisms to inhibit innate host immune responses.

There is currently no licensed tularemia vaccine in the United States. The LVS offers incomplete protection against challenge with fully virulent *F. tularensis*, and the basis for the attenuation of the LVS is not fully understood (25, 26, 30, 196). Therefore, there is need for an improved tularemia vaccine. FPI mutants and other *Francisella* strains that are unable to escape the phagosome or replicate intracellularly do not provide significant protection when used as vaccines, presumably because their growth in vivo is so compromised that they do not effectively trigger adaptive immune responses (47, 48). The problem of overattenuation is also seen during vaccination attempts with *F. tularensis* O-antigen mutants (49, 50). In this regard, the LVS Δ*tolC* mutant may represent an improved live vaccine strain, as it (i) contains a defined genetic lesion; (ii) is attenuated for virulence; (iii) replicates and disseminates within the host, but to lower levels than WT bacteria; and (iv) appears to trigger more effective immune responses compared to the WT LVS. On a broader level, the construction of mutant strains that cause premature induction of host cell death during infection may represent a general strategy to generate effective vaccines against intracellular pathogens.

REFERENCES

1. **Francis E. 1983.** Landmark article April 25, 1925: Tularemia. By Edward Francis. JAMA : the journal of the American Medical Association 250:3216-3224.

2. **Splettstoesser WD, Seibold E, Zeman E, Trebesius K, Podbielski A. 2010.** Rapid differentiation of Francisella species and subspecies by fluorescent in situ hybridization targeting the 23S rRNA. BMC microbiology 10:72.

3. **Sreter-Lancz Z, Szell Z, Sreter T, Marialigeti K. 2009.** Detection of a novel Francisella in Dermacentor reticulatus: a need for careful evaluation of PCR-based identification of Francisella tularensis in Eurasian ticks. Vector Borne Zoonotic Dis 9:123-126.

4. **Johansson A, Ibrahim A, Goransson I, Eriksson U, Gurycova D, Clarridge JE, 3rd, Sjostedt A. 2000.** Evaluation of PCR-based methods for discrimination of Francisella species and subspecies and development of a specific PCR that distinguishes the two major subspecies of Francisella tularensis. J Clin Microbiol 38:4180-4185.

5. **La Scola B, Elkarkouri K, Li W, Wahab T, Fournous G, Rolain JM, Biswas S, Drancourt M, Robert C, Audic S, Lofdahl S, Raoult D. 2008.** Rapid comparative genomic analysis for clinical microbiology: the Francisella tularensis paradigm. Genome research 18:742-750.

6. **Staples JE, Kubota KA, Chalcraft LG, Mead PS, Petersen JM. 2006.** Epidemiologic and molecular analysis of human tularemia, United States, 1964-2004. Emerging infectious diseases 12:1113-1118.

7. **Urich SK, Petersen JM. 2008.** In vitro susceptibility of isolates of Francisella tularensis types A and B from North America. Antimicrob Agents Chemother (Bethesda) 52:2276-2278.

8. **Teutsch SM, Martone WJ, Brink EW, Potter ME, Eliot G, Hoxsie R, Craven RB, Kaufmann AF. 1979.** Pneumonic tularemia on Martha's Vineyard. The New England journal of medicine 301:826-828.

9. **Feldman KA, Enscore RE, Lathrop SL, Matyas BT, McGuill M, Schriefer ME, Stiles-Enos D, Dennis DT, Petersen LR, Hayes EB. 2001.** An outbreak of primary pneumonic tularemia on Martha's Vineyard. The New England journal of medicine 345:1601-1606.

10. **Matyas BT, Nieder HS, Telford SR, 3rd. 2007.** Pneumonic tularemia on Martha's Vineyard: clinical, epidemiologic, and ecological characteristics. Ann N Y Acad Sci 1105:351-377.

11. **Morner T. 1992.** The ecology of tularaemia. Rev Sci Tech 11:1123-1130.

12. **Jackson J, McGregor A, Cooley L, Ng J, Brown M, Ong CW, Darcy C, Sintchenko V. 2012.** Francisella tularensis subspecies holarctica, Tasmania, Australia, 2011. Emerging infectious diseases 18:1484-1486.

13. **Molins CR, Carlson JK, Coombs J, Petersen JM. 2009.** Identification of Francisella tularensis subsp. tularensis A1 and A2 infections by real-time polymerase chain reaction. Diagnostic microbiology and infectious disease 64:6-12.

14. **Molins CR, Delorey MJ, Yockey BM, Young JW, Sheldon SW, Reese SM, Schriefer ME, Petersen JM. 2010.** Virulence differences among Francisella tularensis subsp. tularensis clades in mice. PLoS One 5:e10205.

15. **Gyuranecz M, Rigo K, Dan A, Foldvari G, Makrai L, Denes B, Fodor L, Majoros G, Tirjak L, Erdelyi K. 2011.** Investigation of the ecology of Francisella tularensis during an inter-epizootic period. Vector Borne Zoonotic Dis 11:1031-1035.

16. **Santic M, Al-Khodor S, Abu Kwaik Y. 2010.** Cell biology and molecular ecology of Francisella tularensis. Cell Microbiol 12:129-139.

17. **Keim P, Johansson A, Wagner DM. 2007.** Molecular epidemiology, evolution, and ecology of Francisella. Ann N Y Acad Sci 1105:30-66.

18. **Sjostedt A. 2007.** Tularemia: history, epidemiology, pathogen physiology, and clinical manifestations. Ann N Y Acad Sci 1105:1-29.

19. **Hanke CA, Otten JE, Berner R, Serr A, Splettstoesser W, von Schnakenburg C. 2009.** Ulceroglandular tularemia in a toddler in Germany after a mosquito bite. European journal of pediatrics 168:937-940.

20. **Maurin M, Castan B, Roch N, Gestin B, Pelloux I, Mailles A, Chiquet C, Chavanet P. 2010.** Real-time PCR for diagnosis of oculoglandular tularemia. Emerging infectious diseases 16:152-153.

21. **Steinrucken J, Graber P. 2014.** Oropharyngeal tularemia. CMAJ : Canadian Medical Association journal = journal de l'Association medicale canadienne 186:E62.

22. **Dennis DT, Inglesby TV, Henderson DA, Bartlett JG, Ascher MS, Eitzen E, Fine AD, Friedlander AM, Hauer J, Layton M, Lillibridge SR, McDade JE, Osterholm MT, O'Toole T, Parker G, Perl TM, Russell PK, Tonat K. 2001.** Tularemia as a biological weapon: medical and public health management. JAMA : the journal of the American Medical Association 285:2763-2773.

23. **Faith SA, Smith LP, Swatland AS, Reed DS. 2012.** Growth conditions and environmental factors impact aerosolization but not virulence of Francisella tularensis infection in mice. Front Cell Infect Microbiol 2:126.

24. **2012.** Possession, use, and transfer of select agents and toxins; biennial review. Final rule. Fed Regist 77:61083-61115.

25. **Saslaw S, Eigelsbach HT, Prior JA, Wilson HE, Carhart S. 1961.** Tularemia vaccine study. II. Respiratory challenge. Archives of internal medicine 107:702-714.

26. **Hornick RB, Eigelsbach HT. 1966.** Aerogenic immunization of man with live Tularemia vaccine. Bacteriol Rev 30:532-538.

27. **Foshay L, Hesselbrock WH, Wittenberg HJ, Rodenberg AH. 1942.** Vaccine Prophylaxis against Tularemia in Man. Am J Public Health Nations Health 32:1131-1145.

28. **Coriell LL, King EO, Smith MG. 1948.** Studies on tularemia; observations on tularemia in normal and vaccinated monkeys. J Immunol 58:183-202.

29. **Eigelsbach HT, Downs CM. 1961.** Prophylactic effectiveness of live and killed tularemia vaccines. I. Production of vaccine and evaluation in the white mouse and guinea pig. J Immunol 87:415-425.

30. **Saslaw S, Eigelsbach HT, Wilson HE, Prior JA, Carhart S. 1961.** Tularemia vaccine study. I. Intracutaneous challenge. Archives of internal medicine 107:689-701.

31. **Eigelsbach HT, Tulis JJ, Overholt EL, Griffith WR. 1961.** Aerogenic immunization of the monkey and guinea pig with live tularemia vaccine. Proc Soc Exp Biol Med 108:732-734.

32. **Kamata M, Wu RP, An DS, Saxe JP, Damoiseaux R, Phelps ME, Huang J, Chen IS. 2006.** Cell-based chemical genetic screen identifies damnacanthal as an inhibitor of HIV-1 Vpr induced cell death. Biochem Biophys Res Commun 348:1101-1106.

33. Huntley JF, Conley PG, Rasko DA, Hagman KE, Apicella MA, Norgard MV. 2008. Native outer membrane proteins protect mice against pulmonary challenge with virulent type A Francisella tularensis. Infect Immun 76:3664-3671.

34. Fulop M, Mastroeni P, Green M, Titball RW. 2001. Role of antibody to lipopolysaccharide in protection against low- and high-virulence strains of Francisella tularensis. Vaccine 19:4465-4472.

35. Foster RH, Noble S. 1999. Bivalent cholera and typhoid vaccine. Drugs 58:91-96; discussion 97-98.

36. Pitt JM, Blankley S, McShane H, O'Garra A. 2013. Vaccination against tuberculosis: how can we better BCG? Microb Pathog 58:2-16.

37. Quarry JE, Isherwood KE, Michell SL, Diaper H, Titball RW, Oyston PC. 2007. A Francisella tularensis subspecies novicida purF mutant, but not a purA mutant, induces protective immunity to tularemia in mice. Vaccine 25:2011-2018.

38. Mohapatra NP, Soni S, Bell BL, Warren R, Ernst RK, Muszynski A, Carlson RW, Gunn JS. 2007. Identification of an orphan response regulator required for the virulence of Francisella spp. and transcription of pathogenicity island genes. Infect Immun 75:3305-3314.

39. Jia Q, Lee BY, Bowen R, Dillon BJ, Som SM, Horwitz MA. 2010. A Francisella tularensis live vaccine strain (LVS) mutant with a deletion in capB, encoding a putative capsular biosynthesis protein, is significantly more attenuated than LVS yet induces potent protective immunity in mice against F. tularensis challenge. Infect Immun 78:4341-4355.

40. Sebastian S, Dillon ST, Lynch JG, Blalock LT, Balon E, Lee KT, Comstock LE, Conlan JW, Rubin EJ, Tzianabos AO, Kasper DL. 2007. A defined O-antigen polysaccharide mutant of Francisella tularensis live vaccine strain has attenuated virulence while retaining its protective capacity. Infect Immun 75:2591-2602.

41. Bakshi CS, Malik M, Mahawar M, Kirimanjeswara GS, Hazlett KR, Palmer LE, Furie MB, Singh R, Melendez JA, Sellati TJ, Metzger DW. 2008. An improved vaccine for prevention of respiratory tularemia caused by Francisella tularensis SchuS4 strain. Vaccine 26:5276-5288.

42. Griffin KF, Oyston PC, Titball RW. 2007. Francisella tularensis vaccines. FEMS immunology and medical microbiology 49:315-323.

43. **Pechous RD, McCarthy TR, Zahrt TC. 2009.** Working toward the future: insights into Francisella tularensis pathogenesis and vaccine development. Microbiol Mol Biol Rev 73:684-711.

44. **Michell SL, Dean RE, Eyles JE, Hartley MG, Waters E, Prior JL, Titball RW, Oyston PC. 2010.** Deletion of the Bacillus anthracis capB homologue in Francisella tularensis subspecies tularensis generates an attenuated strain that protects mice against virulent tularaemia. J Med Microbiol 59:1275-1284.

45. **Reed DS, Smith LP, Cole KS, Santiago AE, Mann BJ, Barry EM. 2014.** Live attenuated mutants of Francisella tularensis protect rabbits against aerosol challenge with a virulent type A strain. Infect Immun.

46. **Golovliov I, Twine SM, Shen H, Sjostedt A, Conlan W. 2013.** A DeltaclpB mutant of Francisella tularensis subspecies holarctica strain, FSC200, is a more effective live vaccine than F. tularensis LVS in a mouse respiratory challenge model of tularemia. PLoS One 8:e78671.

47. **Twine S, Bystrom M, Chen W, Forsman M, Golovliov I, Johansson A, Kelly J, Lindgren H, Svensson K, Zingmark C, Conlan W, Sjostedt A. 2005.** A mutant of Francisella tularensis strain SCHU S4 lacking the ability to express a 58-kilodalton protein is attenuated for virulence and is an effective live vaccine. Infect Immun 73:8345-8352.

48. **Pechous RD, McCarthy TR, Mohapatra NP, Soni S, Penoske RM, Salzman NH, Frank DW, Gunn JS, Zahrt TC. 2008.** A Francisella tularensis Schu S4 purine auxotroph is highly attenuated in mice but offers limited protection against homologous intranasal challenge. PLoS One 3:e2487.

49. **Li J, Ryder C, Mandal M, Ahmed F, Azadi P, Snyder DS, Pechous RD, Zahrt T, Inzana TJ. 2007.** Attenuation and protective efficacy of an O-antigen-deficient mutant of Francisella tularensis LVS. Microbiology 153:3141-3153.

50. **Thomas RM, Titball RW, Oyston PC, Griffin K, Waters E, Hitchen PG, Michell SL, Grice ID, Wilson JC, Prior JL. 2007.** The immunologically distinct O antigens from Francisella tularensis subspecies tularensis and Francisella novicida are both virulence determinants and protective antigens. Infect Immun 75:371-378.

51. **Bosio CM, Bielefeldt-Ohmann H, Belisle JT. 2007.** Active suppression of the pulmonary immune response by Francisella tularensis Schu4. J Immunol 178:4538-4547.

52. **Mares CA, Ojeda SS, Morris EG, Li Q, Teale JM. 2008.** Initial delay in the immune response to Francisella tularensis is followed by hypercytokinemia characteristic of

severe sepsis and correlating with upregulation and release of damage-associated molecular patterns. Infect Immun 76:3001-3010.

53. **Andersson H, Hartmanova B, Kuolee R, Ryden P, Conlan W, Chen W, Sjostedt A. 2006.** Transcriptional profiling of host responses in mouse lungs following aerosol infection with type A Francisella tularensis. J Med Microbiol 55:263-271.

54. **Andersson H, Hartmanova B, Back E, Eliasson H, Landfors M, Naslund L, Ryden P, Sjostedt A. 2006.** Transcriptional profiling of the peripheral blood response during tularemia. Genes and immunity 7:503-513.

55. **Conlan JW, Zhao X, Harris G, Shen H, Bolanowski M, Rietz C, Sjostedt A, Chen W. 2008.** Molecular immunology of experimental primary tularemia in mice infected by respiratory or intradermal routes with type A Francisella tularensis. Mol Immunol 45:2962-2969.

56. **Cowley SC, Elkins KL. 2011.** Immunity to francisella. Front Microbiol 2:26.

57. **Poltorak A, Ricciardi-Castagnoli P, Citterio S, Beutler B. 2000.** Physical contact between lipopolysaccharide and toll-like receptor 4 revealed by genetic complementation. Proc Natl Acad Sci U S A 97:2163-2167.

58. **Chow JC, Young DW, Golenbock DT, Christ WJ, Gusovsky F. 1999.** Toll-like receptor-4 mediates lipopolysaccharide-induced signal transduction. J Biol Chem 274:10689-10692.

59. **Poltorak A, He X, Smirnova I, Liu MY, Van Huffel C, Du X, Birdwell D, Alejos E, Silva M, Galanos C, Freudenberg M, Ricciardi-Castagnoli P, Layton B, Beutler B. 1998.** Defective LPS signaling in C3H/HeJ and C57BL/10ScCr mice: mutations in Tlr4 gene. Science 282:2085-2088.

60. **Telepnev MV, Klimpel GR, Haithcoat J, Knirel YA, Anisimov AP, Motin VL. 2009.** Tetraacylated lipopolysaccharide of Yersinia pestis can inhibit multiple Toll-like receptor-mediated signaling pathways in human dendritic cells. J Infect Dis 200:1694-1702.

61. **van der Ley P, Steeghs L, Hamstra HJ, ten Hove J, Zomer B, van Alphen L. 2001.** Modification of lipid A biosynthesis in Neisseria meningitidis lpxL mutants: influence on lipopolysaccharide structure, toxicity, and adjuvant activity. Infect Immun 69:5981-5990.

62. **Matsuura M. 2013.** Structural Modifications of Bacterial Lipopolysaccharide that Facilitate Gram-Negative Bacteria Evasion of Host Innate Immunity. Front Immunol 4:109.

63. **Zipfel PF, Hallstrom T, Riesbeck K. 2013.** Human complement control and complement evasion by pathogenic microbes--tipping the balance. Mol Immunol 56:152-160.

64. **Ben Nasr A, Klimpel GR. 2008.** Subversion of complement activation at the bacterial surface promotes serum resistance and opsonophagocytosis of Francisella tularensis. J Leukoc Biol 84:77-85.

65. **Clay CD, Soni S, Gunn JS, Schlesinger LS. 2008.** Evasion of complement-mediated lysis and complement C3 deposition are regulated by Francisella tularensis lipopolysaccharide O antigen. J Immunol 181:5568-5578.

66. **Sandstrom G, Lofgren S, Tarnvik A. 1988.** A capsule-deficient mutant of Francisella tularensis LVS exhibits enhanced sensitivity to killing by serum but diminished sensitivity to killing by polymorphonuclear leukocytes. Infect Immun 56:1194-1202.

67. **Dai S, Rajaram MV, Curry HM, Leander R, Schlesinger LS. 2013.** Fine tuning inflammation at the front door: macrophage complement receptor 3-mediates phagocytosis and immune suppression for Francisella tularensis. PLoS Pathog 9:e1003114.

68. **Qin A, Mann BJ. 2006.** Identification of transposon insertion mutants of Francisella tularensis tularensis strain Schu S4 deficient in intracellular replication in the hepatic cell line HepG2. BMC microbiology 6:69.

69. **Melillo A, Sledjeski DD, Lipski S, Wooten RM, Basrur V, Lafontaine ER. 2006.** Identification of a Francisella tularensis LVS outer membrane protein that confers adherence to A549 human lung cells. FEMS Microbiol Lett 263:102-108.

70. **Fortier AH, Green SJ, Polsinelli T, Jones TR, Crawford RM, Leiby DA, Elkins KL, Meltzer MS, Nacy CA. 1994.** Life and death of an intracellular pathogen: Francisella tularensis and the macrophage. Immunol Ser 60:349-361.

71. **Anthony LD, Burke RD, Nano FE. 1991.** Growth of Francisella spp. in rodent macrophages. Infect Immun 59:3291-3296.

72. **Bosio CM, Dow SW. 2005.** Francisella tularensis induces aberrant activation of pulmonary dendritic cells. J Immunol 175:6792-6801.

73. **McCaffrey RL, Allen LA. 2006.** Francisella tularensis LVS evades killing by human neutrophils via inhibition of the respiratory burst and phagosome escape. J Leukoc Biol 80:1224-1230.

74. **Horzempa J, O'Dee DM, Stolz DB, Franks JM, Clay D, Nau GJ. 2011.** Invasion of erythrocytes by Francisella tularensis. J Infect Dis 204:51-59.

75. **Balagopal A, MacFarlane AS, Mohapatra N, Soni S, Gunn JS, Schlesinger LS. 2006.** Characterization of the receptor-ligand pathways important for entry and survival of Francisella tularensis in human macrophages. Infect Immun 74:5114-5125.

76. **Ben Nasr A, Haithcoat J, Masterson JE, Gunn JS, Eaves-Pyles T, Klimpel GR. 2006.** Critical role for serum opsonins and complement receptors CR3 (CD11b/CD18) and CR4 (CD11c/CD18) in phagocytosis of Francisella tularensis by human dendritic cells (DC): uptake of Francisella leads to activation of immature DC and intracellular survival of the bacteria. J Leukoc Biol 80:774-786.

77. **Schulert GS, Allen LA. 2006.** Differential infection of mononuclear phagocytes by Francisella tularensis: role of the macrophage mannose receptor. J Leukoc Biol 80:563-571.

78. **Pierini LM. 2006.** Uptake of serum-opsonized Francisella tularensis by macrophages can be mediated by class A scavenger receptors. Cell Microbiol 8:1361-1370.

79. **Celli J, Zahrt TC. 2013.** Mechanisms of Francisella tularensis intracellular pathogenesis. Cold Spring Harb Perspect Med 3:a010314.

80. **Cross AS, Kelly NM. 1990. Bacteria-phagocyte interactions: emerging tactics in an ancient rivalry.** FEMS Microbiol Immunol 2:245-258.

81. **Brune B, Dehne N, Grossmann N, Jung M, Namgaladze D, Schmid T, von Knethen A, Weigert A. 2013. Redox control of inflammation in macrophages.** Antioxidants & redox signaling 19:595-637.

82. **Zahrt TC, Deretic V. 2002.** Reactive nitrogen and oxygen intermediates and bacterial defenses: unusual adaptations in Mycobacterium tuberculosis. Antioxidants & redox signaling 4:141-159.

83. **Lindgren H, Stenmark S, Chen W, Tarnvik A, Sjostedt A. 2004.** Distinct roles of reactive nitrogen and oxygen species to control infection with the facultative intracellular bacterium Francisella tularensis. Infect Immun 72:7172-7182.

84. **Mohapatra NP, Soni S, Rajaram MV, Dang PM, Reilly TJ, El-Benna J, Clay CD, Schlesinger LS, Gunn JS. 2010.** Francisella acid phosphatases inactivate the NADPH oxidase in human phagocytes. J Immunol 184:5141-5150.

85. **Bakshi CS, Malik M, Regan K, Melendez JA, Metzger DW, Pavlov VM, Sellati TJ. 2006.** Superoxide dismutase B gene (sodB)-deficient mutants of Francisella tularensis demonstrate hypersensitivity to oxidative stress and attenuated virulence. J Bacteriol 188:6443-6448.

86. **Melillo AA, Mahawar M, Sellati TJ, Malik M, Metzger DW, Melendez JA, Bakshi CS. 2009.** Identification of Francisella tularensis live vaccine strain CuZn superoxide dismutase as critical for resistance to extracellularly generated reactive oxygen species. J Bacteriol 191:6447-6456.

87. **Lindgren H, Shen H, Zingmark C, Golovliov I, Conlan W, Sjostedt A. 2007.** Resistance of Francisella tularensis strains against reactive nitrogen and oxygen species with special reference to the role of KatG. Infect Immun 75:1303-1309.

88. **Ramond E, Gesbert G, Rigard M, Dairou J, Dupuis M, Dubail I, Meibom K, Henry T, Barel M, Charbit A. 2014.** Glutamate utilization couples oxidative stress defense and the tricarboxylic acid cycle in Francisella phagosomal escape. PLoS Pathog 10:e1003893.

89. **Claus V, Jahraus A, Tjelle T, Berg T, Kirschke H, Faulstich H, Griffiths G. 1998.** Lysosomal enzyme trafficking between phagosomes, endosomes, and lysosomes in J774 macrophages. Enrichment of cathepsin H in early endosomes. J Biol Chem 273:9842-9851.

90. **Clemens DL, Lee BY, Horwitz MA. 2004.** Virulent and avirulent strains of Francisella tularensis prevent acidification and maturation of their phagosomes and escape into the cytoplasm in human macrophages. Infect Immun 72:3204-3217.

91. **Bonquist L, Lindgren H, Golovliov I, Guina T, Sjostedt A. 2008.** MglA and Igl proteins contribute to the modulation of Francisella tularensis live vaccine strain-containing phagosomes in murine macrophages. Infect Immun 76:3502-3510.

92. **Barker JR, Chong A, Wehrly TD, Yu JJ, Rodriguez SA, Liu J, Celli J, Arulanandam BP, Klose KE. 2009.** The Francisella tularensis pathogenicity island encodes a secretion system that is required for phagosome escape and virulence. Mol Microbiol 74:1459-1470.

93. **Jones CL, Napier BA, Sampson TR, Llewellyn AC, Schroeder MR, Weiss DS. 2012.** Subversion of host recognition and defense systems by Francisella spp. Microbiol Mol Biol Rev 76:383-404.

94. **Asare R, Abu Kwaik Y. 2010.** Molecular complexity orchestrates modulation of phagosome biogenesis and escape to the cytosol of macrophages by Francisella tularensis. Environmental microbiology 12:2559-2586.

95. **Meibom KL, Charbit A. 2010.** The unraveling panoply of Francisella tularensis virulence attributes. Current opinion in microbiology 13:11-17.

96. **Alkhuder K, Meibom KL, Dubail I, Dupuis M, Charbit A. 2009.** Glutathione provides a source of cysteine essential for intracellular multiplication of Francisella tularensis. PLoS Pathog 5:e1000284.

97. **Wehrly TD, Chong A, Virtaneva K, Sturdevant DE, Child R, Edwards JA, Brouwer D, Nair V, Fischer ER, Wicke L, Curda AJ, Kupko JJ, 3rd, Martens C, Crane DD, Bosio CM, Porcella SF, Celli J. 2009.** Intracellular biology and virulence determinants of Francisella tularensis revealed by transcriptional profiling inside macrophages. Cell Microbiol 11:1128-1150.

98. **Fuller JR, Craven RR, Hall JD, Kijek TM, Taft-Benz S, Kawula TH. 2008.** RipA, a cytoplasmic membrane protein conserved among Francisella species, is required for intracellular survival. Infect Immun 76:4934-4943.

99. **Parmely MJ, Fischer JL, Pinson DM. 2009.** Programmed cell death and the pathogenesis of tissue injury induced by type A Francisella tularensis. FEMS Microbiol Lett 301:1-11.

100. **von Moltke J, Ayres JS, Kofoed EM, Chavarria-Smith J, Vance RE. 2013.** Recognition of bacteria by inflammasomes. Annu Rev Immunol 31:73-106.

101. **Belhocine K, Monack DM. 2012.** Francisella infection triggers activation of the AIM2 inflammasome in murine dendritic cells. Cell Microbiol 14:71-80.

102. **Jones JW, Kayagaki N, Broz P, Henry T, Newton K, O'Rourke K, Chan S, Dong J, Qu Y, Roose-Girma M, Dixit VM, Monack DM. 2010.** Absent in melanoma 2 is required for innate immune recognition of Francisella tularensis. Proc Natl Acad Sci U S A 107:9771-9776.

103. **Moffitt KL, Martin SL, Walker B. 2010.** From sentencing to execution--the processes of apoptosis. J Pharm Pharmacol 62:547-562.

104. **Schwartz JT, Bandyopadhyay S, Kobayashi SD, McCracken J, Whitney AR, Deleo FR, Allen LA. 2013.** Francisella tularensis alters human neutrophil gene expression: insights into the molecular basis of delayed neutrophil apoptosis. J Innate Immun 5:124-136.

105. **Schwartz JT, Barker JH, Kaufman J, Fayram DC, McCracken JM, Allen LA. 2012.** Francisella tularensis inhibits the intrinsic and extrinsic pathways to delay constitutive apoptosis and prolong human neutrophil lifespan. J Immunol 188:3351-3363.

106. **Santic M, Pavokovic G, Jones S, Asare R, Kwaik YA. 2010.** Regulation of apoptosis and anti-apoptosis signalling by Francisella tularensis. Microbes Infect 12:126-134.

107. **Wickstrum JR, Bokhari SM, Fischer JL, Pinson DM, Yeh HW, Horvat RT, Parmely MJ. 2009.** Francisella tularensis induces extensive caspase-3 activation and apoptotic cell death in the tissues of infected mice. Infect Immun 77:4827-4836.

108. **Weiss DS, Henry T, Monack DM. 2007.** Francisella tularensis: activation of the inflammasome. Ann N Y Acad Sci 1105:219-237.

109. **Henry T, Monack DM. 2007.** Activation of the inflammasome upon Francisella tularensis infection: interplay of innate immune pathways and virulence factors. Cell Microbiol 9:2543-2551.

110. **Peng K, Broz P, Jones J, Joubert LM, Monack D. 2011.** Elevated AIM2-mediated pyroptosis triggered by hypercytotoxic Francisella mutant strains is attributed to increased intracellular bacteriolysis. Cell Microbiol 13:1586-1600.

111. **Schwechheimer C, Sullivan CJ, Kuehn MJ. 2013.** Envelope control of outer membrane vesicle production in Gram-negative bacteria. Biochemistry 52:3031-3040.

112. **Larsson P, Oyston PC, Chain P, Chu MC, Duffield M, Fuxelius HH, Garcia E, Halltorp G, Johansson D, Isherwood KE, Karp PD, Larsson E, Liu Y, Michell S, Prior J, Prior R, Malfatti S, Sjostedt A, Svensson K, Thompson N, Vergez L, Wagg JK, Wren BW, Lindler LE, Andersson SG, Forsman M, Titball RW. 2005.** The complete genome sequence of Francisella tularensis, the causative agent of tularemia. Nature genetics 37:153-159.

113. **Chakraborty S, Monfett M, Maier TM, Benach JL, Frank DW, Thanassi DG. 2008.** Type IV pili in Francisella tularensis: roles of pilF and pilT in fiber assembly, host cell adherence, and virulence. Infect Immun 76:2852-2861.

114. **Gil H, Platz GJ, Forestal CA, Monfett M, Bakshi CS, Sellati TJ, Furie MB, Benach JL, Thanassi DG. 2006.** Deletion of TolC orthologs in Francisella tularensis identifies roles in multidrug resistance and virulence. Proc Natl Acad Sci U S A 103:12897-12902.

115. **McCaig WD, Koller A, Thanassi DG. 2013.** Production of outer membrane vesicles and outer membrane tubes by Francisella novicida. J Bacteriol 195:1120-1132.

116. Wandersman C, Delepelaire P. 1990. TolC, an Escherichia coli outer membrane protein required for hemolysin secretion. Proc Natl Acad Sci U S A 87:4776-4780.

117. Koronakis V, Eswaran J, Hughes C. 2004. Structure and function of TolC: the bacterial exit duct for proteins and drugs. Annual review of biochemistry 73:467-489.

118. Koronakis V. 2003. TolC--the bacterial exit duct for proteins and drugs. FEBS Lett 555:66-71.

119. Eicher T, Brandstatter L, Pos KM. 2009. Structural and functional aspects of the multidrug efflux pump AcrB. Biological chemistry 390:693-699.

120. Tikhonova EB, Zgurskaya HI. 2004. AcrA, AcrB, and TolC of Escherichia coli Form a Stable Intermembrane Multidrug Efflux Complex. J Biol Chem 279:32116-32124.

121. Husain F, Humbard M, Misra R. 2004. Interaction between the TolC and AcrA proteins of a multidrug efflux system of Escherichia coli. J Bacteriol 186:8533-8536.

122. Koronakis V, Sharff A, Koronakis E, Luisi B, Hughes C. 2000. Crystal structure of the bacterial membrane protein TolC central to multidrug efflux and protein export. Nature 405:914-919.

123. Hanekop N, Zaitseva J, Jenewein S, Holland IB, Schmitt L. 2006. Molecular insights into the mechanism of ATP-hydrolysis by the NBD of the ABC-transporter HlyB. FEBS Lett 580:1036-1041.

124. Balakrishnan L, Hughes C, Koronakis V. 2001. Substrate-triggered recruitment of the TolC channel-tunnel during type I export of hemolysin by Escherichia coli. Journal of molecular biology 313:501-510.

125. Thanabalu T, Koronakis E, Hughes C, Koronakis V. 1998. Substrate-induced assembly of a contiguous channel for protein export from E.coli: reversible bridging of an inner-membrane translocase to an outer membrane exit pore. Embo J 17:6487-6496.

126. Hinchliffe P, Symmons MF, Hughes C, Koronakis V. 2013. Structure and operation of bacterial tripartite pumps. Annual review of microbiology 67:221-242.

127. Lecher J, Schwarz CK, Stoldt M, Smits SH, Willbold D, Schmitt L. 2012. An RTX transporter tethers its unfolded substrate during secretion via a unique N-terminal domain. Structure 20:1778-1787.

128. Lee M, Jun SY, Yoon BY, Song S, Lee K, Ha NC. 2012. Membrane fusion proteins of type I secretion system and tripartite efflux pumps share a binding motif for TolC in gram-negative bacteria. PLoS One 7:e40460.

129. Welch RA. 2001. RTX toxin structure and function: a story of numerous anomalies and few analogies in toxin biology. Current topics in microbiology and immunology 257:85-111.

130. Thomas S, Holland IB, Schmitt L. 2013. The Type 1 secretion pathway - The hemolysin system and beyond. Biochim Biophys Acta.

131. Gray L, Mackman N, Nicaud JM, Holland IB. 1986. The carboxy-terminal region of haemolysin 2001 is required for secretion of the toxin from Escherichia coli. Molecular & general genetics : MGG 205:127-133.

132. Gray L, Baker K, Kenny B, Mackman N, Haigh R, Holland IB. 1989. A novel C-terminal signal sequence targets Escherichia coli haemolysin directly to the medium. J Cell Sci Suppl 11:45-57.

133. Kenny B, Haigh R, Holland IB. 1991. Analysis of the haemolysin transport process through the secretion from Escherichia coli of PCM, CAT or beta-galactosidase fused to the Hly C-terminal signal domain. Mol Microbiol 5:2557-2568.

134. Kenny B, Taylor S, Holland IB. 1992. Identification of individual amino acids required for secretion within the haemolysin (HlyA) C-terminal targeting region. Mol Microbiol 6:1477-1489.

135. Stanley P, Koronakis V, Hughes C. 1991. Mutational analysis supports a role for multiple structural features in the C-terminal secretion signal of Escherichia coli haemolysin. Mol Microbiol 5:2391-2403.

136. Platz GJ, Bublitz DC, Mena P, Benach JL, Furie MB, Thanassi DG. 2010. A tolC mutant of Francisella tularensis is hypercytotoxic compared to the wild type and elicits increased proinflammatory responses from host cells. Infect Immun 78:1022-1031.

137. Kayagaki N, Warming S, Lamkanfi M, Vande Walle L, Louie S, Dong J, Newton K, Qu Y, Liu J, Heldens S, Zhang J, Lee WP, Roose-Girma M, Dixit VM. 2011. Non-canonical inflammasome activation targets caspase-11. Nature 479:117-121.

138. Galluzzi L, Blomgren K, Kroemer G. 2009. Mitochondrial membrane permeabilization in neuronal injury. Nat Rev Neurosci 10:481-494.

139. Remaut H, Waksman G. 2004. Structural biology of bacterial pathogenesis. Curr Opin Struct Biol 14:161-170.

140. Frey J, Beck M, Stucki U, Nicolet J. 1993. Analysis of hemolysin operons in Actinobacillus pleuropneumoniae. Gene 123:51-58.

141. Goebel W, Hedgpeth J. 1982. Cloning and functional characterization of the plasmid-encoded hemolysin determinant of Escherichia coli. J Bacteriol 151:1290-1298.

142. Hwang J, Zhong X, Tai PC. 1997. Interactions of dedicated export membrane proteins of the colicin V secretion system: CvaA, a member of the membrane fusion protein family, interacts with CvaB and TolC. J Bacteriol 179:6264-6270.

143. Strathdee CA, Lo RY. 1989. Cloning, nucleotide sequence, and characterization of genes encoding the secretion function of the Pasteurella haemolytica leukotoxin determinant. J Bacteriol 171:916-928.

144. Lally ET, Golub EE, Kieba IR, Taichman NS, Rosenbloom J, Rosenbloom JC, Gibson CW, Demuth DR. 1989. Analysis of the Actinobacillus actinomycetemcomitans leukotoxin gene. Delineation of unique features and comparison to homologous toxins. J Biol Chem 264:15451-15456.

145. Yamanaka H, Kobayashi H, Takahashi E, Okamoto K. 2008. MacAB is involved in the secretion of Escherichia coli heat-stable enterotoxin II. J Bacteriol 190:7693-7698.

146. Duong F, Lazdunski A, Cami B, Murgier M. 1992. Sequence of a cluster of genes controlling synthesis and secretion of alkaline protease in Pseudomonas aeruginosa: relationships to other secretory pathways. Gene 121:47-54.

147. Wassif C, Cheek D, Belas R. 1995. Molecular analysis of a metalloprotease from Proteus mirabilis. J Bacteriol 177:5790-5798.

148. Letoffe S, Delepelaire P, Wandersman C. 1991. Cloning and expression in Escherichia coli of the Serratia marcescens metalloprotease gene: secretion of the protease from E. coli in the presence of the Erwinia chrysanthemi protease secretion functions. J Bacteriol 173:2160-2166.

149. Delepelaire P. 1994. PrtD, the integral membrane ATP-binding cassette component of the Erwinia chrysanthemi metalloprotease secretion system, exhibits a secretion signal-regulated ATPase activity. J Biol Chem 269:27952-27957.

150. Akatsuka H, Kawai E, Omori K, Shibatani T. 1995. The three genes lipB, lipC, and lipD involved in the extracellular secretion of the Serratia marcescens lipase which lacks an N-terminal signal peptide. J Bacteriol 177:6381-6389.

151. Ahn JH, Pan JG, Rhee JS. 1999. Identification of the tliDEF ABC transporter specific for lipase in Pseudomonas fluorescens SIK W1. J Bacteriol 181:1847-1852.

152. Satchell KJ. 2011. Structure and function of MARTX toxins and other large repetitive RTX proteins. Annual review of microbiology 65:71-90.

153. Vigil PD, Wiles TJ, Engstrom MD, Prasov L, Mulvey MA, Mobley HL. 2012. The repeat-in-toxin family member TosA mediates adherence of uropathogenic Escherichia coli and survival during bacteremia. Infect Immun 80:493-505.

154. Morgan E, Bowen AJ, Carnell SC, Wallis TS, Stevens MP. 2007. SiiE is secreted by the Salmonella enterica serovar Typhimurium pathogenicity island 4-encoded secretion system and contributes to intestinal colonization in cattle. Infect Immun 75:1524-1533.

155. Hinsa SM, Espinosa-Urgel M, Ramos JL, O'Toole GA. 2003. Transition from reversible to irreversible attachment during biofilm formation by Pseudomonas fluorescens WCS365 requires an ABC transporter and a large secreted protein. Mol Microbiol 49:905-918.

156. Toporowski MC, Nomellini JF, Awram P, Smit J. 2004. Two outer membrane proteins are required for maximal type I secretion of the Caulobacter crescentus S-layer protein. J Bacteriol 186:8000-8009.

157. Braun M, Kuhnert P, Nicolet J, Burnens AP, Frey J. 1999. Cloning and characterization of two bistructural S-layer-RTX proteins from Campylobacter rectus. J Bacteriol 181:2501-2506.

158. Kawai E, Akatsuka H, Idei A, Shibatani T, Omori K. 1998. Serratia marcescens S-layer protein is secreted extracellularly via an ATP-binding cassette exporter, the Lip system. Mol Microbiol 27:941-952.

159. Binet R, Wandersman C. 1996. Cloning of the Serratia marcescens hasF gene encoding the Has ABC exporter outer membrane component: a TolC analogue. Mol Microbiol 22:265-273.

160. Glaser P, Ladant D, Sezer O, Pichot F, Ullmann A, Danchin A. 1988. The calmodulin-sensitive adenylate cyclase of Bordetella pertussis: cloning and expression in Escherichia coli. Mol Microbiol 2:19-30.

161. Thompson SA, Sparling PF. 1993. The RTX cytotoxin-related FrpA protein of Neisseria meningitidis is secreted extracellularly by meningococci and by HlyBD+ Escherichia coli. Infect Immun 61:2906-2911.

162. Wakeel A, den Dulk-Ras A, Hooykaas PJ, McBride JW. 2011. Ehrlichia chaffeensis tandem repeat proteins and Ank200 are type 1 secretion system substrates related to the repeats-in-toxin exoprotein family. Front Cell Infect Microbiol 1:22.

163. Kaur SJ, Rahman MS, Ammerman NC, Beier-Sexton M, Ceraul SM, Gillespie JJ, Azad AF. 2012. TolC-dependent secretion of an ankyrin repeat-containing protein of Rickettsia typhi. J Bacteriol 194:4920-4932.

164. LoVullo ED, Molins-Schneekloth CR, Schweizer HP, Pavelka MS, Jr. 2009. Single-copy chromosomal integration systems for Francisella tularensis. Microbiology 155:1152-1163.

165. LoVullo ED, Sherrill LA, Pavelka MS, Jr. 2009. Improved shuttle vectors for Francisella tularensis genetics. FEMS Microbiol Lett 291:95-102.

166. Cha-aim K, Fukunaga T, Hoshida H, Akada R. 2009. Reliable fusion PCR mediated by GC-rich overlap sequences. Gene 434:43-49.

167. Chamberlain RE. 1965. Evaluation of Live Tularemia Vaccine Prepared in a Chemically Defined Medium. Applied microbiology 13:232-235.

168. Chalabaev S, Anderson CA, Onderdonk AB, Kasper DL. 2011. Sensitivity of Francisella tularensis to ultrapure water and deoxycholate: implications for bacterial intracellular growth assay in macrophages. Journal of microbiological methods 85:230-232.

169. Ma Z, Banik S, Rane H, Mora VT, Rabadi SM, Doyle CR, Thanassi DG, Bakshi CS, Malik M. 2014. EmrA1 membrane fusion protein of Francisella tularensis LVS is required for resistance to oxidative stress, intramacrophage survival and virulence in mice. Mol Microbiol 91:976-995.

170. Checroun C, Wehrly TD, Fischer ER, Hayes SF, Celli J. 2006. Autophagy-mediated reentry of Francisella tularensis into the endocytic compartment after cytoplasmic replication. Proc Natl Acad Sci U S A 103:14578-14583.

171. Golovliov I, Baranov V, Krocova Z, Kovarova H, Sjostedt A. 2003. An attenuated strain of the facultative intracellular bacterium Francisella tularensis can escape the phagosome of monocytic cells. Infect Immun 71:5940-5950.

172. **Nano FE, Zhang N, Cowley SC, Klose KE, Cheung KK, Roberts MJ, Ludu JS, Letendre GW, Meierovics AI, Stephens G, Elkins KL. 2004.** A Francisella tularensis pathogenicity island required for intramacrophage growth. J Bacteriol 186:6430-6436.

173. **Santic M, Molmeret M, Klose KE, Jones S, Kwaik YA. 2005.** The Francisella tularensis pathogenicity island protein IglC and its regulator MglA are essential for modulating phagosome biogenesis and subsequent bacterial escape into the cytoplasm. Cell Microbiol 7:969-979.

174. **Henry T, Brotcke A, Weiss DS, Thompson LJ, Monack DM. 2007.** Type I interferon signaling is required for activation of the inflammasome during Francisella infection. J Exp Med 204:987-994.

175. **Kirimanjeswara GS, Olmos S, Bakshi CS, Metzger DW. 2008.** Humoral and cell-mediated immunity to the intracellular pathogen Francisella tularensis. Immunological reviews 225:244-255.

176. **Telepnev M, Golovliov I, Grundstrom T, Tarnvik A, Sjostedt A. 2003.** Francisella tularensis inhibits Toll-like receptor-mediated activation of intracellular signalling and secretion of TNF-alpha and IL-1 from murine macrophages. Cell Microbiol 5:41-51.

177. **Weiss DS, Brotcke A, Henry T, Margolis JJ, Chan K, Monack DM. 2007.** In vivo negative selection screen identifies genes required for Francisella virulence. Proc Natl Acad Sci U S A 104:6037-6042.

178. **McCaffrey RL, Schwartz JT, Lindemann SR, Moreland JG, Buchan BW, Jones BD, Allen LA. 2010.** Multiple mechanisms of NADPH oxidase inhibition by type A and type B Francisella tularensis. J Leukoc Biol 88:791-805.

179. **Bublitz DC, Noah CE, Benach JL, Furie MB. 2010.** Francisella tularensis suppresses the proinflammatory response of endothelial cells via the endothelial protein C receptor. J Immunol 185:1124-1131.

180. **Lai XH, Sjostedt A. 2003.** Delineation of the molecular mechanisms of Francisella tularensis-induced apoptosis in murine macrophages. Infect Immun 71:4642-4646.

181. **Zivna L, Krocova Z, Hartlova A, Kubelkova K, Zakova J, Rudolf E, Hrstka R, Macela A, Stulik J. 2010.** Activation of B cell apoptotic pathways in the course of Francisella tularensis infection. Microb Pathog 49:226-236.

182. **Budihardjo I, Oliver H, Lutter M, Luo X, Wang X. 1999.** Biochemical pathways of caspase activation during apoptosis. Annu Rev Cell Dev Biol 15:269-290.

183. **Luo M, Lu Z, Sun H, Yuan K, Zhang Q, Meng S, Wang F, Guo H, Ju X, Liu Y, Ye T, Zhai Z. 2010.** Nuclear entry of active caspase-3 is facilitated by its p3-recognition-based specific cleavage activity. Cell research 20:211-222.

184. **Kamada S, Kikkawa U, Tsujimoto Y, Hunter T. 2005.** Nuclear translocation of caspase-3 is dependent on its proteolytic activation and recognition of a substrate-like protein(s). J Biol Chem 280:857-860.

185. **Kamada S, Kikkawa U, Tsujimoto Y, Hunter T. 2005.** A-kinase-anchoring protein 95 functions as a potential carrier for the nuclear translocation of active caspase 3 through an enzyme-substrate-like association. Molecular and cellular biology 25:9469-9477.

186. **Lindemann SR, Peng K, Long ME, Hunt JR, Apicella MA, Monack DM, Allen LA, Jones BD. 2011.** Francisella tularensis Schu S4 O-antigen and capsule biosynthesis gene mutants induce early cell death in human macrophages. Infect Immun 79:581-594.

187. **Jayakar HR, Parvathareddy J, Fitzpatrick EA, Bina XR, Bina JE, Re F, Emery FD, Miller MA. 2011.** A galU mutant of Francisella tularensis is attenuated for virulence in a murine pulmonary model of tularemia. BMC microbiology 11:179.

188. **Hazlett KR, Caldon SD, McArthur DG, Cirillo KA, Kirimanjeswara GS, Magguilli ML, Malik M, Shah A, Broderick S, Golovliov I, Metzger DW, Rajan K, Sellati TJ, Loegering DJ. 2008.** Adaptation of Francisella tularensis to the mammalian environment is governed by cues which can be mimicked in vitro. Infect Immun 76:4479-4488.

189. **Singh A, Rahman T, Malik M, Hickey AJ, Leifer CA, Hazlett KR, Sellati TJ. 2013.** Discordant results obtained with Francisella tularensis during in vitro and in vivo immunological studies are attributable to compromised bacterial structural integrity. PloS one 8:e58513.

190. **Zarrella TM, Singh A, Bitsaktsis C, Rahman T, Sahay B, Feustel PJ, Gosselin EJ, Sellati TJ, Hazlett KR. 2011.** Host-adaptation of Francisella tularensis alters the bacterium's surface-carbohydrates to hinder effectors of innate and adaptive immunity. PloS one 6:e22335.

191. **Moule MG, Monack DM, Schneider DS. 2010.** Reciprocal analysis of Francisella novicida infections of a Drosophila melanogaster model reveal host-pathogen conflicts mediated by reactive oxygen and imd-regulated innate immune response. PLoS Pathog 6:e1001065.

192. Bertrand R, Solary E, O'Connor P, Kohn KW, Pommier Y. 1994. Induction of a common pathway of apoptosis by staurosporine. Experimental cell research 211:314-321.

193. White-Gilbertson S, Mullen T, Senkal C, Lu P, Ogretmen B, Obeid L, Voelkel-Johnson C. 2009. Ceramide synthase 6 modulates TRAIL sensitivity and nuclear translocation of active caspase-3 in colon cancer cells. Oncogene 28:1132-1141.

194. Forestal CA, Malik M, Catlett SV, Savitt AG, Benach JL, Sellati TJ, Furie MB. 2007. Francisella tularensis has a significant extracellular phase in infected mice. J Infect Dis 196:134-137.

195. Kim TH, Pinkham JT, Heninger SJ, Chalabaev S, Kasper DL. 2012. Genetic modification of the O-polysaccharide of Francisella tularensis results in an avirulent live attenuated vaccine. J Infect Dis 205:1056-1065.

196. McCrumb FR. 1961. Aerosol Infection of Man with Pasteurella Tularensis. Bacteriol Rev 25:262-267.

197. Nakazawa Y, Williams RA, Peterson AT, Mead PS, Kugeler KJ, Petersen JM. 2010. Ecological niche modeling of Francisella tularensis subspecies and clades in the United States. Am J Trop Med Hyg 82:912-918.

198. Huntley JF, Conley PG, Hagman KE, Norgard MV. 2007. Characterization of Francisella tularensis outer membrane proteins. J Bacteriol 189:561-574.

199. Bogomolnaya LM, Andrews KD, Talamantes M, Maple A, Ragoza Y, Vazquez-Torres A, Andrews-Polymenis H. 2013. The ABC-type efflux pump MacAB protects Salmonella enterica serovar typhimurium from oxidative stress. MBio 4:e00630-00613.

200. Ferhat M, Atlan D, Vianney A, Lazzaroni JC, Doublet P, Gilbert C. 2009. The TolC protein of Legionella pneumophila plays a major role in multi-drug resistance and the early steps of host invasion. PLoS One 4:e7732.

201. Padilla E, Llobet E, Domenech-Sanchez A, Martinez-Martinez L, Bengoechea JA, Alberti S. 2010. Klebsiella pneumoniae AcrAB efflux pump contributes to antimicrobial resistance and virulence. Antimicrob Agents Chemother (Bethesda) 54:177-183.

202. Al-Karablieh N, Weingart H, Ullrich MS. 2009. The outer membrane protein TolC is required for phytoalexin resistance and virulence of the fire blight pathogen Erwinia amylovora. Microb Biotechnol 2:465-475.

203. Kulathila R, Indic M, van den Berg B. 2011. Crystal structure of Escherichia coli CusC, the outer membrane component of a heavy metal efflux pump. PLoS One 6:e15610.

204. Su CC, Long F, Zimmermann MT, Rajashankar KR, Jernigan RL, Yu EW. 2011. Crystal structure of the CusBA heavy-metal efflux complex of Escherichia coli. Nature 470:558-562.

205. Gupta A, Matsui K, Lo JF, Silver S. 1999. Molecular basis for resistance to silver cations in Salmonella. Nature medicine 5:183-188.

206. Kelley LA, Sternberg MJ. 2009. Protein structure prediction on the Web: a case study using the Phyre server. Nature protocols 4:363-371.

207. Reed LJ, Muench H. 1938. A simple method of estimating fifty percent endpoints. The American Journal of Hygiene 27:493-497.

208. Lai XH, Wang SY, Edebro H, Sjostedt A. 2003. Francisella strains express hemolysins of distinct characteristics. FEMS Microbiol Lett 224:91-95.

209. Boschiroli ML, Ouahrani-Bettache S, Foulongne V, Michaux-Charachon S, Bourg G, Allardet-Servent A, Cazevieille C, Liautard JP, Ramuz M, O'Callaghan D. 2002. The Brucella suis virB operon is induced intracellularly in macrophages. Proc Natl Acad Sci U S A 99:1544-1549.

210. Sieira R, Comerci DJ, Pietrasanta LI, Ugalde RA. 2004. Integration host factor is involved in transcriptional regulation of the Brucella abortus virB operon. Mol Microbiol 54:808-822.

211. Valdivia RH, Falkow S. 1997. Fluorescence-based isolation of bacterial genes expressed within host cells. Science 277:2007-2011.

212. Seibold GM, Breitinger KJ, Kempkes R, Both L, Kramer M, Dempf S, Eikmanns BJ. 2011. The glgB-encoded glycogen branching enzyme is essential for glycogen accumulation in Corynebacterium glutamicum. Microbiology 157:3243-3251.

213. Garg S, Alam MS, Bajpai R, Kishan KR, Agrawal P. 2009. Redox biology of Mycobacterium tuberculosis H37Rv: protein-protein interaction between GlgB and WhiB1 involves exchange of thiol-disulfide. BMC biochemistry 10:1.

214. Kiel JA, Boels JM, Beldman G, Venema G. 1992. The glgB gene from the thermophile Bacillus caldolyticus encodes a thermolabile branching enzyme. DNA sequence : the journal of DNA sequencing and mapping 3:221-232.

215. Atkins HS, Dassa E, Walker NJ, Griffin KF, Harland DN, Taylor RR, Duffield ML, Titball RW. 2006. The identification and evaluation of ATP binding cassette systems in the intracellular bacterium Francisella tularensis. Research in microbiology 157:593-604.

216. Zgurskaya HI, Krishnamoorthy G, Ntreh A, Lu S. 2011. Mechanism and Function of the Outer Membrane Channel TolC in Multidrug Resistance and Physiology of Enterobacteria. Front Microbiol 2:189.

217. Dhamdhere G, Zgurskaya HI. 2010. Metabolic shutdown in Escherichia coli cells lacking the outer membrane channel TolC. Mol Microbiol 77:743-754.

218. Kirimanjeswara GS, Golden JM, Bakshi CS, Metzger DW. 2007. Prophylactic and therapeutic use of antibodies for protection against respiratory infection with Francisella tularensis. J Immunol 179:532-539.

219. Hsieh SH, Lin JS, Huang JH, Wu SY, Chu CL, Kung JT, Wu-Hsieh BA. 2011. Immunization with apoptotic phagocytes containing Histoplasma capsulatum activates functional CD8(+) T cells to protect against histoplasmosis. Infect Immun 79:4493-4502.

220. Winau F, Weber S, Sad S, de Diego J, Hoops SL, Breiden B, Sandhoff K, Brinkmann V, Kaufmann SH, Schaible UE. 2006. Apoptotic vesicles crossprime CD8 T cells and protect against tuberculosis. Immunity 24:105-117.

221. Bertaux L, Mevelec MN, Dion S, Suraud V, Gregoire M, Berthon P, Dimier-Poisson I. 2008. Apoptotic pulsed dendritic cells induce a protective immune response against Toxoplasma gondii. Parasite Immunol 30:620-629.

222. Fortier AH, Slayter MV, Ziemba R, Meltzer MS, Nacy CA. 1991. Live vaccine strain of Francisella tularensis: infection and immunity in mice. Infect Immun 59:2922-2928.

223. Conlan JW, Chen W, Shen H, Webb A, KuoLee R. 2003. Experimental tularemia in mice challenged by aerosol or intradermally with virulent strains of Francisella tularensis: bacteriologic and histopathologic studies. Microb Pathog 34:239-248.

224. Roberts LM, Tuladhar S, Steele SP, Riebe KJ, Chen CJ, Cumming RI, Seay S, Frothingham R, Sempowski GD, Kawula TH, Frelinger JA. 2014. Identification of Early Interactions Between Francisella and the Host. Infect Immun.

225. Eisen RJ, Yockey B, Young J, Reese SM, Piesman J, Schriefer ME, Beard CB, Petersen JM. 2009. Short report: time course of hematogenous dissemination of Francisella tularensis A1, A2, and Type B in laboratory mice. Am J Trop Med Hyg 80:259-262.

226. Dhamdhere G, Krishnamoorthy G, Zgurskaya HI. 2010. Interplay between drug efflux and antioxidants in Escherichia coli resistance to antibiotics. Antimicrob Agents Chemother (Bethesda) 54:5366-5368.

227. Lau SY, Zgurskaya HI. 2005. Cell division defects in Escherichia coli deficient in the multidrug efflux transporter AcrEF-TolC. J Bacteriol 187:7815-7825.

228. Ge Y, Yoshiie K, Kuribayashi F, Lin M, Rikihisa Y. 2005. Anaplasma phagocytophilum inhibits human neutrophil apoptosis via upregulation of bfl-1, maintenance of mitochondrial membrane potential and prevention of caspase 3 activation. Cell Microbiol 7:29-38.

229. Chen A, Seifert HS. 2011. Neisseria gonorrhoeae-mediated inhibition of apoptotic signalling in polymorphonuclear leukocytes. Infect Immun 79:4447-4458.

230. Sukumaran SK, Fu NY, Tin CB, Wan KF, Lee SS, Yu VC. 2010. A soluble form of the pilus protein FimA targets the VDAC-hexokinase complex at mitochondria to suppress host cell apoptosis. Molecular cell 37:768-783.

231. Verbeke P, Welter-Stahl L, Ying S, Hansen J, Hacker G, Darville T, Ojcius DM. 2006. Recruitment of BAD by the Chlamydia trachomatis vacuole correlates with host-cell survival. PLoS Pathog 2:e45.

232. Schmid MC, Scheidegger F, Dehio M, Balmelle-Devaux N, Schulein R, Guye P, Chennakesava CS, Biedermann B, Dehio C. 2006. A translocated bacterial protein protects vascular endothelial cells from apoptosis. PLoS Pathog 2:e115.

233. Bechelli JR, Rydkina E, Colonne PM, Sahni SK. 2009. Rickettsia rickettsii infection protects human microvascular endothelial cells against staurosporine-induced apoptosis by a cIAP(2)-independent mechanism. J Infect Dis 199:1389-1398.

234. Pearson JS, Giogha C, Ong SY, Kennedy CL, Kelly M, Robinson KS, Lung TW, Mansell A, Riedmaier P, Oates CV, Zaid A, Muhlen S, Crepin VF, Marches O, Ang CS, Williamson NA, O'Reilly LA, Bankovacki A, Nachbur U, Infusini G, Webb AI, Silke J, Strasser A, Frankel G, Hartland EL. 2013. A type III effector antagonizes death receptor signalling during bacterial gut infection. Nature 501:247-251.

235. Faherty CS, Merrell DS, Semino-Mora C, Dubois A, Ramaswamy AV, Maurelli AT. 2010. Microarray analysis of Shigella flexneri-infected epithelial cells identifies host factors important for apoptosis inhibition. BMC Genomics 11:272.

236. Abu-Zant A, Jones S, Asare R, Suttles J, Price C, Graham J, Kwaik YA. 2007. Anti-apoptotic signalling by the Dot/Icm secretion system of L. pneumophila. Cell Microbiol 9:246-264.

237. Woodward JJ, Iavarone AT, Portnoy DA. 2010. c-di-AMP secreted by intracellular Listeria monocytogenes activates a host type I interferon response. Science 328:1703-1705.